Comprehensive Evaluation of the Long-Term Performance of Rubberized Pavement Phase II: The Influence of Rubber and...

Technical Report · December 2014

CITATIONS
0

READS
38

8 authors, including:

Junan Shen
Georgia Southern University
49 PUBLICATIONS **644** CITATIONS
SEE PROFILE

Zhaoxing Xie
Auburn University
27 PUBLICATIONS **27** CITATIONS
SEE PROFILE

GEORGIA DOT RESEARCH PROJECT 12-29
FINAL REPORT

Comprehensive Evaluation of the Long-Term Performance of Rubberized Pavement

Phase II: The Influence of Rubber and Asphalt Interaction on Mixture Durability

OFFICE OF RESEARCH
15 Kennedy Drive
Forest Park, GA 30297

1. Report No.: FHWA-GA-12-1229	2. Government Accession No.	3. Recipient's Catalog No. N/A	
4. Title and Subtitle Comprehensive Evaluation of the Long-Term Performance of Rubberized Pavement: Phase II: The Influence of Rubber and Asphalt Interaction on Mixture Durability		5. Report Date December 2014	
		6. Performing Organization Code N/A	
7. Authors Junan Shen, Zhaoxing Xie, and Bo Li		8. Performing Organization Report No.12-29	
9. Performing Organization Name and Address Georgia Southern University Statesboro, GA 30460-8047, USA		10. Work Unit No. (TRAIS)	
		11. Contract or Grant No.	
12. Sponsoring Agency Name and Address Georgia Department of Transportation Office of Research 15 Kennedy Drive Forest Park, GA 30297-2534		13. Type of Report and Period Covered Final Report January 2013 – January 2015	
		14. Sponsoring Agency Code HOTM	
15. Supplementary Notes Prepared in cooperation with the U.S. Department of Transportation, Federal Highway Administration.			
16. Abstract This project investigated the long-term performance of hot asphalt mixes containing crumb rubber modifiers (CRM) added in dry or wet processes. A total of eight asphalt mixtures—four Porous European Mixtures (PEMs) and four Stone Matrix Asphalts (SMAs)—were designed with PG 76-22 modified with CRM, which was added in either a dry or wet process. These mixtures were compared to control mixtures using an SBS-modified PG 76-22. Mixtures incorporating a "hybrid"-modified PG 76-22 were also evaluated. First, the samples were weathered in the Georgia Weathering Asphalt Device (GWAD) for 1,000 hrs and 3,000 hrs and tested to determine their dynamic modulus, fatigue life, rutting, and Cantabro. Binders extracted from the weathered samples were then evaluated using a dynamic shear rheometer (DSR), gel-permeable chromatography (GPC), and Fourier transform infrared spectroscopy (FTIR). Second, the interactions of dry- and wet-processed CRM with asphalt binder were compared during storage and paving. Results indicated: 1) adding TOR to the CRM binder improved PG grade and separation resistance; 2) the dynamic modulus, $\|E^*\|$, of both rubberized PEM and SMA in dry process did not differ significantly from that of the control mixtures or mixtures using the "hybrid"-modified binders before and after weathering; 3) the fatigue life (N_f) of unaged rubberized PEM and SMA in the dry process was similar to that in wet process, although lower than that of control SBS; 4) after 3000-hrs aging, the fatigue life of the dry-processed rubberized SMA is similar to that of the wet-processed but lower than that of hybrid and SBS SMA, regardless of strain and stress levels or test temperatures; 5) the rutting and Cantabro loss of the rubberized PEM and SMA in dry process were higher than those of control SBS after weathering; 6) CRM and asphalt binder interact during the production and paving stages based on DSR, GPC, FTIR, and AFM results. The effect of weathering on the properties of the asphalt binders in rubberized, dry-processed PEMs and SMAs was similar to that in the wet-processed mixtures but greater than that in the control SBS.			
17. Key Words: pavement, dry process, crumb rubber, long-term performance, rutting, dynamic modulus, fatigue life, interaction, weathering, DSR, GPC, FTIR		18. Distribution Statement: N/A	
19. Security Classification (of this report): Unclassified	20. Security Classification (of this page) Unclassified	21. No. of Pages:	22. Price: N/A

Form DOT 1700.7 (8-69)

GDOT Research Project No. 12-29

Comprehensive Evaluation of the Long-Term Performance of Rubberized Pavement

Phase II: The Influence of Rubber and Asphalt Interaction on Mixture Durability

Final Report

By
Junan Shen, Ph.D.
Associate Professor of Civil Engineering
Director, Asphalt Research Laboratory

Zhaoxing Xie, Ph.D.
Postdoctoral Fellow

Bo Li, Ph.D.
Postdoctoral Fellow

College of Engineering and Information Technology
Georgia Southern University
Forest Dr., Engineering Bldg.
Statesboro, GA 30460-8047, USA

January 2015

Table of Contents

LIST OF FIGURES

LIST OF TABLES

EXECUTIVE SUMMARY

Background

Crumb rubber modifier (CRM), a by-product of the scrap tire industry, is introduced into asphalt binders by a wet process or into asphalt mixtures by a dry process. In both, the crumb rubber is expected to substitute for SBS (styrene-butadiene-styrene) in the polymer-modified asphalt binder normally required by the Georgia Department of Transportation (GDOT) to produce performance-grade (PG) 76-22 in the following types of hot mix asphalt (HMA): porous European mix (PEM), stone matrix asphalt (SMA), and polymer-modified 12.5-mm Superpave mixtures. GDOT has paved several highway sections using dry-processed rubberized PEM and SMA. In 2011, phase 1 of a "Comprehensive Evaluation of the Long-Term Performance of Rubberized Pavements" was launched. This preliminary study, based on visual inspection of the pavements and evaluation of core samples, determined density, permeability, Marshall stability, and flow. Phase II was a comprehensive study comparing the long-term durability of both dry- and wet-processed PEM and SMA to that of mixtures using hybrid and SBS-modified binders. The interaction of CRM and asphalt in the dry process was compared with that in the wet process.

Major Findings

1) The G*/sin (σ) of unaged rubberized asphalt binder increased 14% and 20%, respectively, when 3% and 6% doses of the cross-link agent, transpolyoctenamer (TOR) polymer were added. The absolute difference in failure temperatures for binders taken from the top and bottom of a tube was about 20% less than for those of the wet-processed control when 3% and 6% doses of TOR were added to PG 67-22 asphalt.

2) By following GDOT 114 and 123, PEM and SMA incorporating either dry- or wet-processed CRM binders or hybrid and SBS-modified binders can be successfully designed. The volumetric, rutting, moisture susceptibility, drain-down, and Cantabro loss properties of the designed PEM and SMA met GDOT's requirements, although the rutting depths of PEM and SMA with both dry- and wet-processed CRM were higher than those of control SBS.
3) The dynamic modulus, |E*|, of PEM and SMA with dry-processed CRM did not differ significantly from that of other PEMs and SMAs, regardless of whether samples were unaged or aged for 1,000 or 3,000 hours.
4) No significant difference was found in |E*| between unaged and 1,000-hour aged samples but 3,000-hour aging had a significant effect on |E*| at low frequency or high temperature for both PEM and SMA.
5) The fatigue life of unaged rubberized PEM and SMA modified using either the dry or wet process was similar but generally shorter than that of mixtures using hybrid and SBS-modified binders.
6) After 3000-hours of aging, the fatigue life of the dry-processed rubberized SMA was still similar to that of wet-processed but shorter than that of hybrid and SBS modified SMA, regardless of strain and stress levels or test temperatures. In most of the fatigue tests, aged PEM samples failed at the two ends tested and were deemed unsuccessful.
7) Rutting and Cantabro loss in both dry- and wet-processed PEM and SMA were higher than in the control SBS- and hybrid-modified PEM mixtures, regardless of aging duration.
8) The interaction between CRM and asphalt binder was evident during the production and paving stages based on DSR, GPC, FTIR, and AFM results,

regardless of mixture type.

9) Values of G*sin(δ) differed significantly among the four asphalt binders extracted from PEM and SMA after weathering for 1,000 and 3,000 hrs, regardless of mixture type.

10) The dry- and wet-processed and SBS-modified control PEM pavements in SR 247 Macon exhibited good characteristics after three years of service.

CHAPTER 1 INTRODUCTION

1.1 Background and Objectives

Crumb rubber modifier (CRM) is introduced into asphalt binders by a wet process or into asphalt mixtures by a dry process. A literature review indicates that wet-processed samples better resisted permanent deformation and fatigue than conventional mixtures (Hicks et al. 1995; Huang et al. 2002; Hunt 2002; Kaloush et al. 2003; Love 2014; Lyons 2012; Oliver 2000). In the wet process, lengthy blending at high temperature provides sufficient interaction between the asphalt and CRM to result in good properties. In the traditional dry process, the shorter reaction period made CRM and asphalt interaction negligible (Rahman et al. 2004).

However, recent laboratory research indicates that asphalt/CRM interaction in the dry process during mixing, transporting, and paving is much greater than previously thought (Hernández-Olivares et al. 2009; Lopez-Moro et al. 2013; Rahman et al. 2003; Singleton 2000). Field performance of dry-processed CRM mixtures has been inconsistent, with service life varying from two to twenty years (Rahman et al. 2004), depending on the type of mixture and paving method.

Asphalt mixtures with smaller CRM (less than 30 mesh), lower content (about 10% of the asphalt binder mass), and an added cross-link agent, transpolyoctenamer (TOR) polymer, were used in dry-processed test pavements on I-75 Valdosta (2009), I-20 Augusta (2009), and I-75 Perry (2007) in Georgia (Hines 2007; Shen & Xie 2012; Xie & Shen 2013). CRM was added to the asphalt concrete as a substitute for the SBS binder modifier normally required to produce PG 76-22 in two types of HMA: porous European mix (PEM) and stone matrix asphalt (SMA) (Shen & Xie 2012). Phase 1 of

this project investigated the performance of the dry-processed rubberized pavements after 3-7 years of service. To learn more, Phase 2 quickly followed to determine the:

1. durability of well-designed, wet- and dry-processed rubberized PEM and SMA in the laboratory after long-term weathering;
2. aging resistance of the binders recovered from rubberized PEM and SMA after long-term weathering;
3. interaction of asphalt with crumb rubber added using the dry process: do the rubbers modify the binder or the mixture?
4. performance of both wet- and dry-processed CRM PEM pavement sections from SR-247.

1.2 Report Organization

This report is divided into 11 chapters. Chapter 1 presents a general introduction. Chapter 2 documents the literature review. Chapter 3 describes the properties of rubberized asphalt binder; Chapter 4 summarizes the design of rubberized PEM and SMA. Chapter 5 summarizes findings on their dynamic moduli; Chapter 6, their fatigue life; Chapter 7, the effect of weathering on their performance. Chapter 8 describes the interaction between CRM and asphalt binder, and Chapter 9 summarizes the effect of weathering on their interaction. Chapter 10 summarizes the field inspection of pavement performance, and Chapter 11 presents conclusions and recommendations.

CHAPTER 2 LITERATURE REVIEW

2.1 Scrap Tires and Crumb Rubber Modifiers (CRM)

Scrap tires are discarded at an estimated rate of one per year per capita in the United States (EPA 2010). They are among the most problematic waste sources due to the large volume produced and their resistance to decay (see Fig. 2-1). Of the many ways to deal with them, retreading and recycling are environmentally friendly, while putting them into landfills is not. Recycling tire-derived aggregates and crumb rubbers for construction purposes is one practical solution (Mashaan et al. 2014).

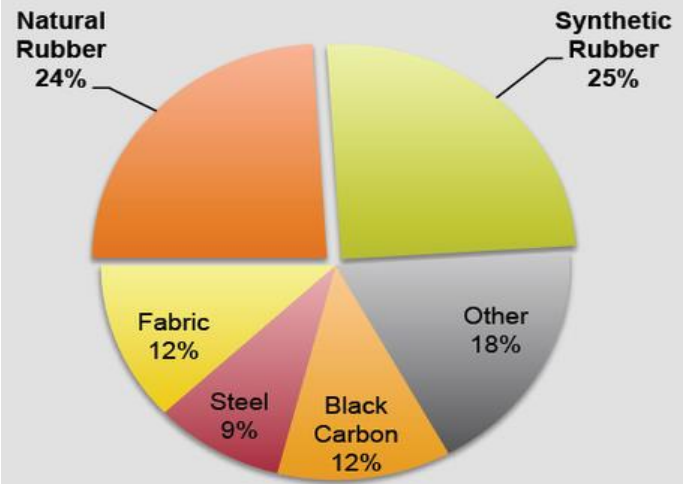

Figure 2-1. Raw materials of tires

Crumb rubber modifier (CRM), sometimes referred to as ground tire rubber (GTR), is used to modify asphalt binder for paving mixtures. Its addition improves the properties of the asphalt binder and the mixture (Presti 2013).

Two types of CRM are processed from scrap tires: ambient and cryogenic. Figure 2-2 shows the main difference in their microstructure (Shen & Amikhanian 2005). Ambient CRM has a porous or fluffy appearance, while cryogenic CRM is angular, with a smooth, cracked surface. Both have white particles, or spots, which are the reinforced steel put into tires and improve the performance of the base asphalt binder.

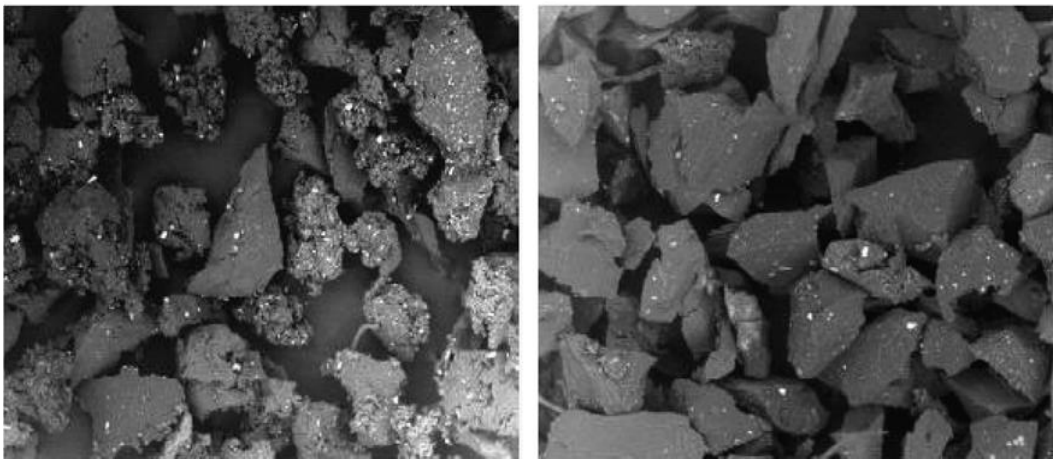

Figure 2-2. Ambient ground rubber (left); cryogenically fractured rubber (right) (Shen & Amikhanian 2005)

2.2 Use of CRM in Asphalt Binders and Mixtures

CRM can be incorporated into asphalt paving mixes using a wet or dry process. In the wet process, CRM particles are well mixed with a base binder to form an asphalt and rubber blend, which is then mixed with aggregate in a mixing chamber (drum or pugmill) at an asphalt plant to produce a rubberized asphalt mixture, following ASTM D 8 (1997). Figure 2-3 shows the steps in wet-processed crumb rubber (CR) modification of asphalt in a continuous blend system at an asphalt mix plant.

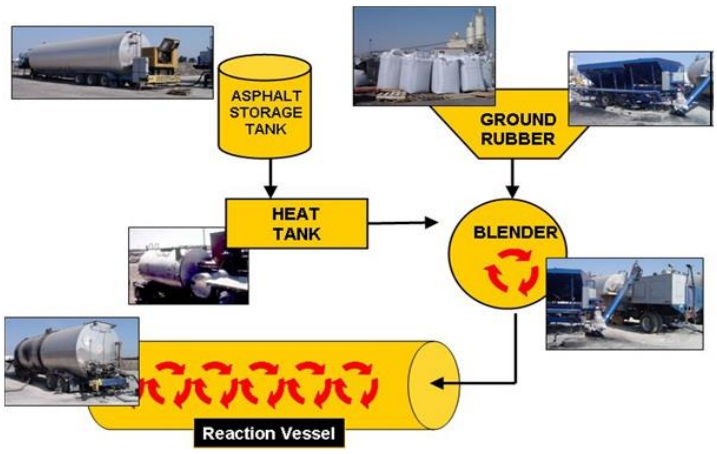

Figure 2-3. CR modification of asphalt in a continuous blend system (http://maxlinktyrerecycling.com)

In the dry process, CRM particles are introduced into the drum simultaneously with the aggregate; then they are mixed with injected asphalt binder to produce a rubberized asphalt mixture. CRM binders can be applied to gap-graded, dense-graded, and open-graded mixtures (Heitzman 1992). Figure 2-4 shows the feed system used for the dry process (Hines 2007).

Figure 2-4. Feed system for the dry process (Hines 2007)

In 1950, the use of CRM in asphalt as a stress-absorbing membrane interlayer (SAMI) was first reported. By 1975, CRM was successfully incorporated into asphalt mixtures, and in 1988, rubberized asphalt was defined in the American Society for Testing and Materials (ASTM) D8 and later specified in D6114-97. In 1992, the 1960s patent for the McDonald process expired; the material became a part of the public domain. From 1991-1997, the US Intermodal Surface Transportation Efficiency Act (ISTEA) mandated its widespread use. The concept started to make a "quiet comeback" (Kuennen 2004), and considerable research has been conducted worldwide to validate and to improve technologies related to rubberized asphalt pavements.

2.2.1 Dry process

The industry uses three main types of dry-process technology:

PlusRide (patented)

Patented in 1950, in PlusRide technology, 1 to 3 percent of granulated rubber per total mix weight was added to aggregate in a hot mix central plant operation before adding asphalt binders (Rahman, 2004). Rubber particles range from 4.2 mm (1/4 in) to 2.0 mm (No. 10 sieve). The target air-void content of the asphalt mix is 2 to 4 percent, which is usually attained when the asphalt binder content is in the 7.5 to 9 percent range. The process is normally applied for gap grading and improving mixture stability.

Generic Dry Technology (not patented)

The generic dry process, also known as the TAK system, was developed in the late 1980s to early 1990s. Up to 3 percent by mass of the weight of mixtures is added to a dense graded mixture. Generally, this system uses less than 1 percent of the weight of the mixture and smaller crumb rubber than PlusRide. The size of the rubber particles for this process ranges from 2 mm to 180 μm, and aggregate gradations of the mixture are conventional in both dense and gap.

Chunk Rubber (not patented)

The US Army Corps of Engineers' Cold Region Research Engineering Laboratory (CRREL) developed this method in the late 1970s and early 1980s to evaluate the ice-disbonding characteristics of asphalt paving materials. The rubber particles typically range in size from 4.75 to 9.5 mm, and mixture gradations must be adjusted to provide space in the aggregate matrix for the substitute rubber particles. Although this process has not yet been field evaluated, laboratory wheel test results indicate that the higher rubber content could increase the incidence of ice cracking (Oliver 1981).

Summary of application performance by state. In the past few years, several states have applied dry-processed CRM asphalt mixtures, as summarized in Table 2-1.

Table 2-1. Some applications of dry-processed CRM asphalt mixtures by state

State	Method/type of mixture	Observations
Alabama	CRM/AC-10	• No significant difference from wet mixes in resilient modulus, indirect tension, and dynamic creep (Buncher1995)
Alaska	PlusRide gap-graded	• Deeper ruts and faster rut accumulation rate than conventional HMA mixes' (Saboundjian 1997)
Arkansas	AC-30 (1, 2, 3% by wt. of aggregate)	• Slightly better if rubber was pretreated with extender oil prior to mixing • Inferior to control and wet-processed mixtures (Gowda 1996; Khalid 2012)
Caltrans	PlusRide /dense-graded	• 2 of 4 dry-process projects out-performed conventional mixtures; one was comparable; one was not properly designed and required an overlay (Van Kirk 1991)
Georgia	PEM/SMA/Superpave 10% CRM with mesh -30/TOR	• Performed as well as SBS mixtures after 3-5 years' service based on visual inspection • Core samples did not differ significantly in density, permeability, and Marshall stability from SBS control. Cantabro loss was slightly greater
Illinois	HMA	• Lower performance than conventional asphalts (Volle 2000)
Louisiana	PlusRide/gap-graded	• Lower initial structural capacities (DYNAFLECT structural number) than the conventional dense-graded control
Minnesota	PlusRide/dense-graded overlay	• Performed well, with improved crack reflection • Benefits did not offset higher cost (Turgeon 1989)
New York	Overlay project	• After 3 years, no economic or structural benefit (Shook 1990)
Oregon	PlusRide	• Poor performance (premature degradation) • Cost 50-100% more than conventional pavements (Hunt 2002)
South Carolina	PlusRide	• Pelham Road has deteriorated in the 8 years since it was paved • Other asphalt rubber projects appear to be in satisfactory condition (Amirkhanian 2001)
Texas	Generic dry process/ dense-graded (0.5% by wt. of aggregate)	• Less propensity for rutting but possibly more cracking • Remained in discrete particles (Rebala 1995)
Washington	PlusRide	• The performance of 7 sections ranged from excellent to immediate failure • Overall, did not improve performance (Dong 2001)

2.2.2 Wet process

In the 1960s, Charles McDonald invented a wet process that fully mixes CRM with asphalt binder. It now uses two production systems: continuous blend and terminal blend. In the former, the asphalt binder and rubber are blended in separate tanks; the latter uses industrial mixing plant units.

The properties of wet-processed CRM-modified binders depend on 1) mixing conditions, including temperature, duration, and mixer type (Huffman 1980); 2) type of binder; 3) type of CRM (ambient or cryogenic, mesh size, percentage) (Hicks, 2000) and 4) type of additives. At high temperatures, they perform better than base asphalt binder.

Table 2-2. Some applications of wet-processed CRM asphalt mixtures by state

State	Applications	Conclusions
Alabama	PG 67-22 +11% CRM (#30-40 mesh)	• After one year, rubberized and conventional mixtures show no practical difference in field performance with regard to rutting and texture (Richard 2014)
Arizona	Gap-graded HMA with 20% CRM	• Asphalt rubber reduced reflective cracking and improved rutting performance and smoothness • Less average maintenance cost (George 1999)
Arkansas	5, 10, and 15% CRM	• Increased rutting resistance • Resilience and tensile properties were not enhanced when tested at 25 ℃ • Performance-related properties did not differ significantly (Gowda 1996)
Caltrans	18% ± 1% CRM/gap and dense-graded	• Over 7+ years, asphalt mixes with 15% CRM outperformed all other mixes in crack reflection mitigation (Holikatti 2013)
Florida	10% CRM	• Routinely used in friction courses and SAMI layers since 1994 • Better resistance to rutting and cracking than that of unmodified binders (Page 1992)
Illinois	No more than 5 pounds of CRM per ton of HMA	• No substantial difference in rut values between CRM and control sections (Illinois DOT 2000)
Kansas	18% CRM MacDonald process	• Rubber did not inhibit crack development in the higher density mixes (Fager 1992) • None of the rubber projects have rutted
Louisiana	5% Neste Wright Wet Process, 10% Rouse Wet Process, 17% Arizona Wet Process, 16-mesh CRM	• The conventional mixtures exhibited higher laboratory strength characteristics than the CRM mixtures • Better performance indices (rut depth, fatigue cracks, IRI numbers) than the corresponding control sections after 5-7 years of traffic (Huang 2002)
Minnesota	20%CRM	• Wear courses exhibited less cracking than the control sections (Turgeon 1989)
New Mexico	OGFC	• Better or comparable to conventional non-CRM materials • CRM OGFC pavements performed well in the short (2-4 years) and long terms (5-9 years) (Bandini 2011)
Oregon	ISI ARC/open-graded	• Varying results (Hunt 2002)
Pennsylvania	Thin overlays Chip seals and/or fog seals	• Enhanced signs of wear and cracking • Performance unsatisfactory in comparison to the DOT standard ID-2 wearing course (Lucas 1998)

(continued on next page)

Table 2-2. (Continued)

State	Applications	Conclusions
Texas	Chip seal SAM Terminal blend Open-graded	• The mix raveled severely (Estakhri 1992) • SAMs exhibit improved resistance to alligator cracking and raveling, but resistance to shrinkage cracking was not improved by chip seals • AC-20-5TR, a terminal blend, had excellent chip retention and resistance to flushing and tracking • Most open-graded mixes improved cracking resistance and prevented binder drain-down in permeable mixes
Washington	SAM/SAMI OGFC	• Did not justify the added expense of their construction • OGFC exhibited good-to-very-good performance, except for one bridge deck overlay (Swearingen 1992)

2.2.3 Wet process, terminal blend

Terminal blend, a type of CRM binder manufactured in an asphalt terminal, is typically sized to a -30 mesh, or smaller than 0.6 mm, and wet-processed to improve storage stability. In some systems, CRM is completely digested in asphalt binder with no particulate matter remaining. Sometimes, polymers are added with fine CRM, typically at 5-10% CRM weight of total binder. Terminal blends look different from traditionally produced asphalt rubber binders (Fig. 2-5).

Figure 2-5. Asphalt rubber (left); terminal blends (right)

2.2.4 Some applications of CRM overseas

Since 1981, CRM technology has been widely reported in Austria, Belgium, the Czech Republic, France, Germany, Greece, Italy, the Netherlands, Poland, Portugal, Spain, Sweden, and the UK. The Czech Republic, Italy, Portugal, Spain, and Sweden have the greatest number of applications.

On the basis of early positive experiences, Brazil is strongly investing CRM technology for road pavement (Widyatmoko 2007). In Asia, Taiwan adopted the Arizona DOT gap-graded and open-graded rubberized asphalt mixtures for flexible pavement rehabilitation (Hsu 2011), and Beijing used the technology in new and maintenance work to prepare for the 2008 Olympics (Bressette 2008).

2.3 Mechanisms of CRM Binders

2.3.1 Interaction between asphalt and CRM in the dry process

In both the dry and wet processes, CR modifies the properties of the resulting binders (TFHRC 2005), although it is sometimes used to replace fine aggregates (Takallou 2003; Visser 2005). In the dry process, some interaction takes place during the production-to-laying stages depending on CRM gradation (Buncher 1994; Green 1997), but it was deemed insignificant compared to that in the wet process. Later research demonstrated a greater increase in the stiffness of dry-processed rubberized mixtures after short-term age conditioning compared to conventional mixtures (Moreno 2011; Singleton 2000). A microscopy study indicated that the rubber-bitumen interaction in the dry process changed the shape and porosity of CRM particles (Javier 2013).

2.3.2 Interaction between asphalt and CRM in the wet process

Many studies have focused on understanding the mechanisms of CRM-asphalt binder interaction (Gualliard 2004; Miknis 1997; Shen & Amirkhanian 2005; Tortum et al. 2005). It was traditionally not deemed chemical but attributed to CRM swelling as it absorbed the light part of the asphalt binder. Other studies claimed that the increase in binder viscosity could not be accounted for by rubber swelling alone (Bahia 1994). In fact, the main mechanism is the rubber particles' absorption of light-weight fractions, which causes the residual binder to stiffen (Abdelrahman 1999; Airey 2003). Since the swelling process reduces the free space between rubber particles, they have less freedom to move into the binder matrix, causing its mass viscosity to increase with time.

2.4 Performance Properties of CRM Asphalt and Mixtures

2.4.1 CRM asphalt binder

Viscosity

The most pronounced effect of adding CRM is the increased viscosity of the CRM binder. Viscosity has typically been used to measure the interaction of CRM binders and the compatibility of different combinations of CRM and asphalt binder (Bahia 1994; 1995; Billiter 1996; Chehovit 1993; Roberts 1989; Rosner 1981; Shuler 1985; West 1998). While increasing a binder's viscosity indicates better interaction and compatibility, the excessively high binder viscosities that may result from CR modification have disadvantages, including difficulty in pumping the binder and mixing and compacting the HMA (Oliver 1982).

High-temperature performance

Use of CRM in asphalt binders improves pavement properties at high temperatures. The dynamic shear rheometer (DSR) has been used to measure CRM binders'

resistance to shear deformation (Abdelrahman 1999; Buncher 1995; Tayebali 1997). In general, the same factors influence both CRM binder viscosity and high-temperature properties.

Low-temperature performance

Using a bending-beam rheometer (BBR), CRM binders have been found less stiff and less likely to fail at low temperatures.

2.4.2 CRM asphalt mixtures

Dynamic Modulus

Dynamic modulus is a key material property that determines strains and displacements in pavement structure (NCHRP 2003; Witczak 2002). However, few researchers have measured the dynamic moduli of crumb rubber asphalt mixes. Bennert et al. (2004) reported that the stiffness of AR-HMA was similar to that of PG76-22 at high test temperatures and much less at the low test temperature. Kaloush et al. (2003) indicated that an asphalt rubber gap-graded mix provides better resistance to low-temperature cracking (softer modulus at lower temperatures) and permanent deformation (stiffer modulus at higher temperatures). A simple performance test (SPT) indicated that the dynamic behavior of CRM asphalt mixtures was better than that of the standard asphalt mixture (Dong et al. 2012).

Fatigue resistance

Rubberized mixtures had better fatigue behavior than the control (Dong 2011; Huang 2009; Kök 2013; Mashaan 2013; Vahidi 2014; Zeiada et al. 2012), depending on rubber content and gradation, aggregate gradation, mixing temperature, and curing time prior to compaction. Increasing an asphalt mixture's rubber content using a coarse gap-graded particle size distribution resulted in better fatigue resistance than a

rubber-modified, dense-graded mixture (Takallou 1986). Curing conditions had mixed effects: some prolonged fatigue life (Pinheiro 2003; Takallou 1986); others made no change (Airey et al. 2003).

Rutting resistance

Research indicated in most cases that rubberized mixtures had greater rutting resistance than conventional control mixtures (Airey 2004; Fontes et al. 2010; Lee 2008; Olivares 2009).

2.5 Findings and Further Studies

CRM asphalt binder is used in dry or wet processes. Among dry processes, use of the patented PlusRide dominated; most field observations have been negative, although they varied with CRM type, percentage, and mesh size. Of the many wet-processed rubberized asphalt mixtures, most performed better than base asphalt binder and the same as SBS-modified asphalt.

The following areas where data are lacking should be studied before implementing CRM technology in Georgia:

- Long-Term Pavement Performance (LTPP) for durability and aging;
- mechanism of the CRM-asphalt binder interaction, especially in the dry process;
- E* and fatigue performance, the key inputs for the new Mechanistic-Empirical Pavement Design Guide (MEPDG), for CRM asphalt mixtures; and
- comparative performance of rubberized and traditional mixtures: dry processed, wet processed, and SBS-modified PEM.

CHAPTER 3 PROPERTIES OF RUBBERIZED BINDER

3.1 Introduction

The performance properties of rubberized asphalt binders depend on binder source, grade, manufacturing method (ambient or cryogenic), mesh size, percentage mixed, and mixing conditions related to temperature range, time, and agitation speed. Newer technologies add cross-linking agents, such as TOR, to improve stability, uniformity, and workability, but its influence on other properties of rubberized asphalt binder, such as high- and low-temperature properties and separation and aging resistance, is unclear.

This chapter investigates the effect of different doses of TOR on these properties. PG 67-22 and PG 64-22 base asphalts were mixed with three doses of CRM and TOR. DSR, BBR, and separation tests were then conducted on unaged and aged rubberized asphalt binder to evaluate the effects (Fig. 3-1).

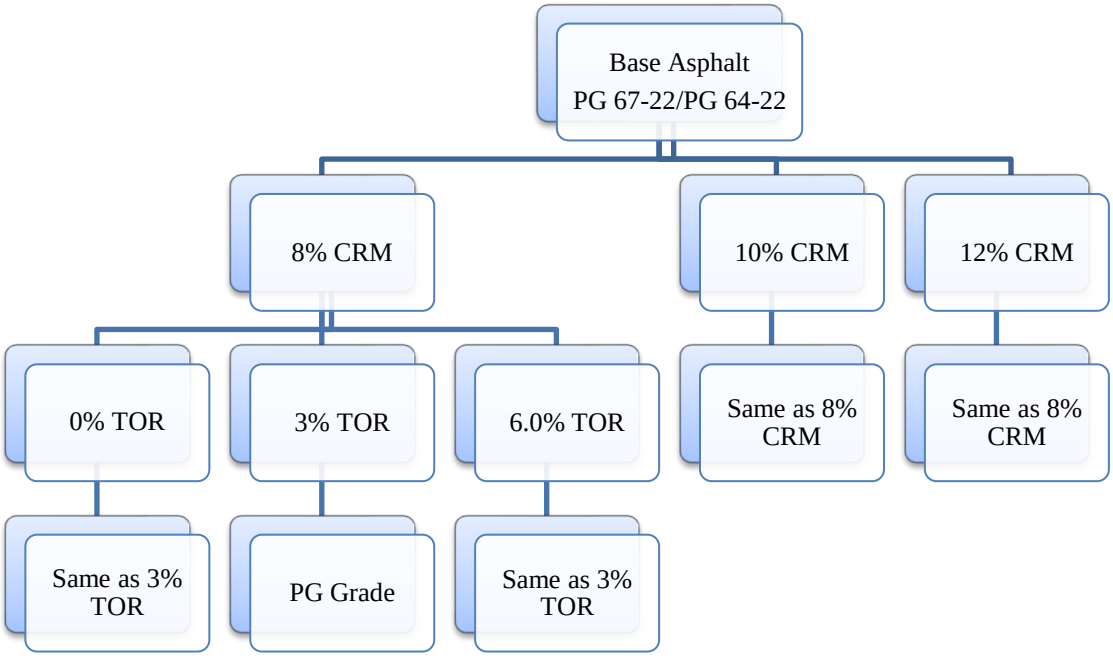

Figure 3-1. Flow chart for testing rubberized asphalt binder properties

3.2 Materials and Test Procedures

The materials used include an ambient grind of 30-mesh CRM (Fig. 3-2 left), two types of base asphalt binder (PG 67-22 and PG 64-22), three doses of CRM (8%, 10%, 12%), and three doses of TOR (0%, 3%, 6%) (Fig. 3-2 right). The rubberized asphalt binder was mixed at 170 °C and 900 RPM for 45 minutes in the laboratory. Table 3-1 shows CRM gradation.

Figure 3-2. CRM (left) and TOR (right)

Table 3-1 CRM Gradations

Sieve	No. 16	No. 30	No. 50	No. 100
Percent Passing (%)	100	99.0	40.4	7.7

Aging was accelerated in the standard rolling thin-film oven (RTFO) at 163 ºC for 85 minutes and a pressure-aging vessel (PAV) at 2.1MPa, 100 ºC for 20 hours to generate aged rubberized asphalt binders (Figs. 3-3; 3-4).

The high-temperature rheological properties of each rubberized asphalt binder were measured using DSR (Fig. 3-5) in accordance with AASHTO T315. A one-millimeter gap for each was used based on NCAT Report 12-09. Each binder's complex shear modulus (G*) and phase angle (δ) were measured at 76 ºC.

BBR testing (Fig. 3-6) was used to evaluate the creep-stiffness properties of the

aged binder at -12 ºC in accordance with AASHTO T313. The measured creep stiffness and m-value were applied to describe aged rubberized asphalt binders.

Figure 3-3. Rolling thin-film oven

Figure 3-4. Pressure-aging vessel

Figure 3-5. Dynamic shear rheometer

Figure 3-6. Bending-beam rheometer

The separation tube test was performed to determine CRM tendency to separate from rubberized asphalt binder during static, heated storage. Testing was conducted in accordance with ASTM D7173-11, Standard Practice for Determining the Separation Tendency of Polymer from Polymer Modified Asphalt. Figure 3-7 shows the specimens.

Figure 3-7. Separation tube test

3.3 Results and Discussion

3.3.1 Effect of TOR on high-temperature properties

To evaluate the performance of rubberized asphalt binder with TOR at high service temperatures, a complex shear modulus and phase angle were measured for both unaged binders and RTFO-aged residue.

Unaged rubberized asphalt binder

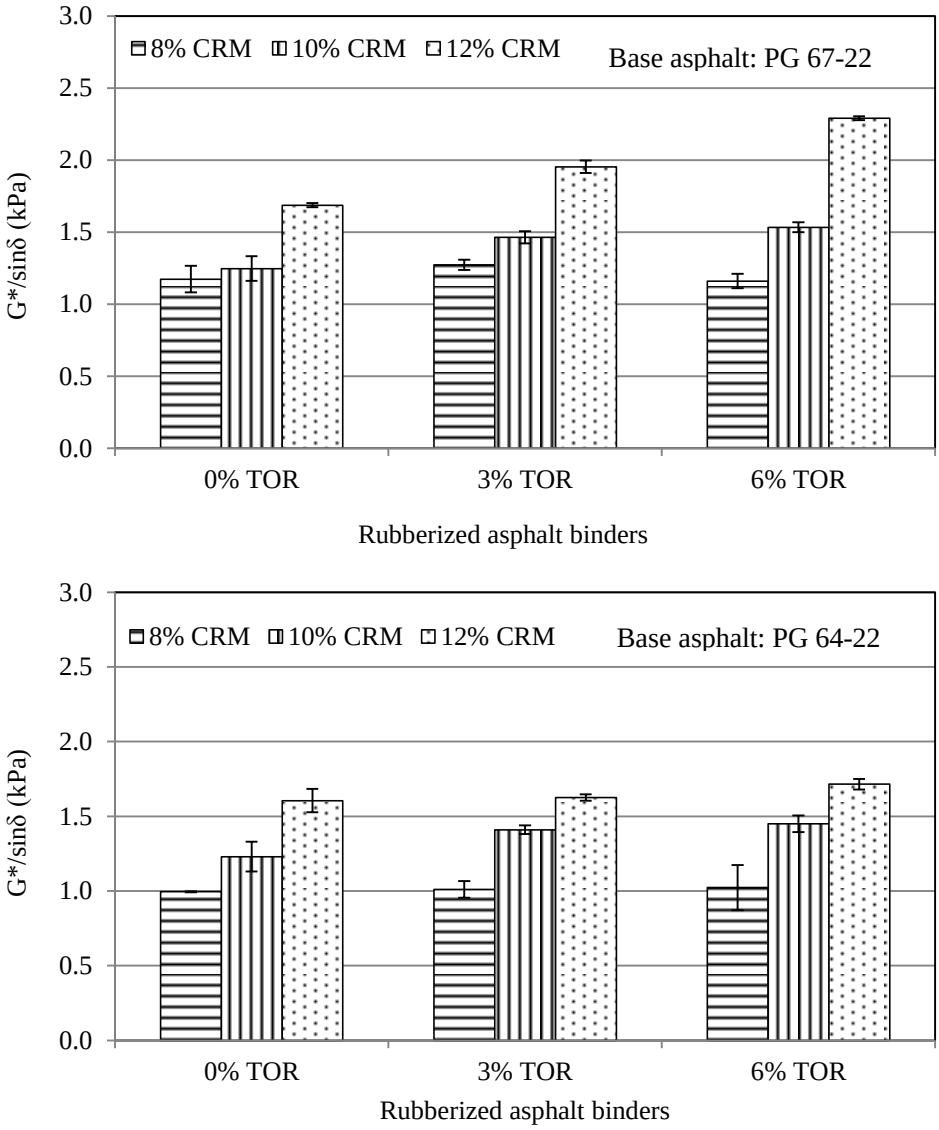

Figure 3-8. G*/sin(δ) of unaged rubberized asphalt binder at 76 ºC

Figure 3-8 shows the values of G*/sin(δ) and phase angle at 76 ºC for the binders

tested. In general, the G*/sin(δ) of unaged rubberized asphalt binder increased with TOR dose, regardless of CRM dose added and grade of base asphalt binder. G*/sin(δ) values also increased as the CRM dose increased from 8% to 12%, regardless of TOR dose added and grade of the base asphalt binder (Fig. 3-8).

Many previous laboratory and field studies have shown that rubberized asphalt binder generally has a higher G*/sin(δ) than base asphalt binders. Adding TOR did not change the trend; CRM content still increases the G*/sin(δ) of rubberized asphalt binder. Adding TOR only increased it further.

For PG 67-22 asphalt with 8% CRM tested with 3% and 6% TOR, G*/sin(δ) values were 8.5% and 0.9% higher, respectively, than those of the controls (CRM asphalt binders without TOR). For those with 10% CRM, the G*/sin(δ) of binders tested with 3% and 6% TOR was, respectively, 17.4% and 23.0% higher than the controls'. For those with 12% CRM, the G*/sin(δ) of binders tested with 3% and 6% TOR was, respectively, 15.8% and 35.8% higher than the controls'. G*/sin(δ) increased, on average, 14% and 20%, respectively, with 3% and 6% doses of TOR.

For PG 64-22 base asphalt binder, G*/sin(δ) increased on average 4.3% and 6.7%, respectively, with the addition of 3% and 6% TOR. Note that TOR had more influence on G*/sin(δ) values when a higher percentage of CRM and a high-temperature-grade base binder were used.

To determine whether TOR's effect on G*/sin(δ) was statistically significant, an analysis of variance was performed. Table 3-2 shows that TOR had no significant statistical effect on the G*/sin(δ) of any rubberized asphalt binder with PG 64-22 but did with PG 67-22 and higher rubber content (10% and 12%).

Table 3-2. Statistical analysis of the G*/sin(δ) of unaged rubberized asphalt binders

Base Asphalt	CRM (%)	TOR 0% ~ TOR 3%	TOR 0% ~ TOR 6%	TOR 3% ~ TOR 6%
PG 67-22	8%	N	N	N
	10%	Y	Y	N
	12%	Y	Y	Y
PG 64-22	8%	N	N	N
	10%	N	N	N
	12%	N	N	N

Note: Y: P-value < α = .05 (significant difference); N: P-value > α = .05 (no significant difference).

The phase angle of the unaged rubberized asphalt binders decreased as the dose of TOR increased from 0% to 6%, regardless of CRM dose added or the grade of base asphalt binder. It also increased as CRM dose increased from 8% to 12%, regardless of TOR dose added and the grade of the base binders (Fig. 3-9).

Previous studies have established that rubberized asphalt binders generally have a lower phase angle than base asphalt binder. However, adding TOR helps to decrease their phase angle. When PG 67-22 was used as the base for unaged rubberized asphalt binder using 8% CRM, the phase angles of the binders tested with 3% and 6% TOR were 1.5% and 1.0% lower, respectively, than controls'. At 10% CRM, they were 0.5% and 0.7% lower, respectively; and at 12% CRM, 2.7% and 3.8% lower, respectively. Average phase angle decreased 1.6% or 1.8% at a 3% or 6% dose of TOR.

When PG 64-22 base asphalt binder was used, phase angles decreased an average of 0.5% and 0.8% at a 3% and 6% dose of TOR, respectively. Obviously, TOR had a greater effect on phase angle when a higher percentage of CRM was used. The grade of the base asphalt binder did not seem to affect the sensitivity of the phase angle of the rubberized asphalt binders with TOR.

To determine whether TOR has a significant effect on the phase angle of unaged rubberized asphalt binders, an analysis of variance was performed. Table 3-3 indicates that TOR had no significant influence on binders with PG 64-22 but did with PG 67-22 and 12% crumb rubber.

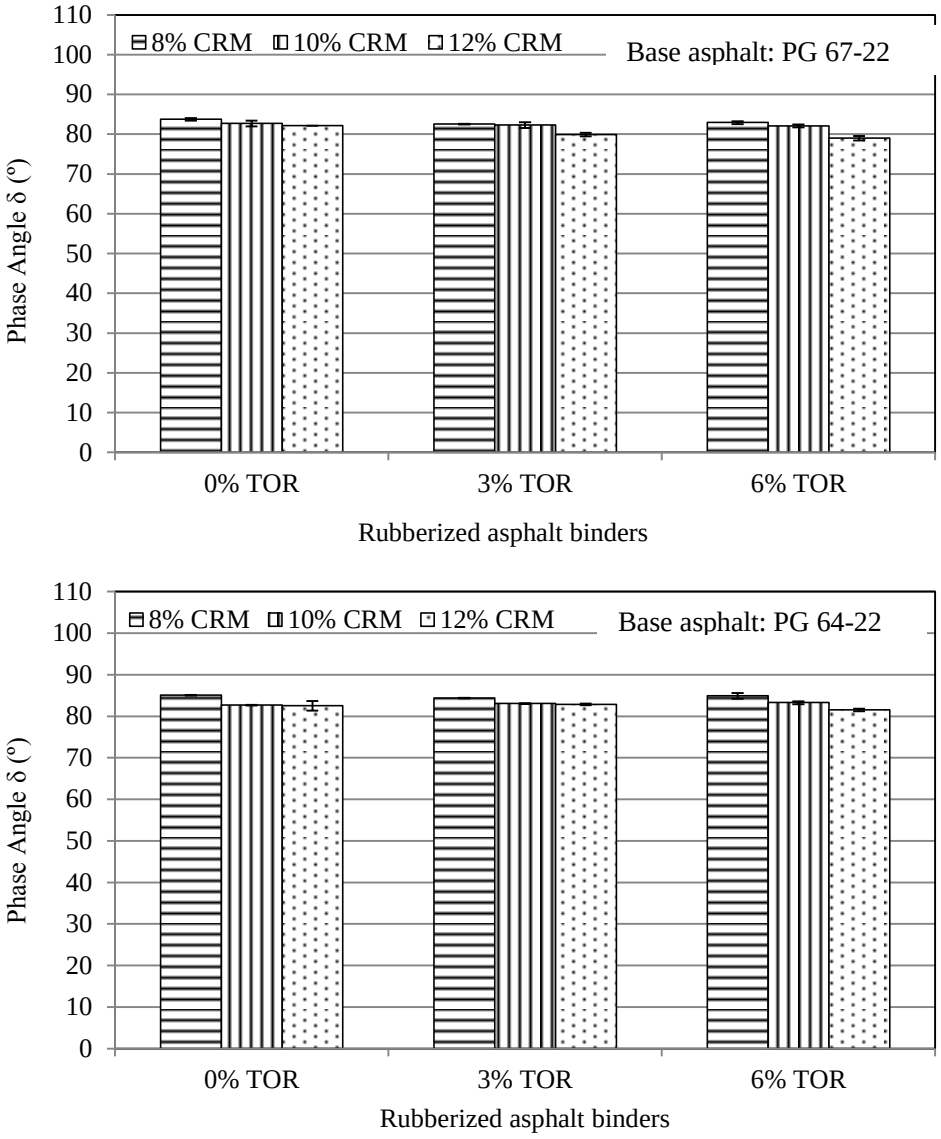

Figure 3-9. Phase angle of unaged rubberized asphalt binders at 76 ºC

Table 3-3. Statistical analysis of the phase angle of unaged rubberized asphalt binders

Virgin Binder	CRM (%)	TOR 0% ~ TOR 3%	TOR 0% ~ TOR 6%	TOR 3% ~ TOR 6%
PG 67-22	8%	N	N	N
	10%	N	N	N
	12%	Y	Y	Y
PG 64-22	8%	N	N	N
	10%	N	N	N
	12%	N	N	N

Note: Y: P-value < α = .05 (significant difference); N: P-value > α = .05 (no significant difference).

In addition, the fail temperature of rubberized asphalt binders increased by 9.1-15.2 ºC and 9.4-14.0 ºC for PG 67-22 and PG 64-22, respectively, with different doses of CRM and TOR (Figure 3-10). At fail temperature, the G*/sin(δ) of unaged

asphalt binder reached 1.0 kPa. Adding 12% CRM to the binder can increase it two PG grades (12.0 ºC) at high temperature, regardless of the type of base asphalt.

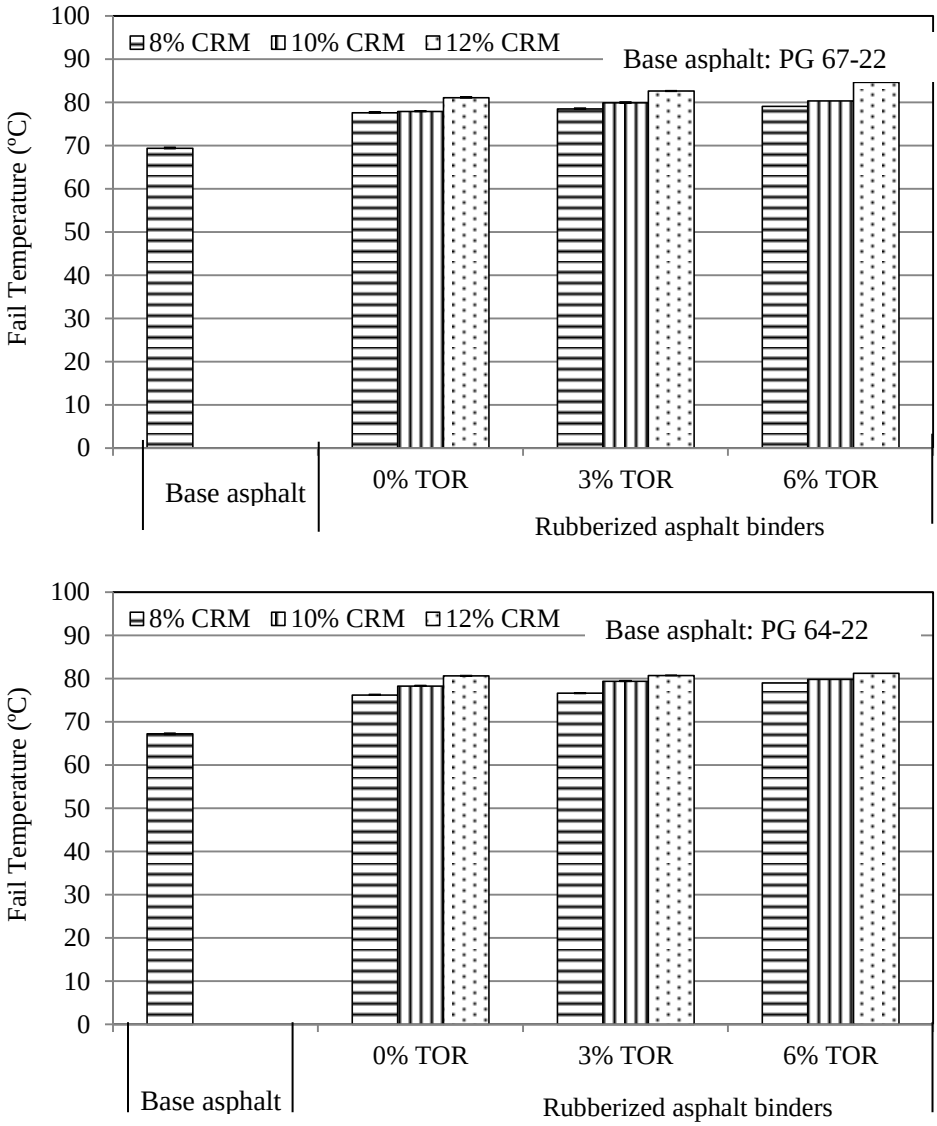

Figure 3-10. Fail temperature of unaged rubberized asphalt binders

RTFO-aged rubberized asphalt binder

RTFO residue showed a trend similar to that for unaged rubberized asphalt binder: the G*/sin(δ) increased with TOR dose, regardless of CRM dose. G*/sin(δ) values also increased as CRM increased from 8% to 12%, regardless of TOR dose and grade of base binder (Fig. 3-11).

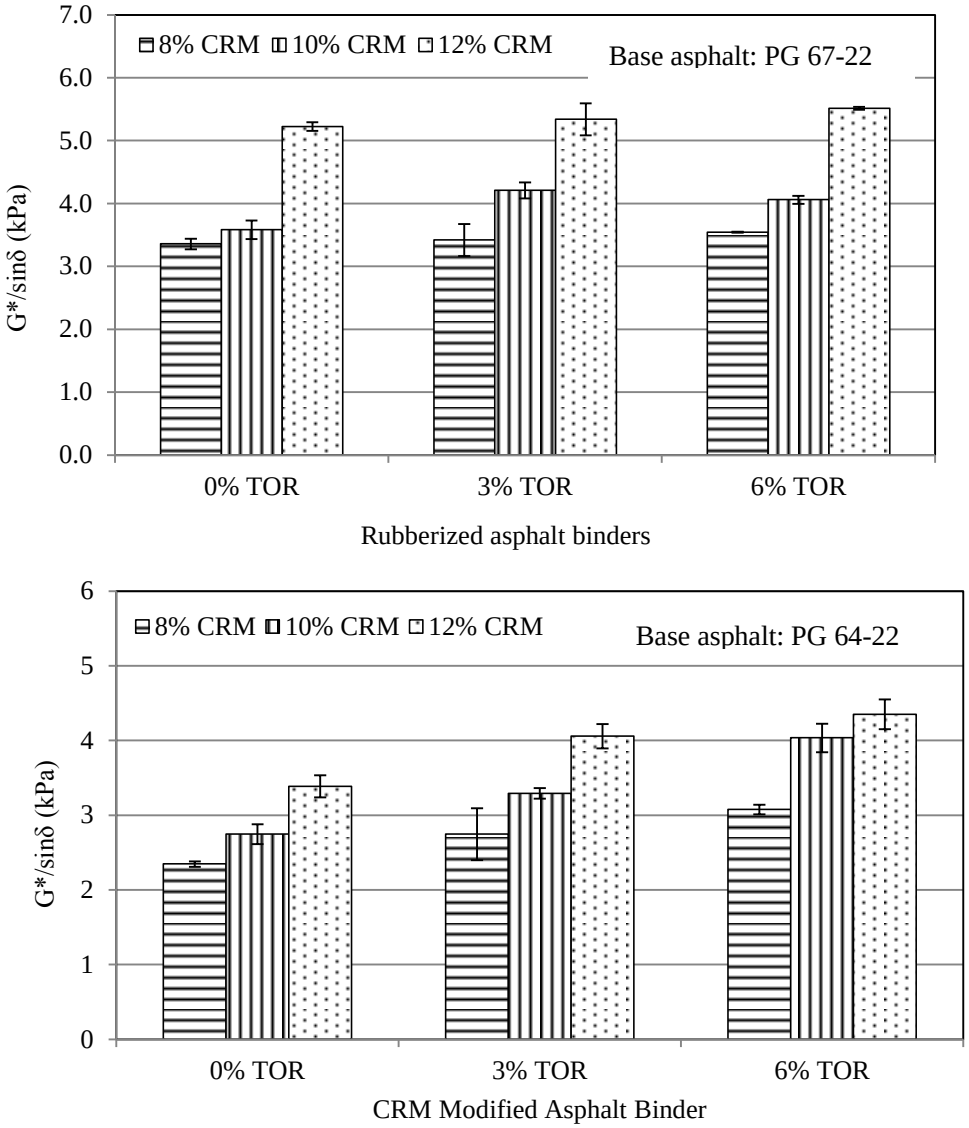

Figure 3-11. G*/ sinδ of RTFO residuals at 76ºC

For an RTFO-aged rubberized asphalt binder consisting of a PG 67-22 asphalt and 8% CRM, those tested with 3% and 6% TOR had G*/sin(δ) values 1.9% and 5.6% higher, respectively, than the controls'(CRM asphalt binders without TOR). For 10% CRM, the G*/sin(δ) values were 17.5% and 13.3% higher, and for 12% CRM, they were 2.2% and 5.6% higher. Average increases of 6.8% and 8.0 % in the G*/sin(δ) were found when 3% and 6% TOR, respectively, were added. When PG 64-22 was used, average G*/sin(δ) increases of 8.3% and 10.0% were found when 3% and 6% TOR, respectively, were added.

Similarly, the phase angle of RTFO-aged rubberized asphalt binder decreased as TOR dose increased, regardless of CRM dose and base binder grade. The phase angle increased as CRM dose increased from 8% to 12%, regardless of TOR dose and base binder grade (Fig. 3-12).

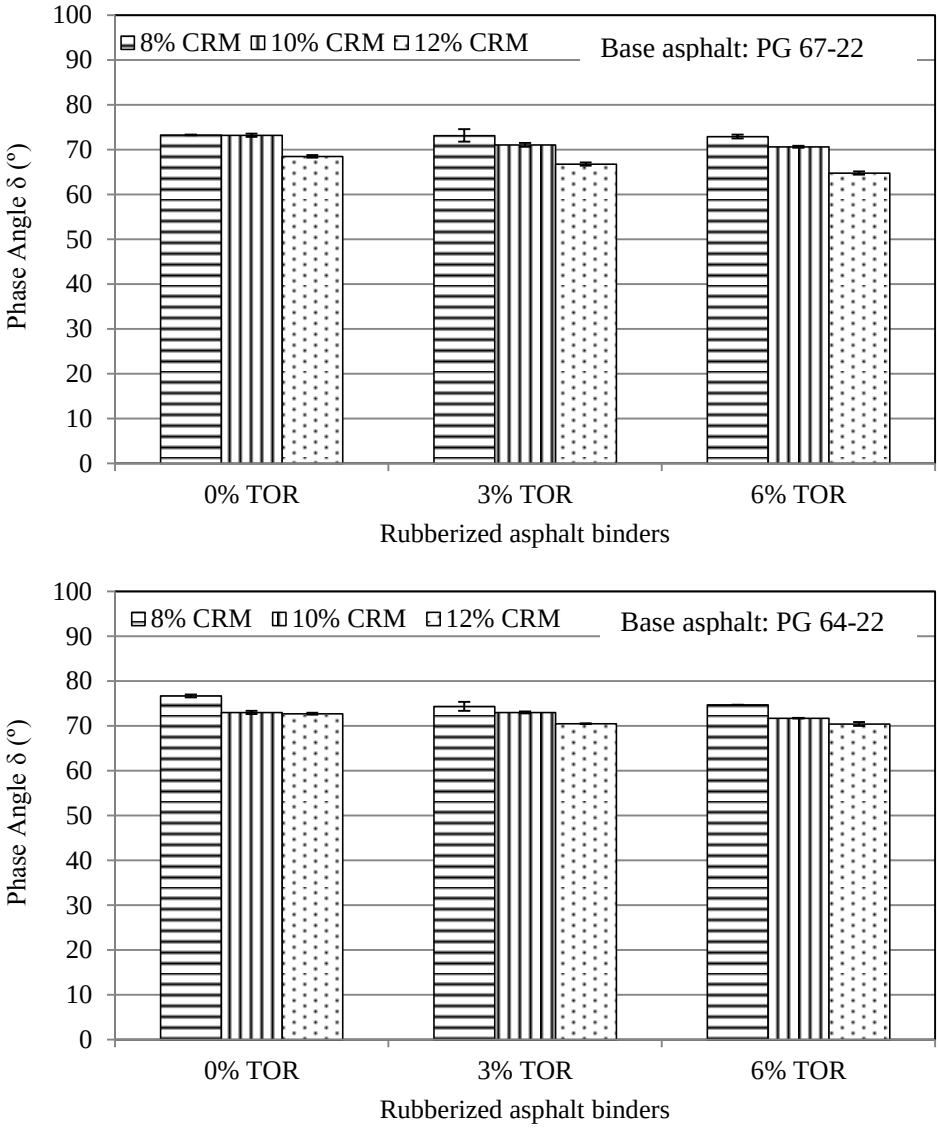

Figure 3-12. Phase angle of RTFO residuals at 76 ºC

For RTFO-aged, rubberized asphalt binder consisting of a PG 67-22 base binder and 8% CRM, the phase angles of the binders tested with 3% and 6% TOR were 0.2% and 0.5% lower, respectively, than the controls'. For 10% CRM, they were 2.9% and 3.5% lower, and for 12% CRM, 2.5% and 5.5% lower. Phase angles decreased on

average 1.6% and 3.1% with 3% and 6% TOR doses, respectively.

When PG 64-22 base binder was used, phase angle decreased on average 0.2% and 1.1% with 3% and 6% TOR doses, respectively. Obviously, TOR had a greater effect on phase-angle decrease at higher percentages of CRM. The grade of the base binder did not affect phase-angle sensitivity to TOR.

3.3.2 Effect of TOR on low-temperature properties

The BBR test is commonly used to measure the low-temperature properties of RTFO+PAV aged binders; that is, how much a binder deflects or creeps under a constant load at a constant low temperature. If creep stiffness is too high, the asphalt will be brittle; cracking is likely at low temperatures, and to prevent it, creep stiffness must be limited to 300 MPa. A high m-value is desirable because as the temperature drops, and thermal stresses accumulate, stiffness changes relatively quickly, and the binder tends to shed stresses that would otherwise lead to low-temperature cracking. Superpave binder specifications require a minimum m-value of 0.300.

The creep stiffness values for all CRM asphalts with TOR (Fig. 3-13) are less than 300 MPa, and the m-values of all CRM asphalts exceed 0.300 (Fig. 3-14). CRM reduces creep stiffness, but TOR increases it to some extent.

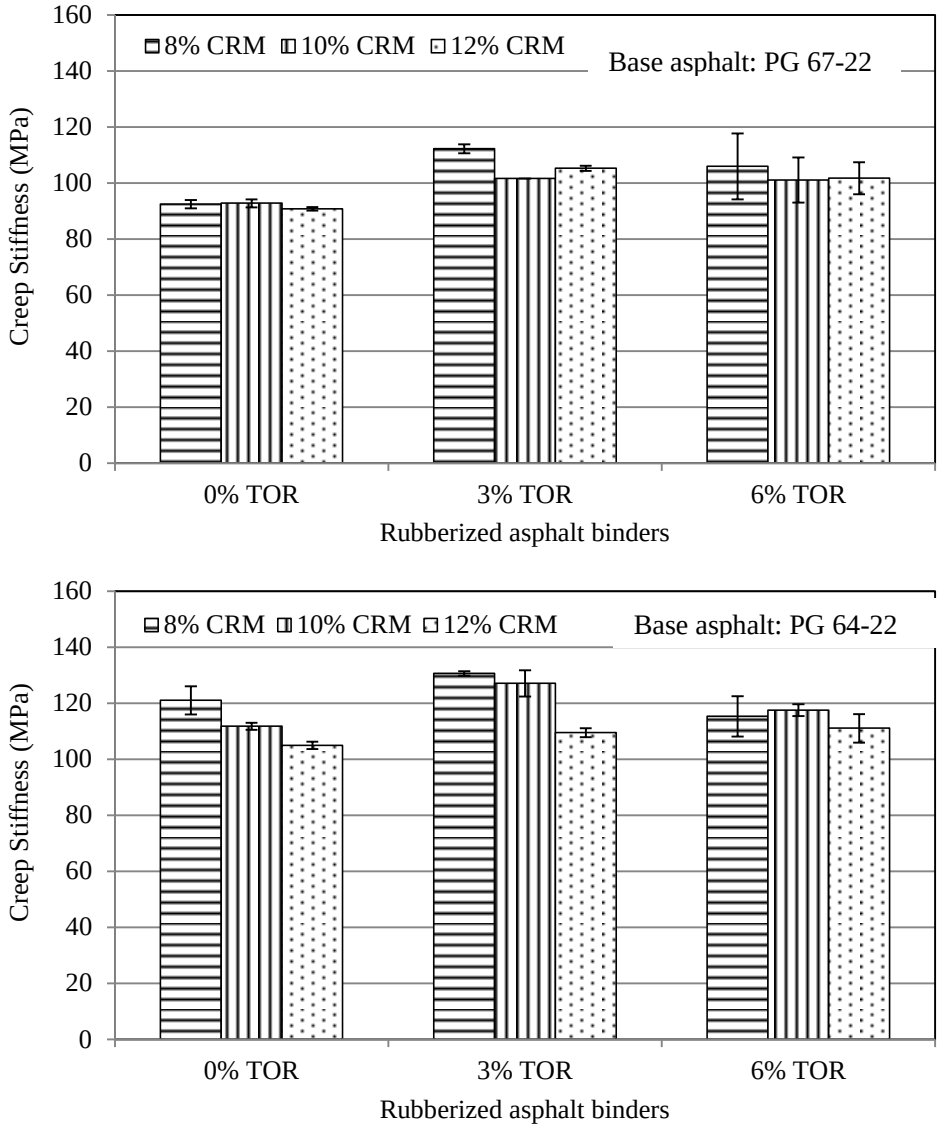

Figure 3-13. Creep stiffness of PAV-aged rubberized asphalt binder at -12 ºC

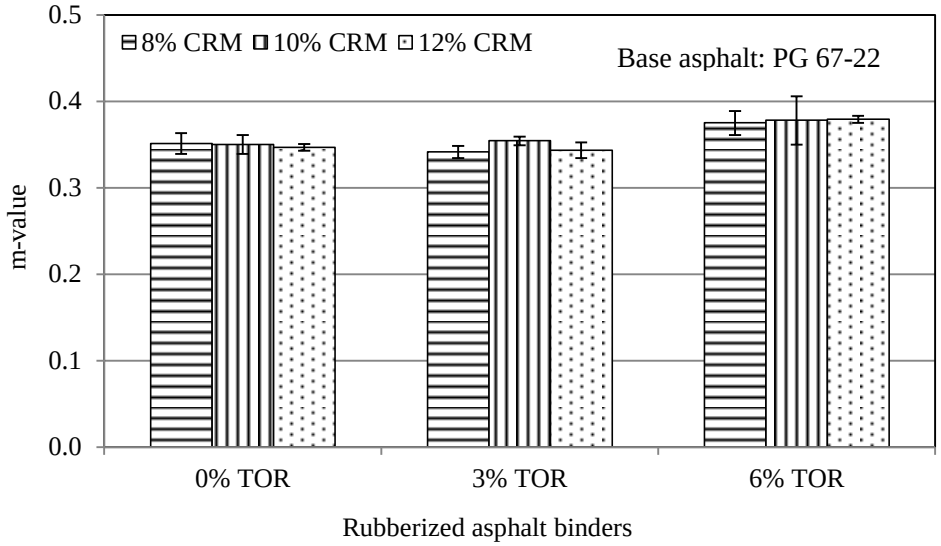

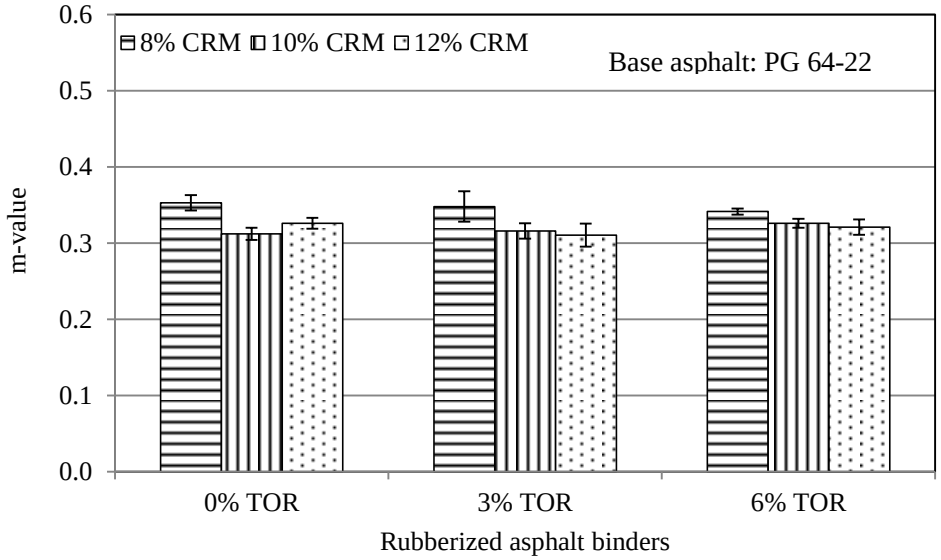

Figure 3-14. m-values of PAV-aged rubberized asphalt binder at -12 ºC

3.3.3 Effect of TOR on separation resistance

Separation tubes were used in conjunction with the DSR to determine whether varying CRM and TOR dose rates affected the overall separation of CRM particles from asphalt binder. The amount of separation was quantified by the difference in fail temperature between CRM binder removed from the top and bottom halves of the separation tube (Fig. 3-15). Results indicate that the difference increases with an increased dose of CRM and decreases with an increased dose of TOR, indicating that

to some extent, TOR reduces separation severity in rubberized asphalt binder.

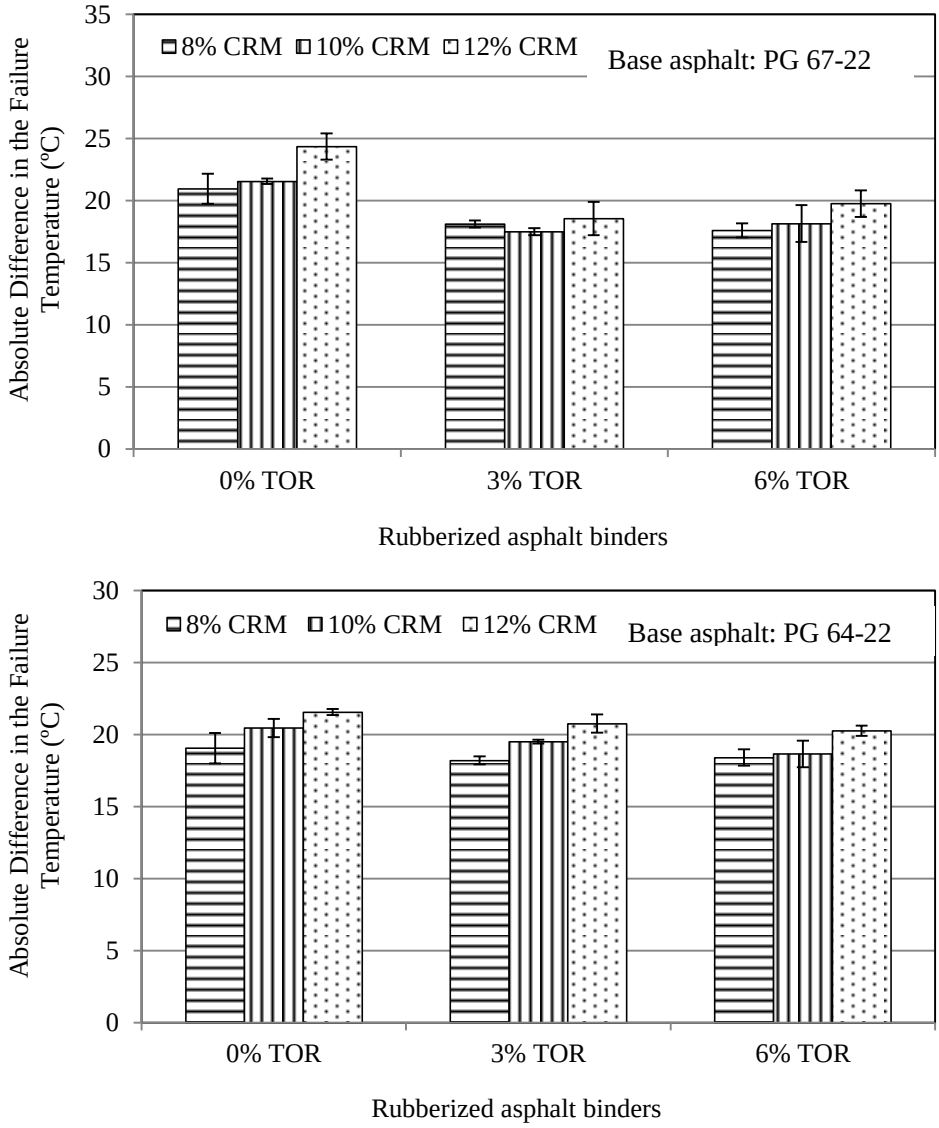

Figure 3-15. Separation Tube DSR Results

3.4 Summary and Conclusions for Rubberized Binder Properties

Two base asphalt binders (PG 67-22 and PG 64-22), three doses of crumb rubber (8%, 10%, and 12% of the weight of binder), and three doses of TOR (0%, 3%, and 6% of the weight of CRM binder) were used to produce rubberized asphalt binders. High- and low-temperature properties were evaluated using the DSR and BBR tests, and stability was evaluated by the tube method in conjunction with DSR tests. The following conclusions can be drawn from the results:

1. Doses of 3% and 6% TOR increased the G*/sin (delta) of unaged rubberized asphalt binder 14% and 20%, respectively. The rate for RTFO-aged residue was lower. Adding TOR increased the high-temperature properties of rubberized asphalt binder.

2. The phase angle of rubberized asphalt binder decreased up to 1.8% when TOR was added to both unaged binders and RTFO residue. Adding TOR to rubberized asphalt binder improved its elastic properties.

3. The absolute difference in failure temperatures for binders taken from the top and bottom of a tube was about 20% less than the controls' when a dose of 3% TOR was added to PG 67-22 asphalt. Increasing the TOR dose did not further decrease the absolute difference in failure temperatures.

4. TOR had less influence on separation in PG 64-22 asphalt binder than in PG 67-22, so it may depend on the type of base asphalt binder.

CHAPTER 4 DESIGN OF RUBBERIZED PEM AND SMA

4.1 Introduction

Porous European mix (PEM) is an open-graded surface course used by GDOT, and stone matrix asphalt (SMA) is gap-graded, Binders containing wet- and dry-processed CRM were designed.

This chapter evaluates the effectiveness of the design protocols applied to Georgia's dry- and wet-processed PEM and SMA mixes and their performance properties with both dry- and wet-processed CRM binders (Fig. 4-1).

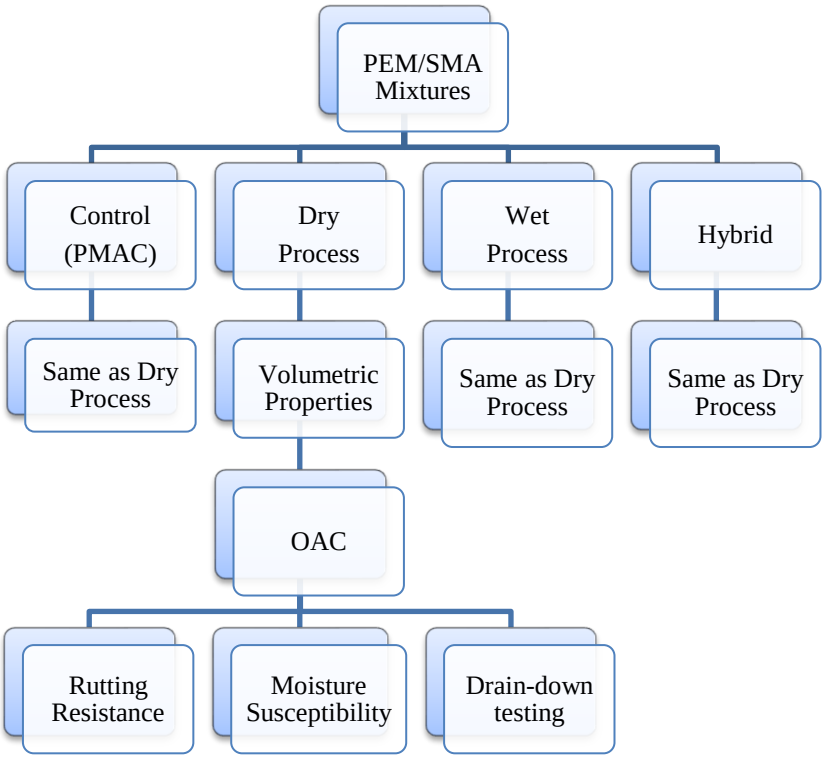

Figure 4-1. Flow chart for the design of rubberized PEM and SMA

4.2 Materials and Test Procedures

Four types of asphalt binder were selected: wet-processed rubberized asphalt binder; dry-processed rubberized asphalt concrete mixtures; terminal blend CRM asphalt binder (termed hybrid binder), which uses smaller CRM particles and polymers; and

SBS-modified binder as a control.

In addition, mineral and cellulose fibers (Fig. 4-1) were added at 0.4% and 0.35% by weight of the total mixture, respectively, to the PEM and SMA mixtures to prevent excessive drain-down. Note that cellulose fiber is more easily dispersed than mineral fiber during mixing. To prevent stripping, hydrated lime was added to all mixtures at 1.0% by weight of the total aggregate. Furthermore, a cross-link agent (TOR polymer) was introduced into dry-processed rubberized HMA at 4.5% of the weight of the CRM. Class C fly ash was used in the SMA. Tables 4-1 to 4-4 show the properties of the materials tested.

Table 4-1. Properties of materials used

Test Item		Value	Test Method
Bulk Specific Gravity	Coarse Aggregate-A	2.597	ASTM128
	Coarse Aggregate-B	2.607	
Apparent Specific Gravity	Coarse Aggregate-A	2.656	ASTM D7370
	Coarse Aggregate-B	2.656	
	Fine aggregate	2.680	
	Lime	2.225	
	Fly Ash	2.308	
	Rubber	1.177	
Flat & Elongated > 3:1 (%)	Coarse Aggregate-A	8.2	GDT 129
	Coarse Aggregate-B	9.6	

Table 4-2. Properties of cellulose fibers*

Test Item	Values
Fiber Length max., in. (mm)	0.25 (6.0)
Ash Content (%)	13.0 - 23.0
PH	6.5 - 8.5
Oil Absorption x fiber weight (mass)	4.0 - 6.0

* The data are from the manufacturer, Fiberand, Inc. (Miami, FL).

Table 4-3. Properties of mineral fibers*

Test Item		Values
Composition: Weight (%)	SiO_2	34-46
	Al_2O_3	8-15
	CaO	24-44
	MgO	4-13
	Fe_2O_3	0-4
	Other	0-4
Other Properties	PH Value	8.5 - 10.5
	Specific Gravity	2.7 - 2.9
	Fiber Diameters (μ)	4 – 6
	Fiber Length (in.)	0.25 Max
	Fiber Tensile Strength (psi)	80,000

* The data are from the manufacturer, Fiberand, Inc. (Miami, FL).

Table 4-4. Properties of the binders

Aging States	Test Properties	CRM binder (wet process)	Hybrid modified binder	SBS modified binder
Unaged Binder	G*/sin (delta) at 76 ºC (kPa)	1.46	1.73	1.58
RTFO-Aged Residue	G*/sin (delta) at 76 ºC (kPa)	4.19	4.21	3.76
PAV-Aged Residue	G*·sin (delta) at 19 ºC (kPa)	2733	4320	3103
	Stiffness at -12 ºC (MPa)	101.7	117.4	129.1
	m-value at -12 ºC	0.360	0.354	0.362

Figure 4-2. Mineral fibers

Figure 4-3. Cellulose fibers

These materials were combined to produce gradations similar to those for GDOT-approved mix designs. The gradations of 12.5-mm PEM and SMA (Fig. 4-4) were designed in accordance with Georgia mix-design procedures (Section 828), and the asphalt content of the PEM and SMA mixtures was optimized according to the requirements of GDOT 114 and GDOT 123, respectively. Both PEM and SMA gradations meet the control tolerances and design criteria of the Standard Specifications, Section 828.

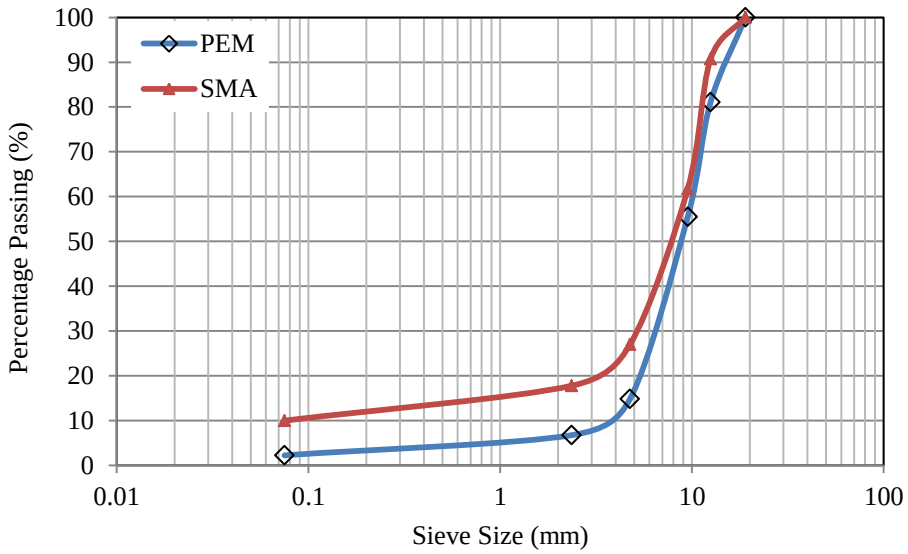

Figure 4-4. Aggregate gradations of PEM and SMA used for this study

In the wet process, rubberized asphalt binder was first produced by mixing -30-mesh CRM at 10% of the weight of the asphalt binder with a base binder of PG 67-22 at 170 °C at 700 RPM for 45 minutes in the laboratory. Next, it was blended with the aggregates. In the dry process, the same CRM and base binder were blended with the aggregates and TOR polymer.

4.3 Design Process

PEM

GDOT 114 guided the determination of optimal asphalt content (OAC) for PEM mixtures based on the surface-capacity (KC) method, the modified Marshall method, and the drain-down test.

Surface capacity method

In this step, 100 grams of dry aggregate (4.75-9.5 mm) were placed in the funnel and completely immersed in S.A.E. No. 10 oil for 5 minutes by plugging the funnel outlet. The aggregate was drained for 2 minutes at room temperature, then 15 minutes in a 140 °F (60 °C) oven. The percent of oil retained (based on 100 g of dry aggregate) was calculated (Fig. 4-5); the KC value determined based on the KC-factor curve (Fig. 4-6) from GDOT 114, and the asphalt content was calculated by Equation 4-1:

$$\text{Percent Asphalt} = 2.0(KC) + 3.5 \qquad 4\text{-}1$$

Figure 4-5. Surface-capacity test

Table 4-5 shows surface-capacity test results. The asphalt content obtained is 5.9%.

Table 4-5. Surface-capacity test results

Mass of Dry Aggregate (g)	Mass of Aggregate + Oil, after Draining (g)	Percent Oil Retained (%)		KC Factor	Asphalt Content (%)
			Average		
100.00	102.75	2.75	2.735	1.20	5.9
100.23	102.96	2.72			

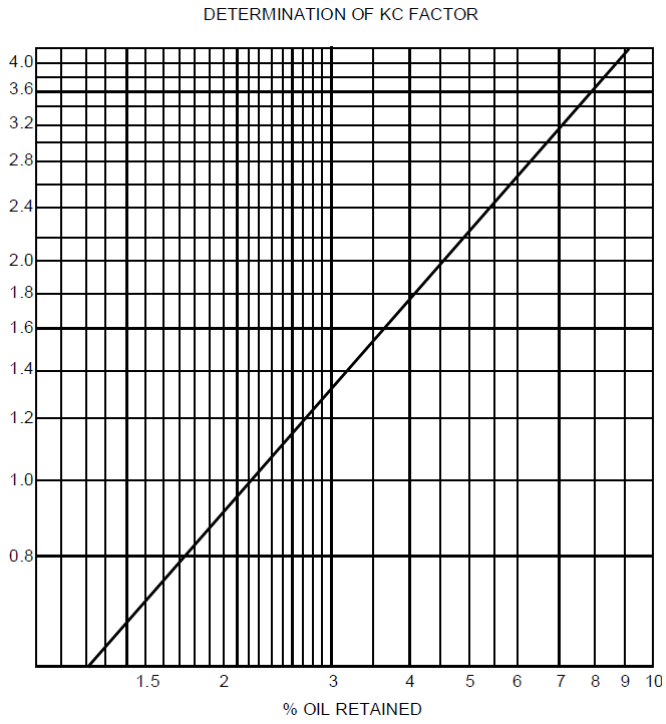

Figure 4-6. KC-factor curve (from GDOT 114)

Modified Marshall Method

Dry-processed PEM is mixed in the following steps: (1) aggregates are mixed with lime and water, then heated in a 100 °C oven; (2) mineral fiber is mixed with aggregates until the fiber separates well; (3) asphalt binder is added and mixed until it coats the other ingredients; and (4) a blend of CRM and TOR is added uniformly. The steps in mixing wet-processed PEM, SBS, and hybrid PEM are as follows: (1) aggregates are mixed with lime and water, and then heated in a 100 °C oven; (2) fiber is mixed with aggregates until it separates well; and (3) modified binder (wet-processed CRM, SBS, or hybrid) is added and mixed until the aggregates are well-coated.

In the modified Marshall test, the aggregates were preheated for 5 hours in a 135 °C oven, then mixed with one of three asphalt binders whose asphalt content was set at the 0.5% intervals closest to the AC established in the KC method. The samples were compacted with 25 blows on each side at 120 °C. Their bulk specific gravity

(G_{mb}) was determined using Equation 4-2:

$$G_{mb} = \frac{W}{\frac{(\pi r^2 h)}{0.9970}} = \frac{(Weight\ (g))(0.0048417)}{Height} \qquad 4\text{-}2$$

where:

W = specimen weight in grams;

r = specimen radius in centimeters;

h = specimen height in centimeters; and

0.99707 = density of water at 77 °F (25 °C).

Maximum specific gravity (G_{mm}) was measured according to AASHTO T 209. Air void (AV) content was calculated from mixture bulk and theoretical maximum specific gravity. Voids in the mineral aggregate (VMA) are the volume of voids and effective binder (VB) in a compacted HMA. Voids filled with asphalt (VFA) are the percentage of VMA filled with binder. The asphalt content at the lowest point on the VMA curve represented maximum specific gravity.

Table 4-6 summarizes the asphalt content at the lowest VMA point for four PEM mixtures. Figure 4-7 shows the relationships between asphalt-binder content and VMA for the four mixtures as determined by the modified Marshall test. AC was determined as the value at which VMA reached the lowest point on the curve plot.

Table 4-6. Asphalt content as determined by the modified Marshall method

PEM Type	Asphalt content at the lowest point of VMA (%)
Dry Process	6.1
Wet process	6.6
SBS	6.0
Hybrid	6.0

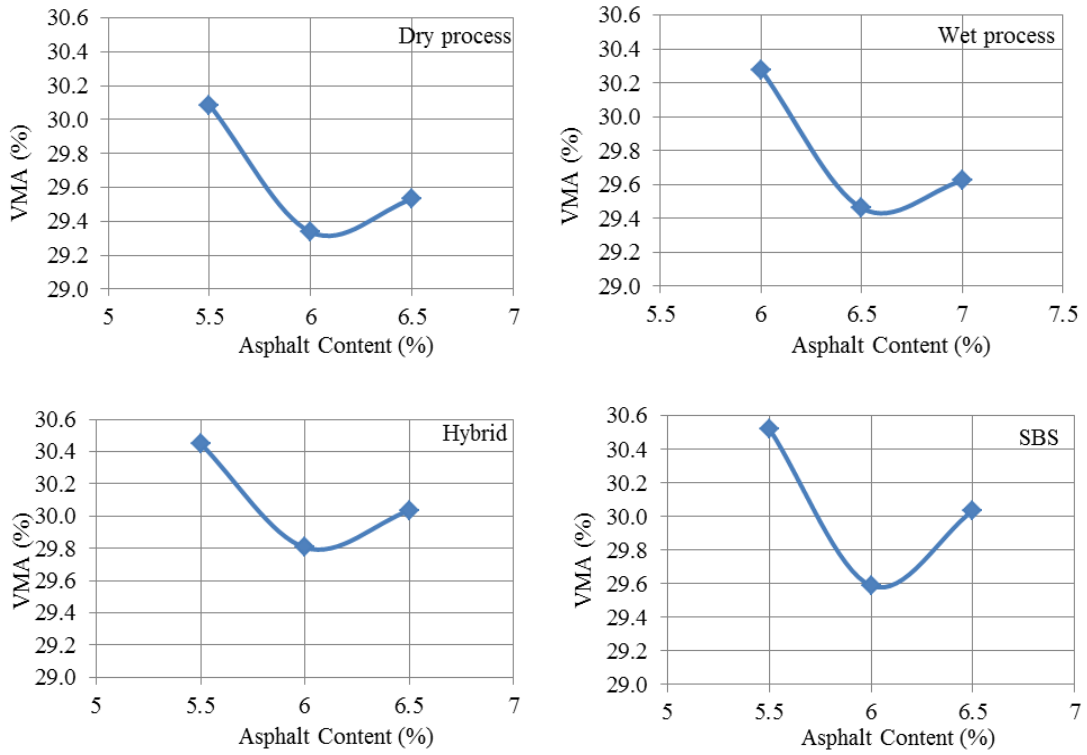

Figure 4-7. VMA curves for PEM

Drain-down test

The amount of drain-down in uncompacted PEM mixtures was determined in accordance with GDOT 127 and uses the average AC determined by the two methods above. For each mixture, two replicates were used. Approximately 1,200 grams of loose mixture were transferred to the tarred test basket, which was placed on a foil pan and into an oven set at 177 ± 2 °C. After an hour, drain-down was calculated. If it was greater than 0.3% by the weight of total mixture, the fiber content was increased 0.1%, and the tests detailed above were repeated.

Table 4-7 shows the results of drain-down testing for the PEM mixture samples. All met the 0.3% criterion. Hybrid and SBS PEM had slight drain-down; both dry- and wet-processed rubberized PEM had none. The OACs for the four PEM mixtures were determined by the three tests above and field experience. The asphalt content of wet-processed rubberized PEM was adjusted to 6.5% based on field experience. Table

4-8 presents the OAC and other volumetric properties of the four PEM.

Table 4-7. Results of drain-down testing

Mix Type	Asphalt Content for Drain-down Test (%)	Drain-down (%)
Dry process	6.0	0.00
Wet process	6.3	0.00
SBS	6.0	0.08
Hybrid	6.0	0.04

Table 4-8. Volumetric properties of PEMs

Mix Type	OAC (%)	G_{mm}	G_{mb}	AV (%)	VMA (%)	VFA (%)
Dry Process	6.0	2.406	1.955	18.7	29.3	36.1
Wet process	6.5	2.402	1.962	18.3	29.5	37.8
SBS	6.0	2.427	1.948	19.7	29.6	33.3
Hybrid	6.0	2.420	1.942	19.8	29.8	33.6

Note: OAC = optimal asphalt content; G_{mm} = maximal specific gravity; Gmb = bulk specific gravity; AV = air voids; VMA = voids in mineral aggregate; VFA = voids filled with asphalt.

Based on these tests, the final OAC was 6.5% for wet-processed rubberized mixtures and 6.0% for all others (Table 4-8). Note that the OAC for wet-processed mixtures is 0.5% higher than that for the dry-processed, but the asphalt binder used in the wet process contained CRM. In other words, the actual asphalt content added to the two mixtures is very similar.

SMA

GDOT 123 was followed to determine the OAC for the SMA mixtures. Marshall samples were compacted with 50 blows on each side at 160 °C. The G_{mb} of the compacted samples was measured in accordance with AASHTO T 166. G_{mm} was measured according to AASHTO T 209.

To determine the OAC, each SMA mixture was tested at three asphalt levels based on field experience: 5.5%, 6.0%, and 6.5% for dry-processed, hybrid, and SBS-

modified SMA; 6.5%, 7.0%, and 7.0% for wet-processed. The volumetric properties of each were measured, and OAC determined to ensure that the AV, VMA, and VFA satisfied the design criteria of Standard Specifications Section 828 (AV: 3.5±0.5%; VMA>17.0%; VFA: 70-90%) and that each yielded 3.5% air voids using a 50-blow Marshall hammer (Fig. 4-8). Table 4-9 presents the volumetric properties for all SMA mixtures at OAC.

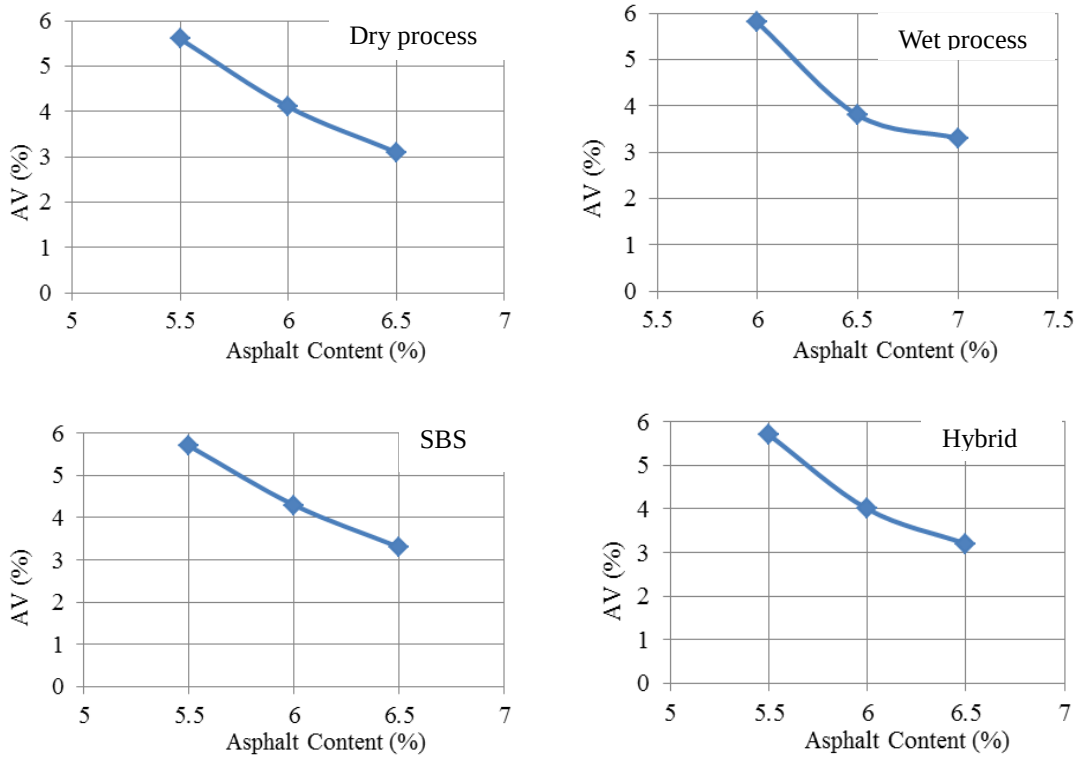

Figure 4-8. AV curves for SMA

Table 4-9. Volumetric properties of SMA mixtures

Mix Type		OAC (%)	G_{mm}	VMA (%)	VFA (%)
SMA	Dry Process	6.3	2.396	17.9	77.0
	Wet process	6.9	2.398	17.8	77.1
	SBS	6.4	2.412	18.0	71.9
	Hybrid	6.3	2.405	17.6	75.9

Note: OAC = optimal asphalt content; Gmm = maximal specific gravity; AV = air voids; VMA = voids in mineral aggregate; VFA = voids filled with asphalt.

4.4 Design Validation by Selected Mixture Properties

Selected properties, such as rutting resistance, moisture susceptibility, and drain-down, were tested to validate the PEM and SMA mixture designs.

Specimen fabrication

Aggregates and asphalt binders were heated in the oven for 5 hours before mixing at 165.5 ± 3 °C. Samples were aged in a forced-draft oven for 2 h ± 5 minutes before compaction to simulate short-term aging and stirred every 60 ± 5 minutes to maintain uniform conditioning. They were then compacted using a Superpave gyratory compactor (SGC) at 160 ± 3 °C. Samples that met the height requirement were allowed to cool for at least 45 minutes prior to extraction from the mold.

Rutting Resistance

Rutting resistance of the PEM and SMA mixtures was evaluated using an asphalt pavement analyzer (APA) (Fig. 4-11) following GDOT 115. Six replicates with air voids of 17 ± 1% (PEMs) or 5 ± 1% (SMAs) at 64 °C were loaded by a 100-pound steel wheel on a pneumatic hose at 100 psi of pressure for 8,000 cycles.

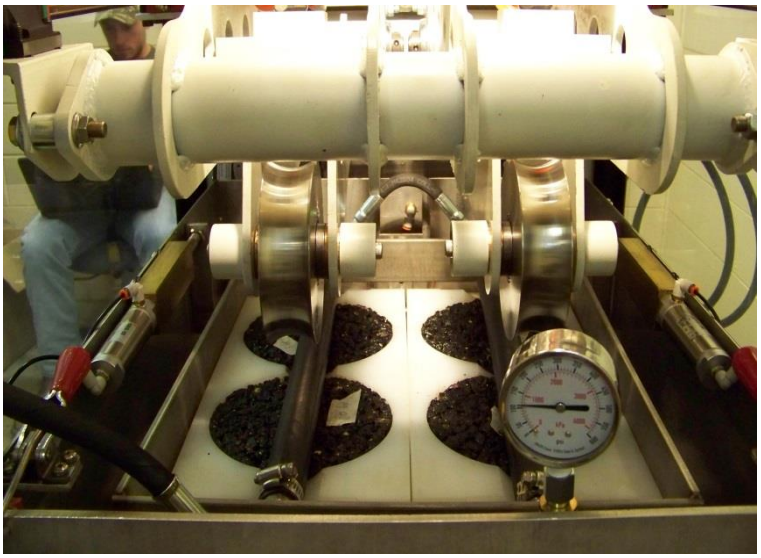

Figure 4-9. APA Test

Figures 4-10 and 4-11 show the results. Note that PEM rutting was most significant (3.2 mm) in the wet-processed samples and least significant in the hybrid samples (2.1 mm). The SBS and dry-processed samples had rutting depths of 2.65 mm and 2.56 mm, respectively. For SMA samples, rutting was most significant in dry processed (2.40 mm) and least significant in wet processed (1.68 mm). Hybrid and SBS samples were nearly identical, with 2.08 mm and 2.14 mm rut depths, respectively.

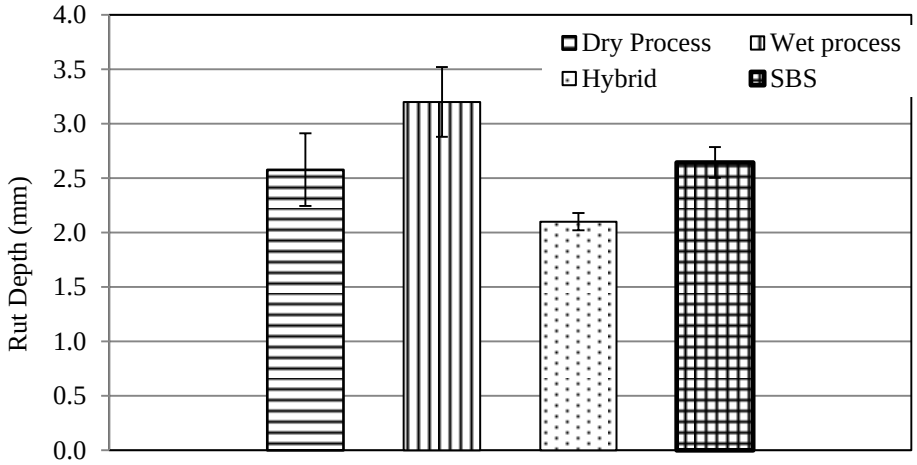

Figure 4-10. PEM average rut depths

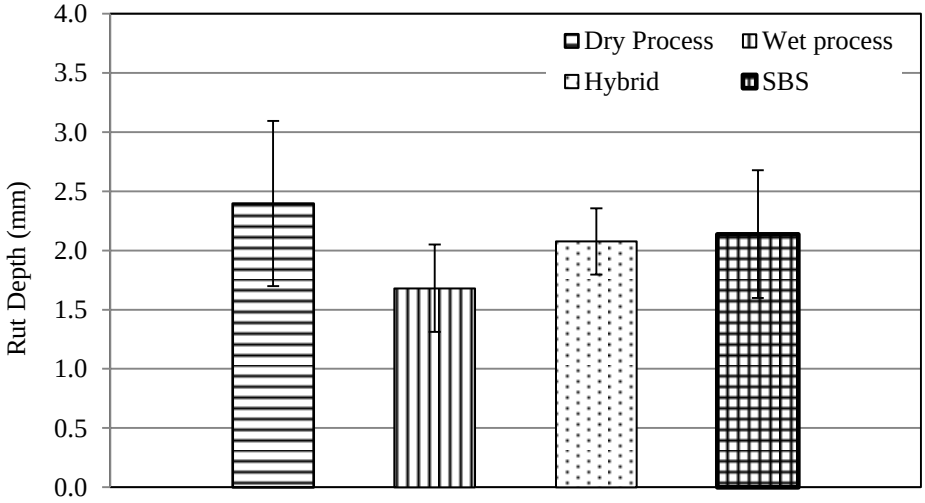

Figure 4-11. SMA average rut depths

Moisture Susceptibility

The Hamburg wheel-tracking device (HWTD) is widely used to investigate HMA susceptibility to moisture damage. A retrofitted APA test was used to evaluate the moisture-damage susceptibility of warm mix asphalts, finding a significant linear correlation with rutting rates (Brandon et al. 2014), although these results were not reliable due to an unstable steel wheel.

Since our asphalt lab had no HWTD at the time of the project, we performed the retrofitted APA test based on AASHTO T-324 (Fig. 4-12). Steel wheels, 1.85 inches wide with an 8-inch diameter, made 52 ± 2 passes across the specimen per minute. The load on each wheel was 158 ± 1.0 lb. Linear variable differential transformers (LVDTs) measured rut depth or deformation at 5 points along the length of each specimen.

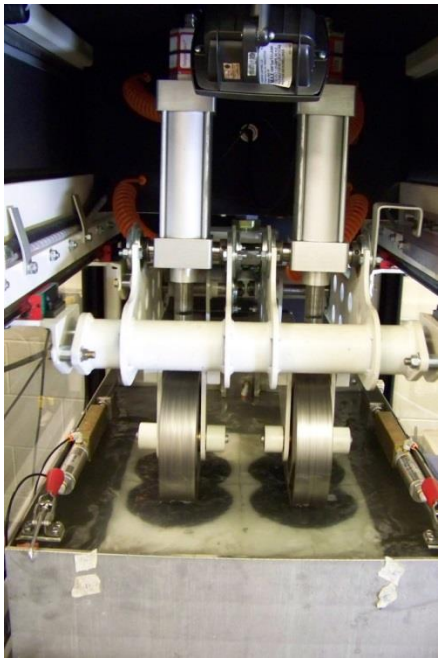

Figure 4-12. Retrofitted APA testing

Figures 4-13 and 4-14 show the results for PEM and SMA samples. Rutting depth for dry-processed rubberized PEM was highest (12.1 mm), followed by wet-processed (10.2 mm). Hybrid and SBS PEM had the lowest rutting depth (5.6 mm and 5.5 mm).

Again, GDOT does not specify rutting performance for PEM mixtures, so we have no criterion, but the test results do tell us the influence of different asphalt binders on rutting. No PEM exhibited a stripping inflection point, suggesting that after 20,000 wheel passes, no sample had significant moisture damage. In addition, all PEM samples met the criterion of a rutting depth of 12.5 mm after 20,000 passes, a trend similar to that found using SMA retrofitted APA testing (Figure 1-14).

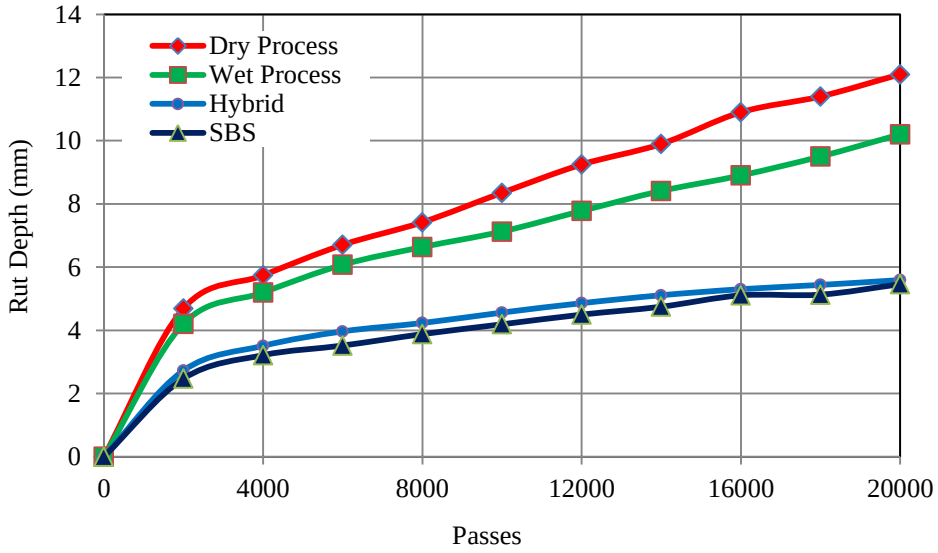

Figure 4-13. Results of retrofitted APA testing for PEM

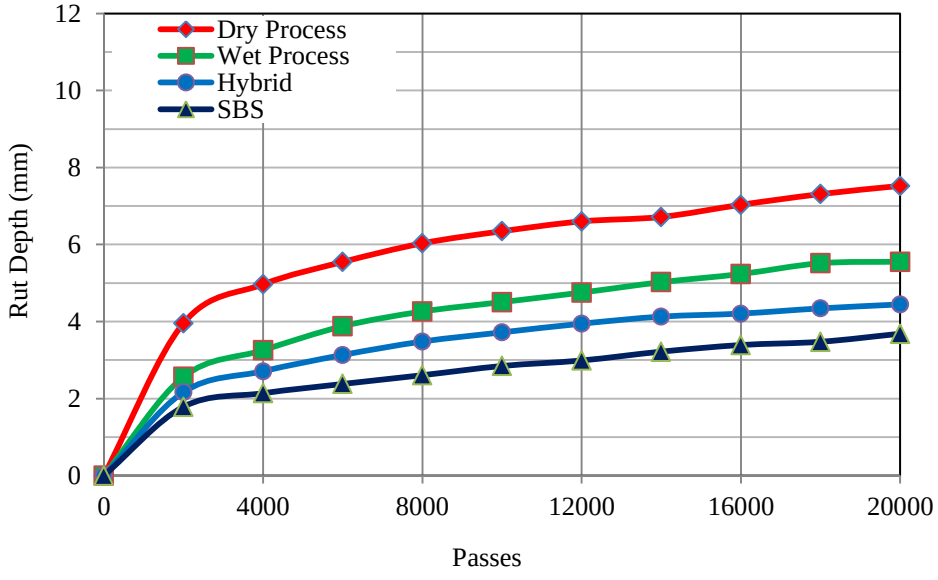

Figure 4-14. Results of retrofitted APA testing for SMA

Drain-down testing

The amount of drain-down in uncompacted PEM and SMA was determined in accordance with GDOT 127. For each mixture, two replicates were used. Approximately 1,200 grams of loose mixture were transferred to the tarred test basket and placed in a foil pan for transfer into a 177 °C ± 2 °C oven (Fig. 4-15).

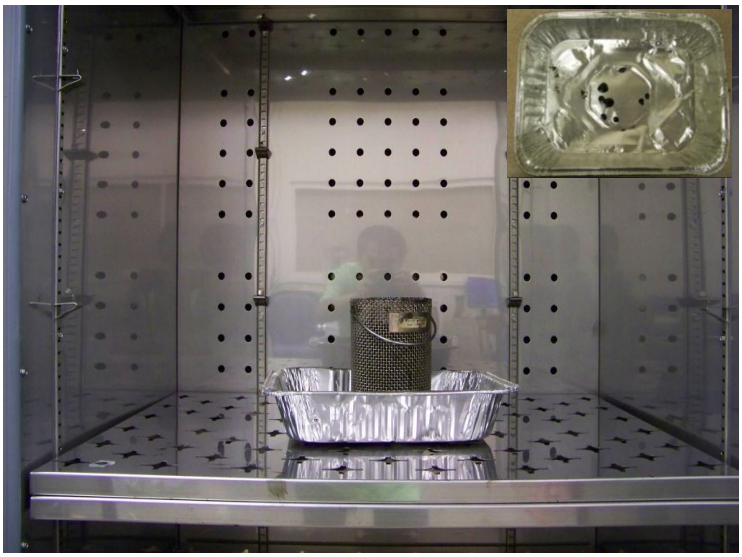

Figure 4-15. Drain-down testing

After one hour, drain-down was calculated using Equation 4-3:

$$D = 100\ (P_f - P_i)/M \qquad 4\text{-}3$$

where

P_i = initial paper-plate mass (grams); P_f = final paper-plate mass (grams);

M = mix mass (grams); D = % drain-down

Table 4-10 shows the results of drain-down testing for the PEM and SMA samples, which all met the 0.3% criterion. The SBS and hybrid PEM mixtures had some drain-down while the others had none.

Table 4-10. Results of drain-down testing

Mix Type		Drain-down (%)
PEM	Dry process	0.00
	Wet process	0.00
	Hybrid	0.04
	SBS	0.08

SMA	Dry process	0.00
	Wet process	0.00
	Hybrid	0.00
	SBS	0.00

4.5 Summary and Conclusions for Mix Design Verification

The volumetric properties of both PEM and SMA mixed with wet- and dry-processed CRM, hybrid, and SBS-modified asphalt binders were evaluated according to GDOT 114 and 123. The designs were also validated by testing their rutting resistance, moisture susceptibility, and drain-down. The following conclusions were drawn:

1. By following GDOT 114 and 123, respectively, PEM and SMA mixtures can be successfully designed to incorporate CRM, hybrid, or SBS-modified binders. Volumetric properties met GDOT requirements.

2. Rutting resistance was best in hybrid PEM mixtures, although similar for SBS and dry-processed PEM mixtures. Wet-processed samples showed the least rutting resistance. GDOT does not perform a rutting test on PEM, so there is no criterion.

3. For SMA, rutting resistance was least in dry-processed and most in wet-processed samples. Hybrid and SBS samples were nearly identical, with 2.08 mm and 2.14 mm rut depths, respectively. All rutting values were much below the state's 5 mm limit.

4. Using the retrofitted APA test, no inflection stripping point was found for all four PEMs and SMAs, indicating that their designs passed the moisture-susceptibility requirement.

5. All PEMs and SMAs met the 0.3% drain-down criterion.

CHAPTER 5 DYNAMIC MODULUS OF RUBBERIZED PEM AND SMA

5.1 Introduction

Dynamic modulus, |E*|, is a key input parameter in the MEPDG, and a comprehensive database of dynamic moduli would help to ensure that designers select cost-effective local materials for successful MEPDG implementation. However, few have investigated the dynamic moduli of dry-processed rubberized PEMs and SMAs as compared to their wet-processed and SBS-modified analogues. PEM dynamic moduli remain generally overlooked since PEM is normally paved in a thin layer that, while not a structural layer, still contributes, more or less, to structural performance.

We examined the dynamic moduli of rubberized PEMs and SMAs and the influence of introducing dry- and wet-processed CRM. The test scope included two types of aggregate gradation (PEM and SMA), four types of modified binders (dry- and wet-processed CRM, SBS-modified, and a hybrid combining CRM and SBS), and a typical aggregate granite used by GDOT. Table 5-1 shows the types of data collected. Figure 5-1 presents a flow chart of testing. E* were measured at different temperatures and frequencies, according to AASHTO 13 TP79-12.

Table 5-1. Dynamic modulus test matrix

Temperature (°C)	Frequency (Hz)	Mixes							
		Dry process		Wet process		Hybrid		SBS	
		PEM	SMA	PEM	SMA	PEM	SMA	PEM	SMA
4	10, 1, 0.1	√	√	√	√	√	√	√	√
20	10, 1, 0.1	√	√	√	√	√	√	√	√
45	10, 1, 0.1,0.01	√	√	√	√	√	√	√	√

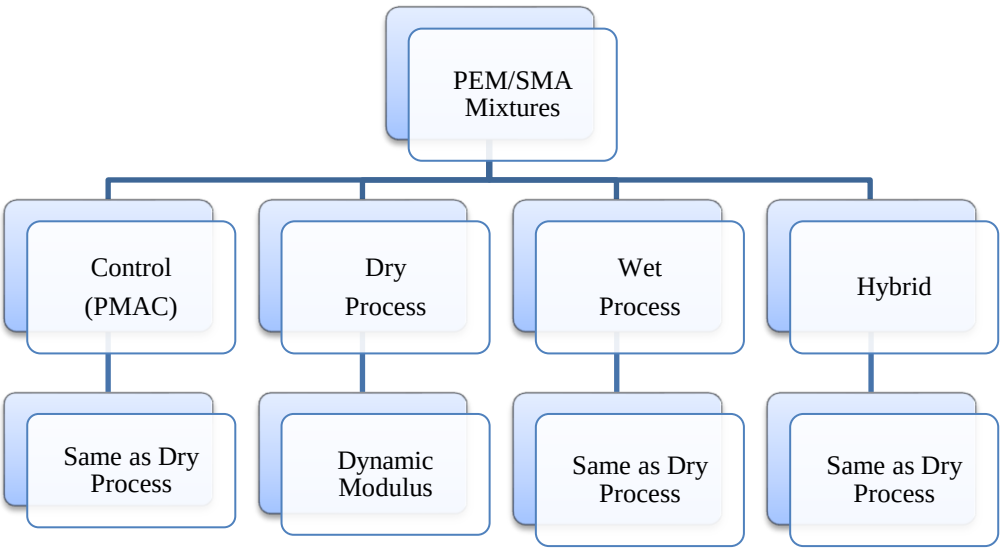

Figure 5-1. Flow chart for determining the dynamic moduli of rubberized PEM and SMA

5.2 Materials and Test Procedures

Four asphalt binder types were selected: wet- and dry-processed rubberized, hybrid (CRM and SBS combined), and SBS-modified (control) asphalt binders. Tables 4-1 to 4-4 provided detailed information on, and properties of, the materials.

The short-term aged mixtures were compacted by the Superpave gyratory compactor to obtain the required air voids, which were measured for each specimen. PEM air voids are measured using the Corelok method. All the PEM and SMA mixture specimens used in this study had target air voids of 17±0.5% and 5±0.5%, respectively. Note that laboratory experiment indicates that a 17% air void as measured by the Corelok method is close to 19% as measured by dimensional analysis. Next, a coring rig was used to obtain the required 100-mm diameter by 150-mm tall specimens, which were conditioned in an environmental chamber to reach the test temperature mandated by AASHTO 13 TP79-12. Three replicate specimens at the target air-void level were tested at four loading frequencies (0.01 Hz,

0.1 Hz, 1 Hz, 10 Hz) for 18 hours at 4 °C, 3 hours at 20 °C, and 3 hours at 45 °C.

Figure 5-2. Gyratory compaction of PEM and SMA specimens

Figure 5-3. Specimen coring and cutting

Dynamic modulus testing was conducted for each PEM and SMA mixture with an IPC Global - Asphalt Mixture Performance Tester (AMPT). The axial deformation value was measured with three spring-loaded linear variable differential transducers (LVDTs) placed vertically on diametrically opposed sides of the specimen (Fig. 5-3). Stress-versus-strain values were captured continuously, and the testing software used them to calculate dynamic modulus values.

Figure 5-4. Dynamic modulus samples and conditioning

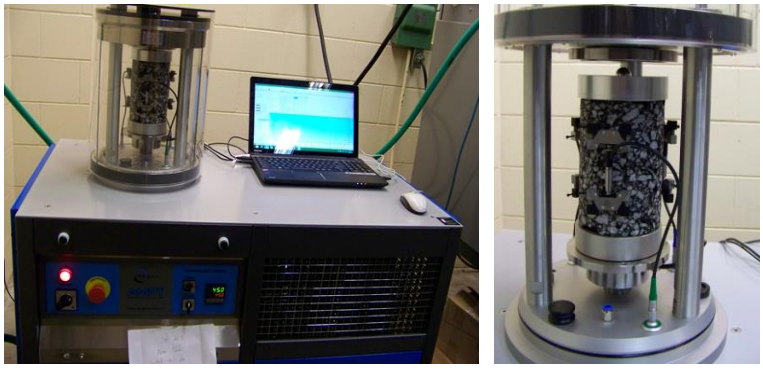

Figure 5-5. AMPT device and instrumentation

5.3 Results and Discussions

5.3.1 PEM dynamic modulus and phase angle

Dependence of dynamic modulus on temperature

Figures 5-6 to 5-8 present the relationships between dynamic modulus and temperature. Note that the slopes of the |E*|-temperature curves of dry-processed rubberized PEM mixture are a little steeper than those of the other three PEM mixtures as testing temperature increased from 4 °C to 20 °C, indicating that the temperature sensitivity of its dynamic modulus was slightly higher than that of the other PEM. On the other hand, as the testing temperature increased from 20 °C to 45 °C, the |E*|-temperature curves of all PEM mixtures had similar slopes.

In addition, the dynamic moduli of all PEM mixtures significantly decreased with increased test temperature, indicating that they were highly dependent on temperature.

For example, when the loading frequency was 10 Hz, the |E*| for all PEM mixture asphalt binder types at 45 °C was 90-92% lower than at 4 °C.

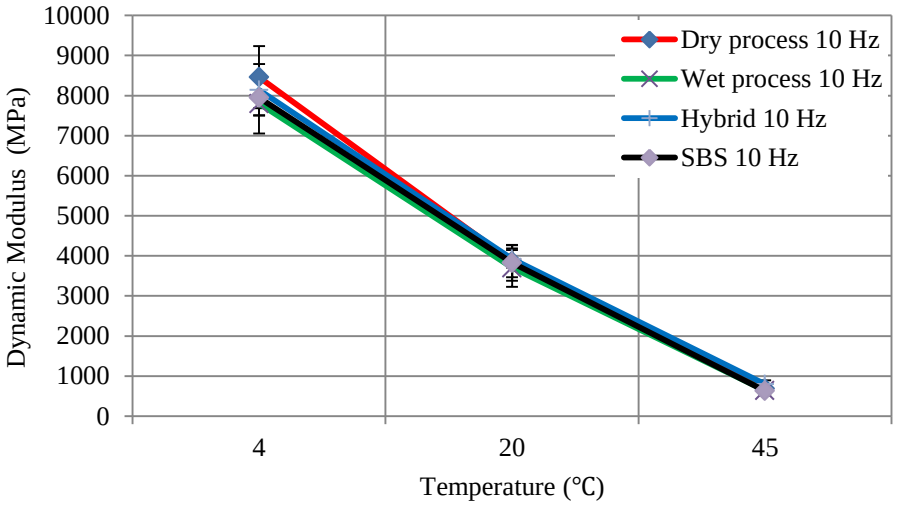

Figure 5-6. PEM dynamic modulus vs. temperature at 10 Hz

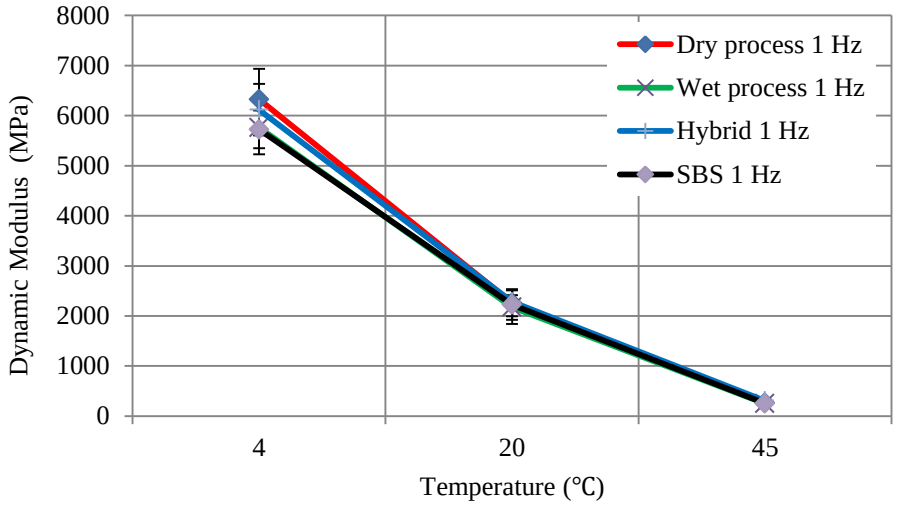

Figure 5-7. PEM dynamic modulus vs. temperature at 1 Hz

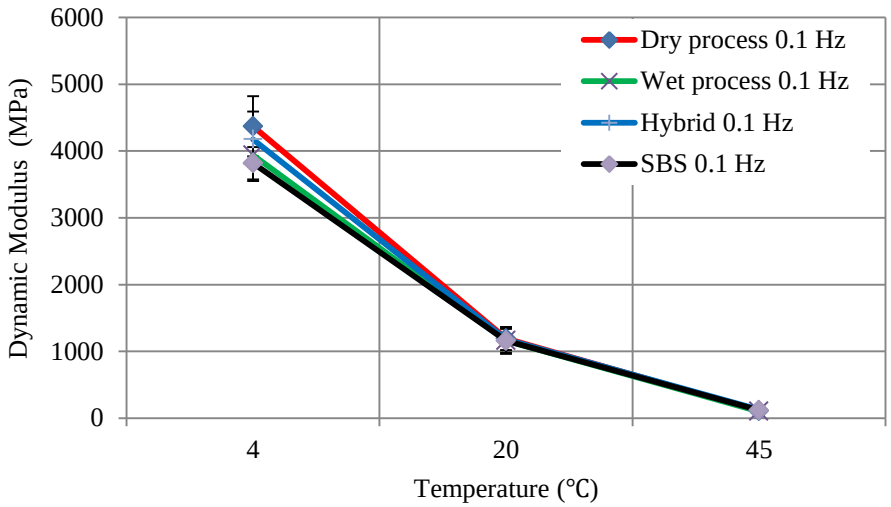

Figure 5-8. PEM dynamic modulus vs. temperature at 0.1 Hz

Dynamic modulus dependence on load frequency

Figures 5-9 to 5-11 present the relationships between dynamic modulus and load frequency. Under a constant test temperature, the dynamic moduli of all PEM mixtures increased with load frequency.

Figures 5-9 to 5-11 show that dry-processed rubberized PEM had a slightly higher dynamic modulus than the other PEM mixtures at 4 °C, but it was similar to the others at 20 °C, regardless of test frequency. The slopes of the |E*|-frequency curves of dry-processed rubberized PEM are similar to those of the other PEMs at 4 °C and 20 °C, indicating that the sensitivity of their dynamic modulus to load frequency grows similar as the test temperature lowers. The slopes of the |E*|-frequency curves of the dry-processed rubberized PEM were slightly higher than those of the wet-processed and SBS-modified PEM mixtures with higher load frequency (1 Hz and 10 Hz) but slightly lower than that of the hybrid PEM mixture at 45 °C.

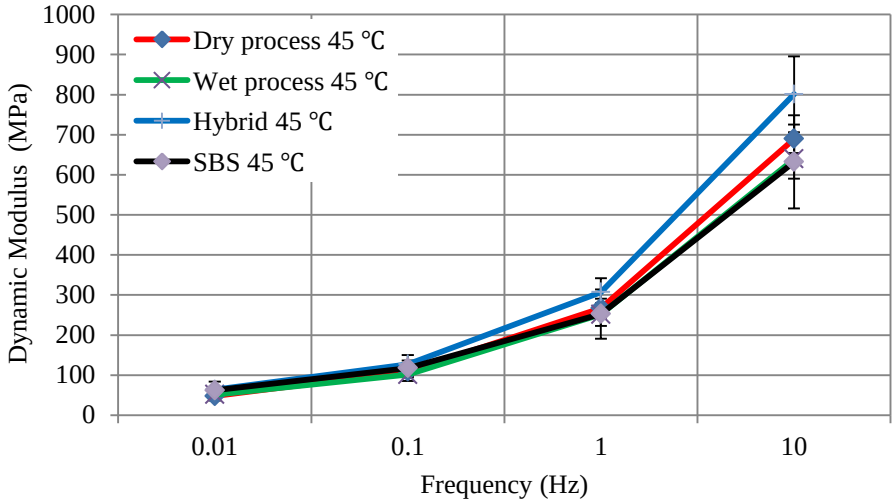

Figure 5-9. PEM dynamic modulus vs. frequency at 45 °C

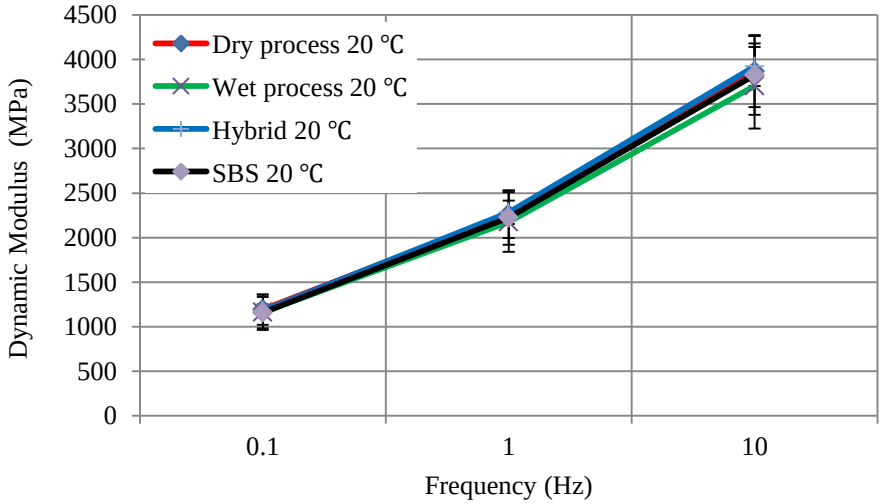

Figure 5-10. PEM dynamic modulus vs. frequency at 20 °C

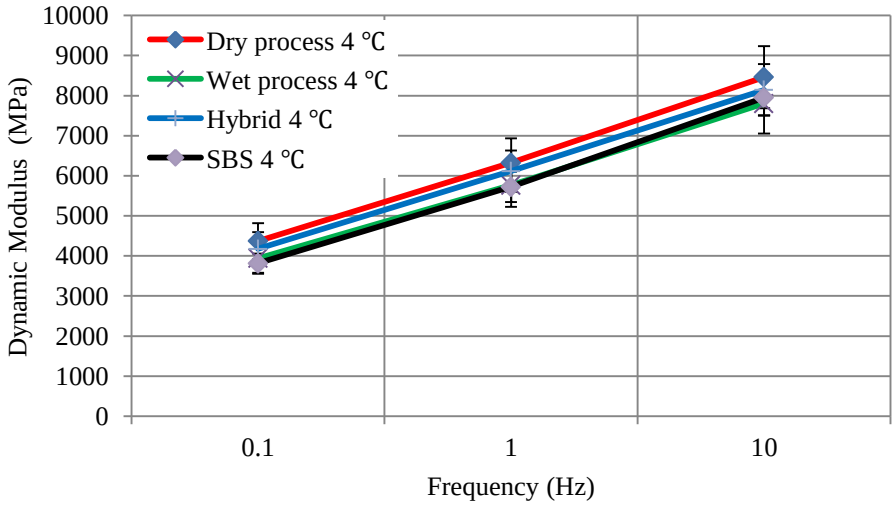

Figure 5-11. PEM dynamic modulus vs. frequency at 4 °C

Phase angle dependence on temperature

Phase angle was obtained simultaneously with |E*|. The time lag between the applied stress and resulting strain is defined as phase angle δ. This parameter determines the elastic or viscous properties of asphalt mixes. A small phase angle indicates greater elasticity.

Figures 5-12 to 5-14 present the relationships between phase angle and temperature in the samples. Generally, the phase angle of all PEM mixtures increases with the increase in test temperature when loading frequency exceeds 0.1 Hz. Thus, higher temperatures enhance PEM mixtures' viscosity, increasing their deformation. For instance, when loading frequency was 10 Hz, the average phase angle of dry- and wet-processed rubberized, hybrid, and SBS-modified PEM mixtures at 45 °C were 235%, 213%, 230%, and 194% higher, respectively, than those at 4 °C. However, at a lower load frequency (0.1Hz), the PEM mixture's phase angle increase was significantly lower and even decreased as the test temperature increased from 20 °C to 45 °C (Fig. 5-14). Dry-processed rubberized PEM's phase angle was slightly higher than the other PEMs' at 45 °C; similar to those of hybrid and SBS-modified PEM at 20 °C; and slightly lower than hybrid and SBS-modified PEM at 4 °C.

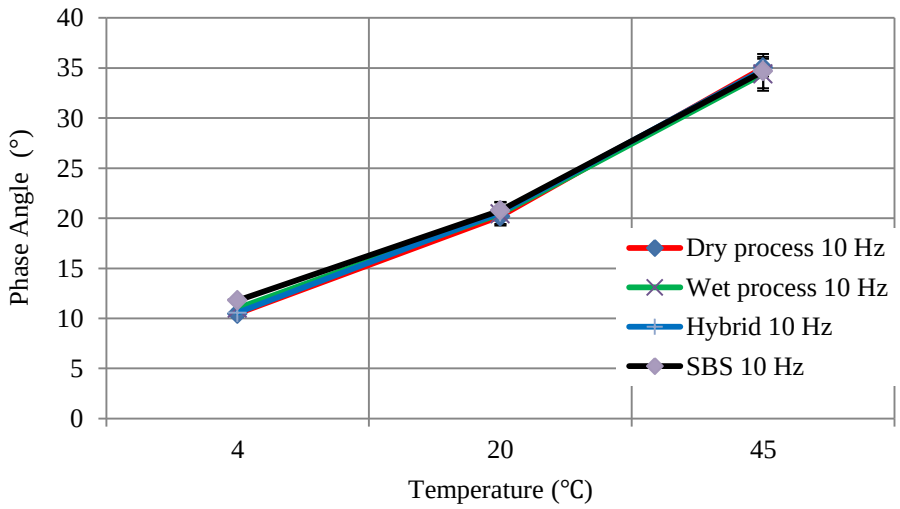

Figure 5-12. PEM phase angle vs. temperature at 10 Hz

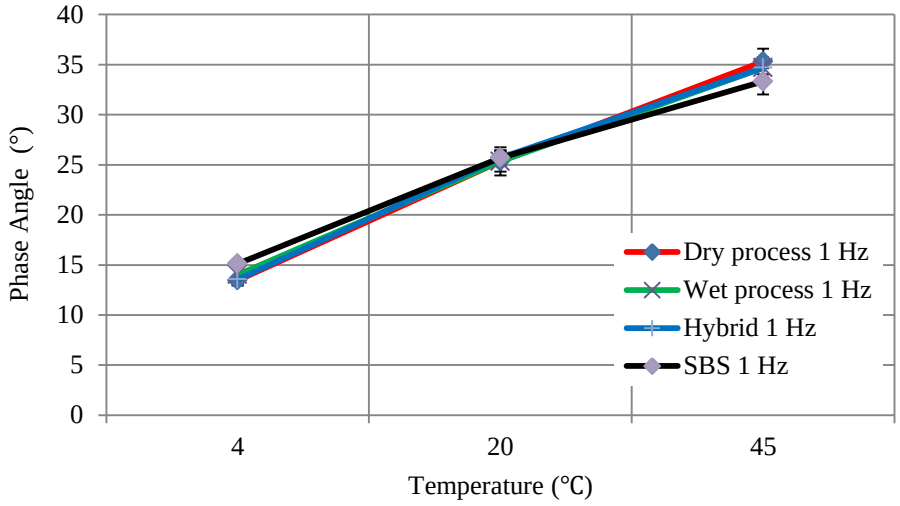

Figure 5-13. PEM phase angle vs. temperature at 1 Hz

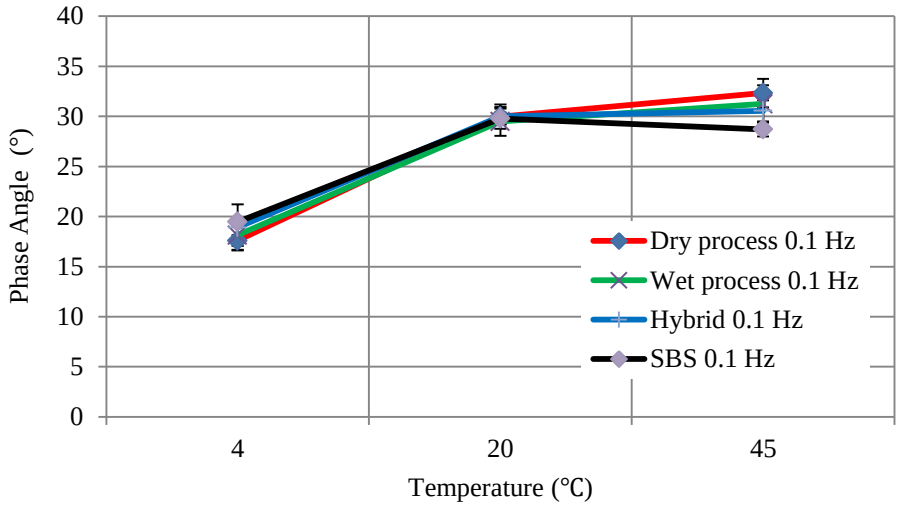

Figure 5-14. PEM phase angle vs. temperature at 0.1 Hz

Phase angle dependence on load frequency

Figures 5-15 to 5-17 present the relationships between phase angle and load frequency. At 4 ºC and 20 ºC, the phase angles of all PEM samples decrease with increased load frequency; for 45 °C, the phase angles increase as the test frequency increases from 0.01 Hz to 1Hz and decrease slightly as it increases from 1 Hz to 10Hz, except for SBS-modified PEM. The dry-processed rubberized PEM mixture has a slightly higher phase angle than the other PEMs at 45 °C and a similar phase angle at 20 °C, regardless of test frequency. It is similar to that of wet-processed and hybrid-modified

PEM mixtures, while slightly lower than SBS-modified PEM at 4 °C. Its sensitivity to load frequency is similar to the others' at 4 °C and 20 °C.

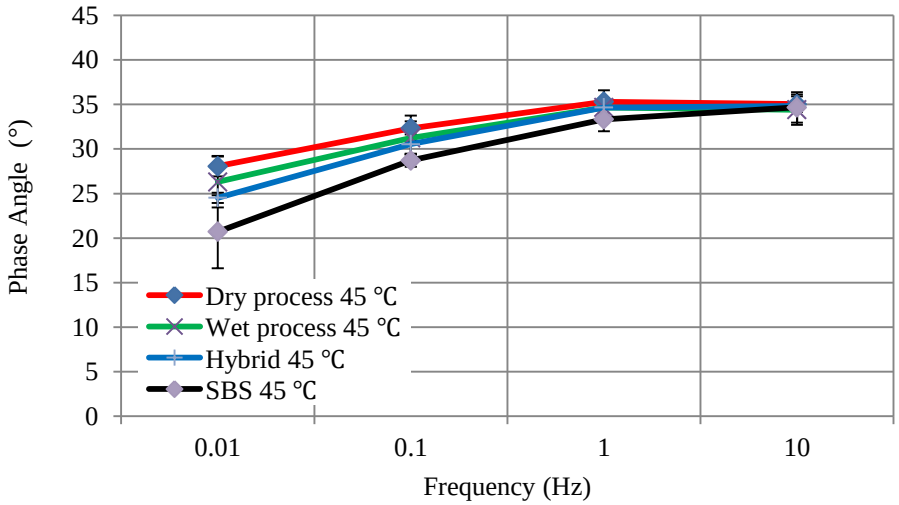

Figure 5-15. PEM phase angle vs. frequency at 45 °C

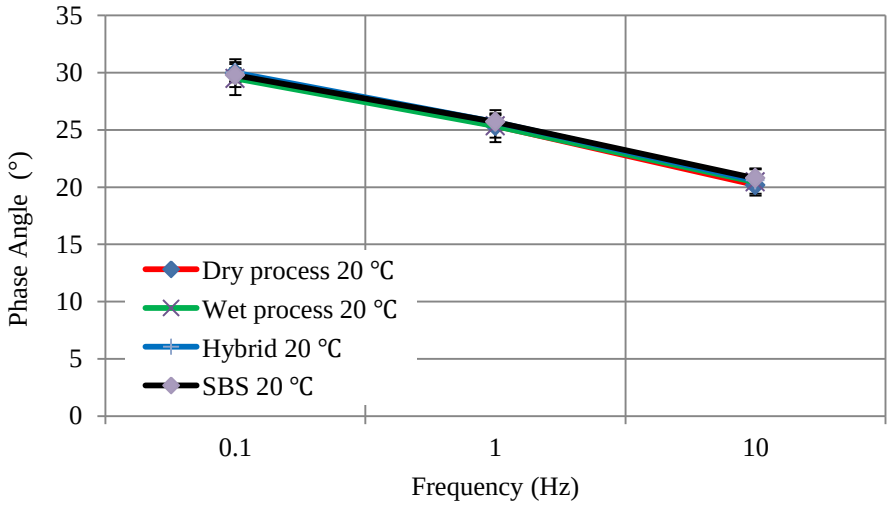

Figure 5-16. PEM phase angle vs. frequency at 20 °C

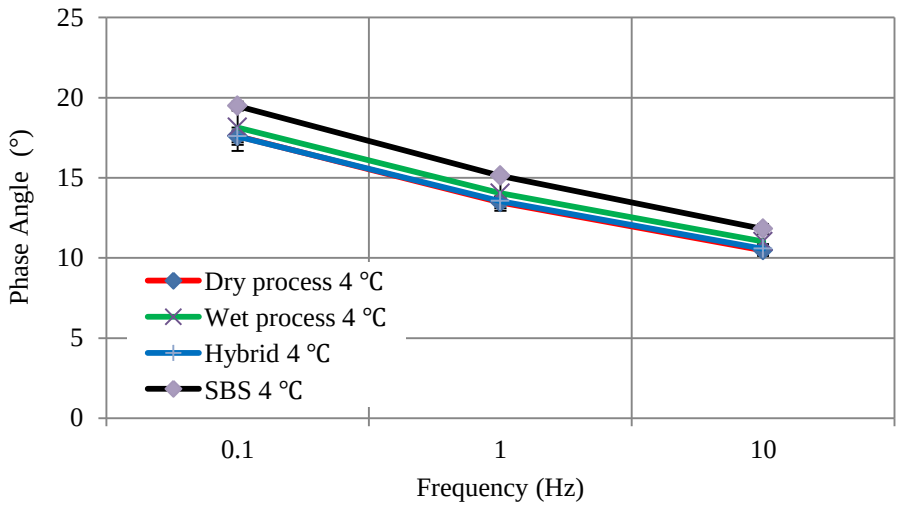

Figure 5-17. PEM phase angle vs. frequency at 4 °C

Master curve of dynamic moduli

Master curves of asphalt mixtures allow performance comparisons over extended frequency and temperature ranges. They are usually generated using the time-temperature superposition principle, which allows test data collected at different temperatures and frequencies to shift horizontally relative to a reference temperature or frequency, thereby aligning the various curves to form a single master curve. In this study, master curves for the dynamic moduli of all mixtures were constructed at the reference temperature of 70 °F (21 °C).

The construction of dynamic modulus master curves using the AMPT is standardized in AASHTO PP61. Dynamic modulus data were collected at three temperatures and four frequencies. A sigmoidal model (Eq. 5-1) was used to describe the master curves. A nonlinear analysis was performed using an available optimization routine (Microsoft Excel™) to obtain the model parameters of the master curve by minimizing the sum of the squares of error between the predicted and measured values. These master curves (Fig. 5-18) show no major difference in dynamic modulus over the entire range of frequencies for four different asphalt

mixtures, although it was slightly lower for dry-processed rubberized PEM than the three other mixes when the test frequency was lower.

$$\log(|E^*|) = \delta + \frac{\alpha}{1+e^{[\beta+\gamma(\log f_r)]}} \qquad 5\text{-}1$$

where f_r = loading frequency at the reference temperature; δ =minimum value of dynamic modulus; δ +α = maximum value of dynamic modulus; and β, γ = parameter describing the shape of the sigmoidal function.

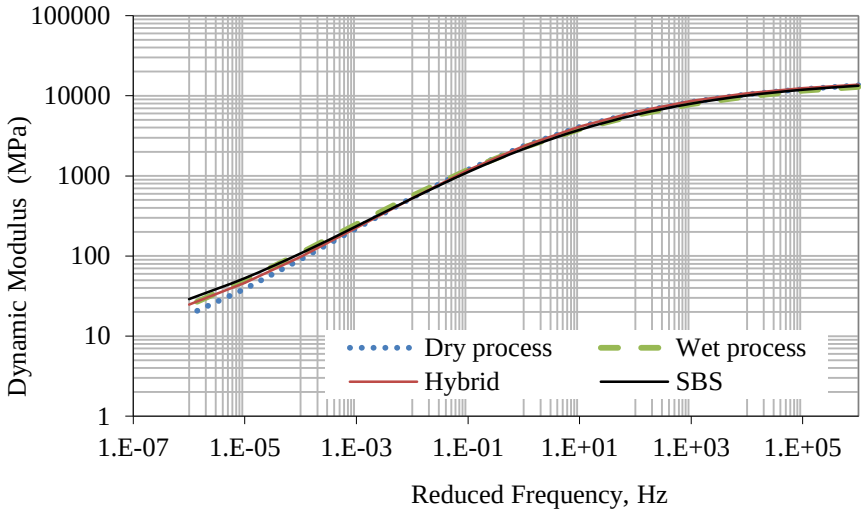

Figure 5-18. Master curves of PEM dynamic moduli

To determine whether dry-processed rubberized PEM performs as well as the other three PEM mixtures with regard to dynamic modulus, an analysis of variance with a 5% level of significance was performed. Table 5-2 indicates no statistically significant difference between the dynamic modulus of dry-processed rubberized PEM and those of the other three PEM mixtures.

Table 5-2. Statistical analysis of PEM dynamic modulus

Test Condition	Dry Process~ Wet Process	Dry Process~ Hybrid	Dry Process~ SBS
4 ℃, 10 Hz	N	N	N
4 ℃, 1.0 Hz	N	N	N
4 ℃, 0.1 Hz	N	N	N
20 ℃, 10 Hz	N	N	N
20 ℃, 1.0 Hz	N	N	N
20 ℃, 0.1 Hz	N	N	N
45 ℃, 10 Hz	N	N	N
45 ℃, 1.0 Hz	N	N	N
45 ℃, 0.1 Hz	N	N	N
45 ℃, 0.01 Hz	N	N	N

Note: Y: P-value < α = .05 (significant difference); N: P-value > α = .05 (no significant difference).

Master curve of phase angles

The master curve of the phase angles of four PEM mixtures (Fig. 5-19) shows that the phase angle decreases as the reduced frequency increases beyond 0.01 Hz and exhibits the opposite trend at less than 0.01 Hz. Asphalt binder softens as the temperature increases, and aggregate interlocking significantly overtakes its rheological behavior.

At higher frequencies (equivalent to low test temperatures), the phase angles of the dry- and wet-processed rubberized, and hybrid-modified PEM mixtures are similar and slightly lower than that of SBS-modified PEM. At lower frequencies (equivalent to high test temperatures), the phase angles of dry- and wet-processed rubberized PEM mixes are similar and higher than those of hybrid and SBS-modified PEM mixtures, suggesting that they may be less elastic and more viscous than hybrid and SBS-modified PEM at higher temperatures.

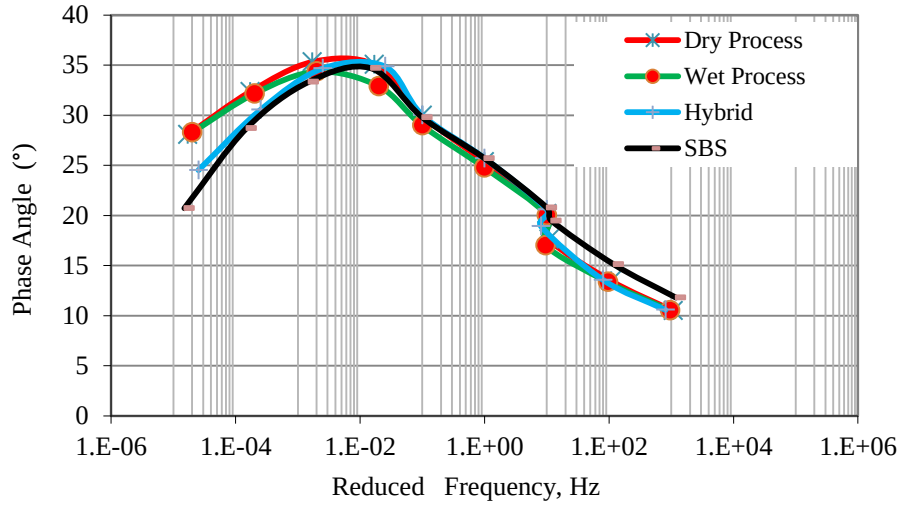

Figure 5-19. Master curves of PEM phase angles

5.3.2 SMA dynamic modulus and phase angle

Dynamic modulus dependence on temperature and load frequency

Figures 5-20 to 5-25 show the dynamic modulus test results for all SMA mixtures. As expected, they were significantly lower as testing temperature increased and loading frequency decreased. They were similar for all SMA samples at 4 and 20 ºC. Both dry- and wet-processed rubberized SMA mixtures exhibited a slightly lower dynamic modulus at low frequency and high temperature (0.01 or 0.1Hz at 45 °C).

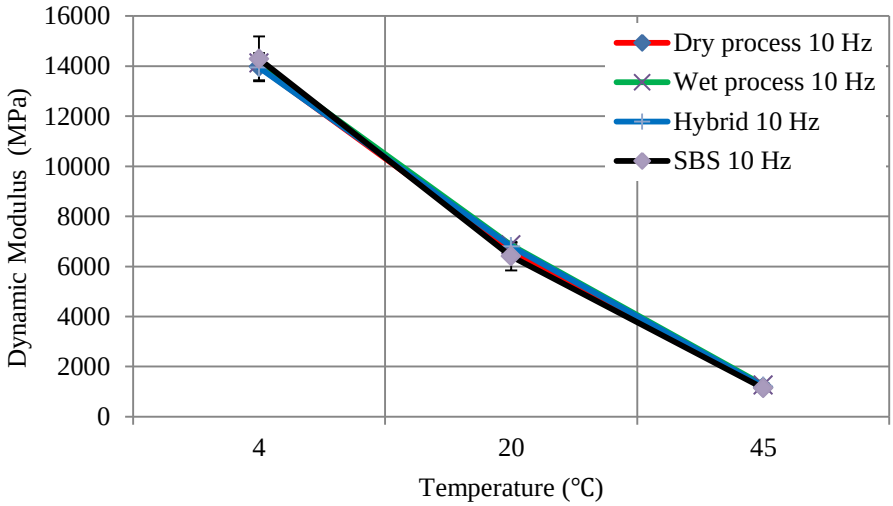

Figure 5-20. SMA dynamic modulus vs. temperature at 10 Hz

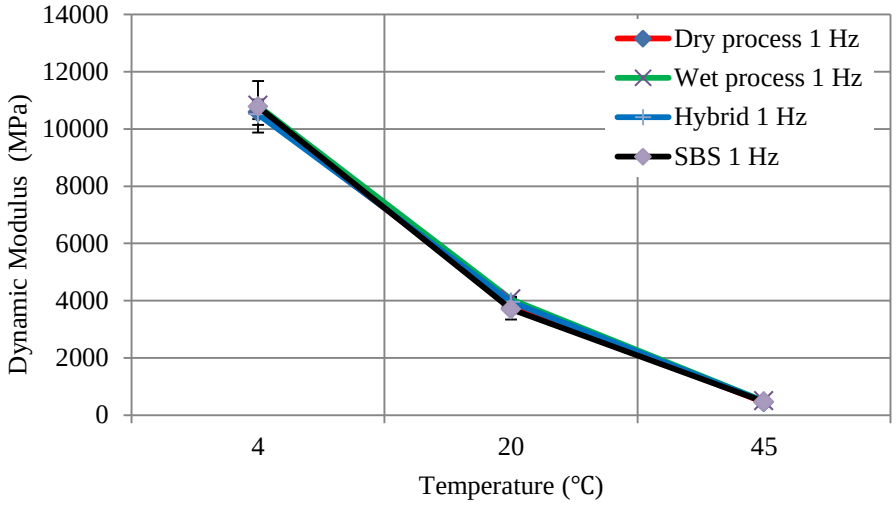

Figure 5-21. SMA dynamic modulus vs. temperature at 1 Hz

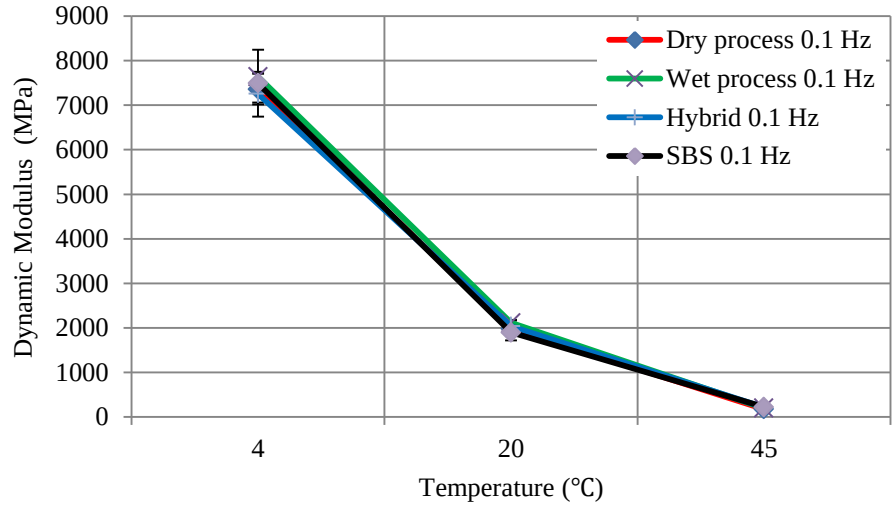

Figure 5-22. SMA dynamic modulus vs. temperature at 0.1 Hz

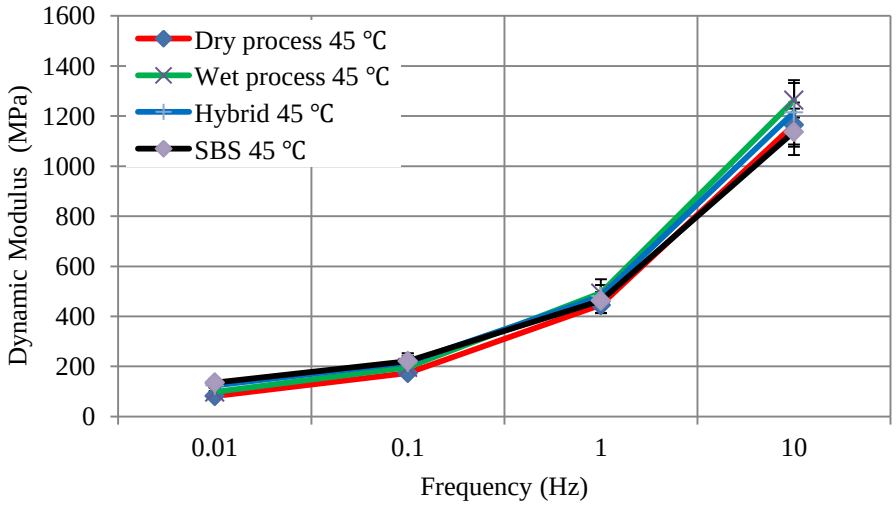

Figure 5-23. SMA dynamic modulus vs. frequency at 45 °C

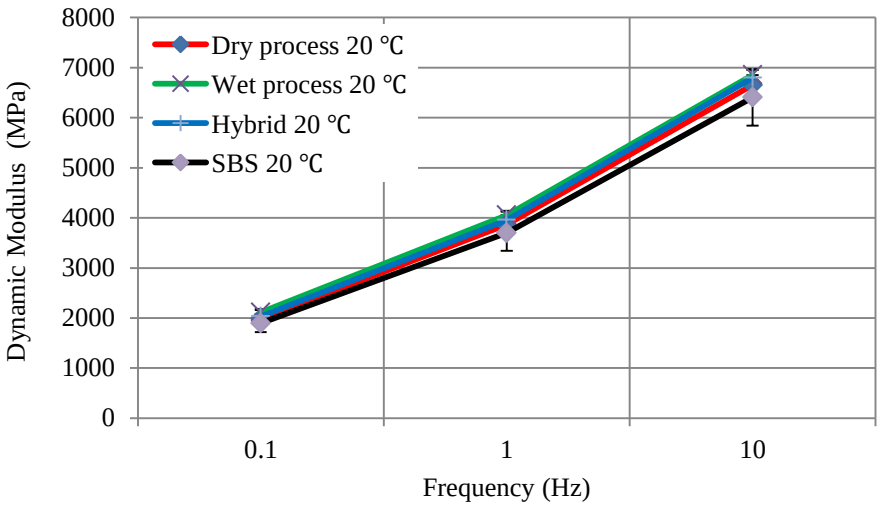

Figure 5-24. SMA dynamic modulus vs. frequency at 20 °C

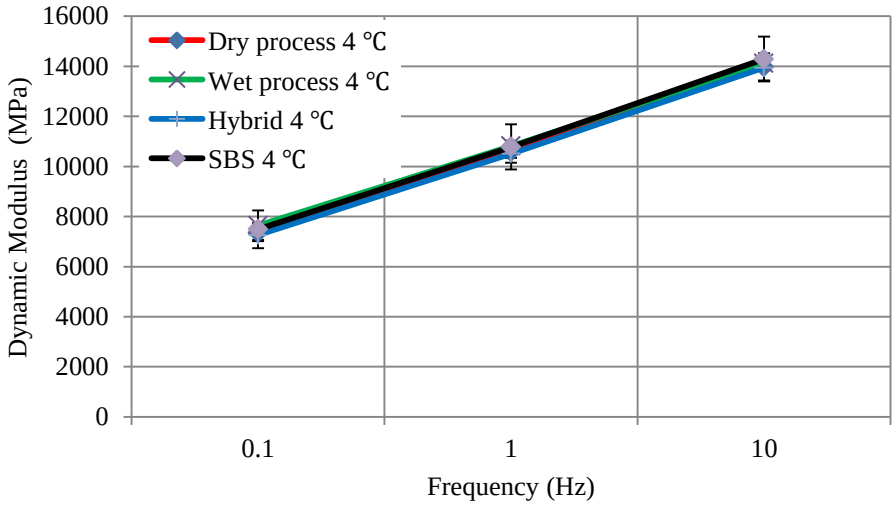

Figure 5-25. SME dynamic modulus vs. frequency at 4 °C

Master curve of dynamic moduli

Master curves of dynamic moduli at 21 °C were plotted (Fig. 5-26). They were similar at higher frequency, but dry- and wet-processed SMA mixtures had slightly lower values than hybrid and SBS-modified SMA mixtures at reduced frequency. To determine whether the difference between the E* of dry-processed SMA and those of other three SMA mixtures was significant, a statistical F-test of variance at the 5% significance level was performed (Table 5-3). Results showed that the dynamic modulus of the dry-processed SMA mixture did not differ significantly from the others'.

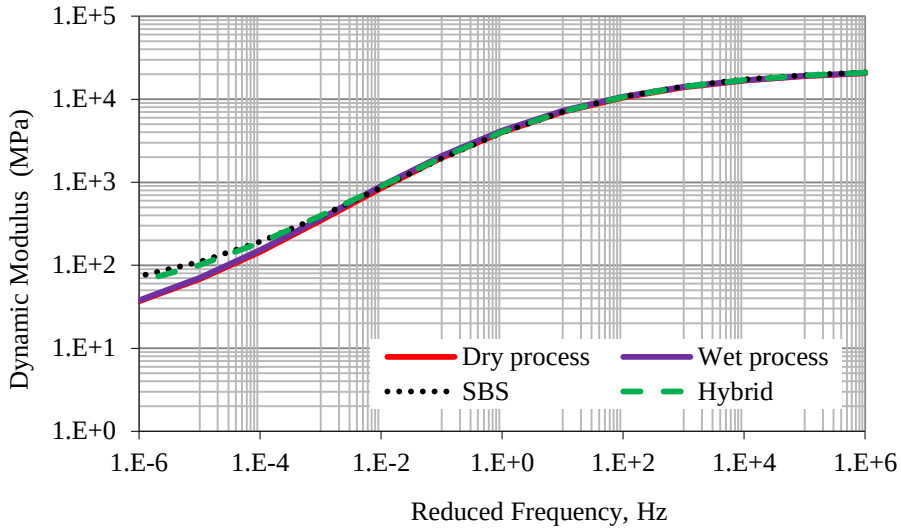

Figure 5-26. Master curves of SMA dynamic modulus

Table 5-3. Statistical analysis of SMA dynamic modulus

	dry ~ wet process	dry process ~ Hybrid	dry process ~ SBS
4 ℃, 10 Hz	N	N	N
4 ℃, 1.0 Hz	N	N	N
4 ℃, 0.1 Hz	N	N	**N**
20 ℃, 10 Hz	N	N	N
20 ℃, 1.0 Hz	N	N	N
20 ℃, 0.1 Hz	N	N	**N**
45 ℃, 10 Hz	N	N	N
45 ℃, 1.0 Hz	N	N	N
45 ℃, 0.1 Hz	N	N	N
45 ℃, 0.01 Hz	N	N	N

Note: Y: P-value < α = 0.05 (significant difference); N: P-value > α =0 .05 (no significant difference).

Dynamic modulus dependence on temperature and load frequency

The E* test determines the elastic or viscous properties of an SMA mix. It is used to determine phase angle, which indicates the relative amounts of temporary and permanent deformation. Lower phase angle indicates better resistance to deformation.

Figures 5-27 to 5-32 show the phase angle results for four SMA mixtures. They were similar at 4 and 20 °C, while dry-processed rubberized SMA's was slightly higher at high temperature (45 °C) than the others', regardless of load frequency. Furthermore, the phase angle of the dry- and wet-processed modified SMA mixes at 10 Hz and 1 Hz increased at a slightly higher rate than those of the hybrid and SBS-modified SMA mixtures as the testing temperature increased from 20 to 45 °C. At 10 Hz and 1 Hz, the phase angle of all SMA mixtures increased significantly with the testing temperature. At 0.1 Hz, the phase angle of hybrid and SBS-modified SMA mixtures decreased slightly and those of the dry- and wet-processed rubberized SMA increased slightly as the testing temperature increased from 20 to 45 °C.

Figures 5-31 to 5-32 reveal that at 4 and 20 ºC, the phase angles of all SMA samples decreased with increased frequency, while at 45 °C, they increased.

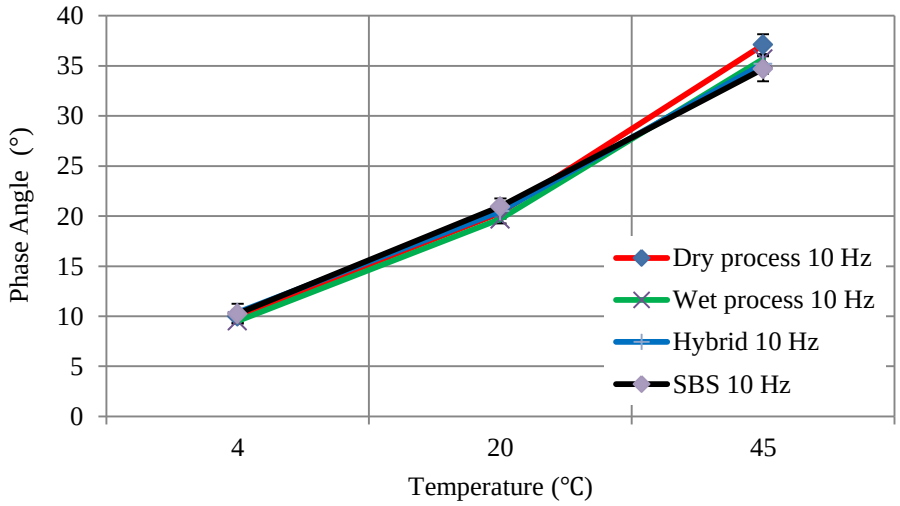

Figure 5-27. SMA phase angle vs. temperature at 10 Hz

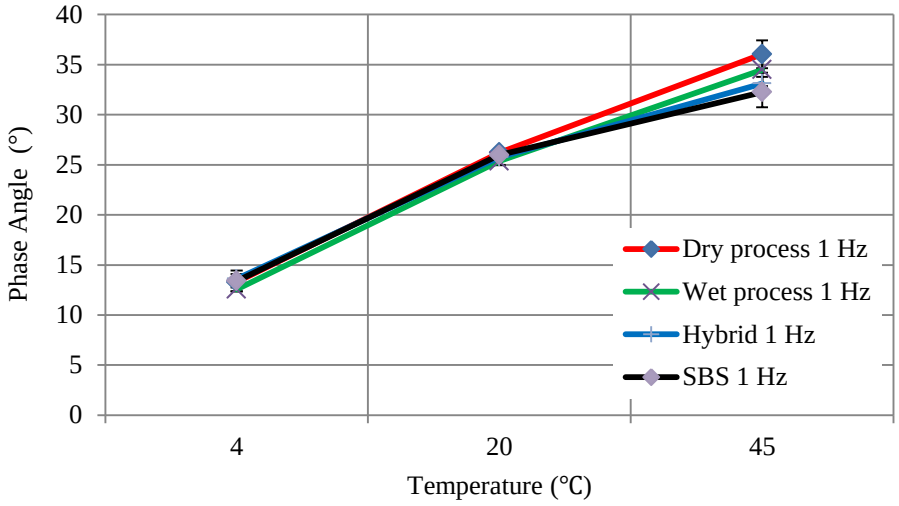

Figure 5-28. SMA phase angle vs. temperature at 1 Hz

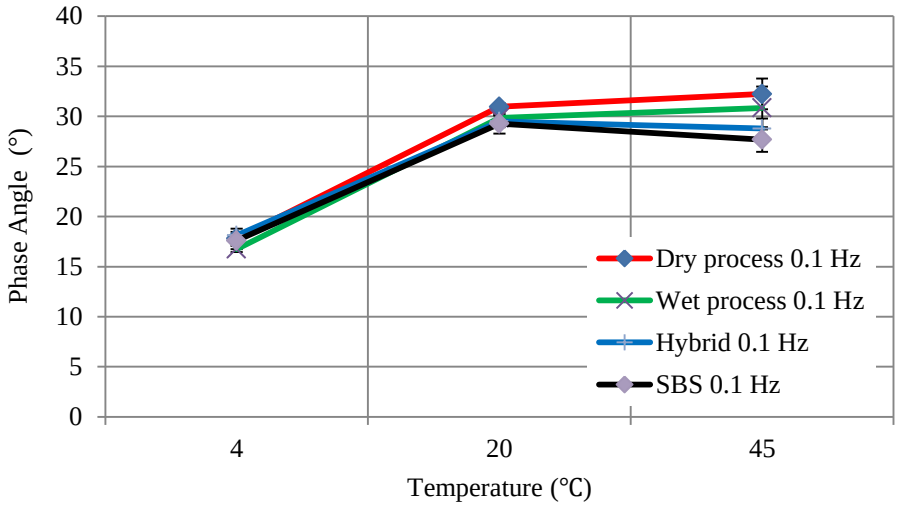

Figure 5-29. SMA phase angle vs. temperature at 0.1 Hz

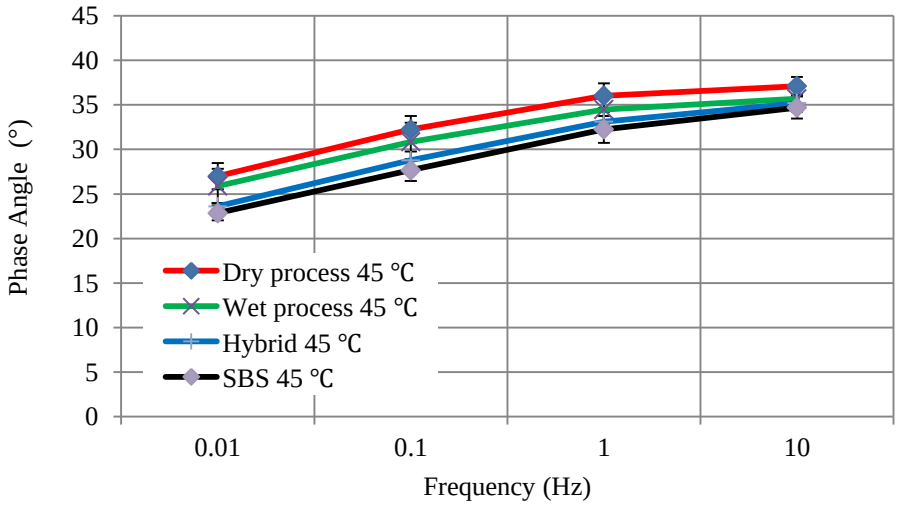

Figure 5-30. SMA phase angle vs. frequency at 45 °C

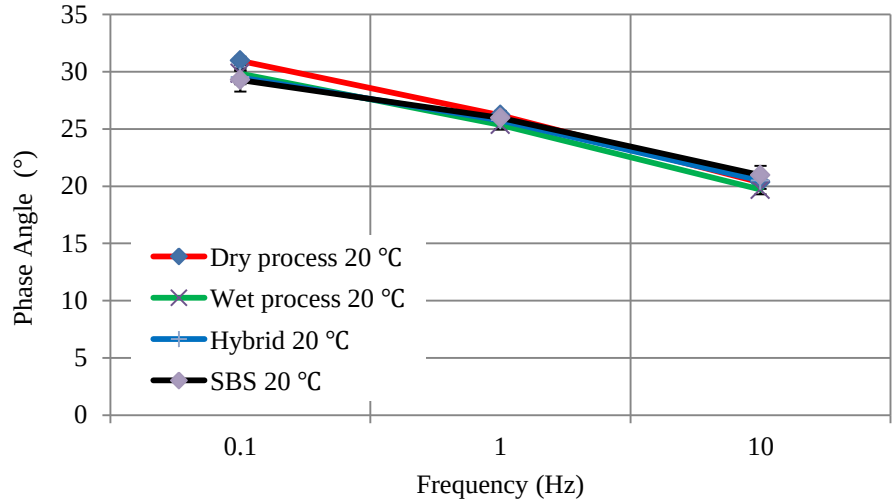

Figure 5-31. SMA phase angle vs. frequency at 20 °C

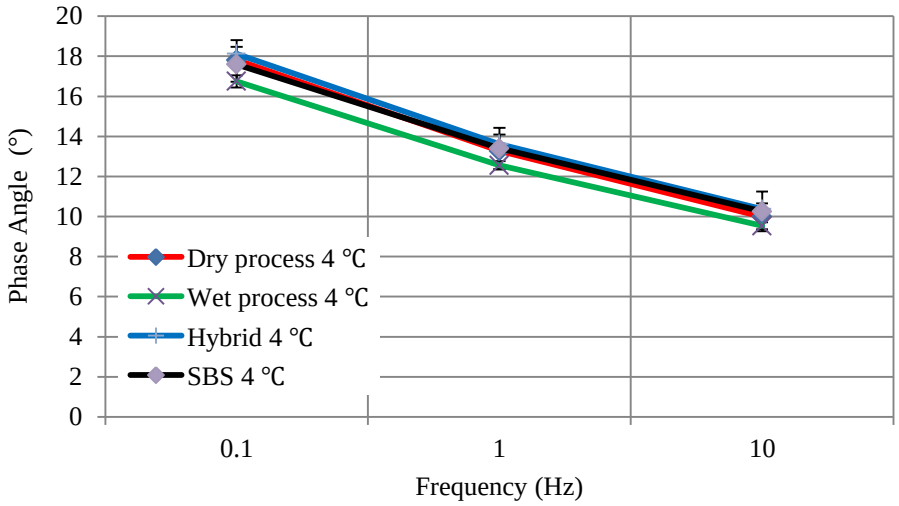

Figure 5-32. SMA phase angle vs. frequency at 4 °C

A statistical F-test of variance at the 5% significance level was conducted for the phase angle of the four SMA mixtures (Table 5-4). Results revealed that the phase angle of dry-process modified SMA did not differ significantly from the others', regardless of test frequency and temperature.

Table 5-4. Statistical analysis of SMA phase angle

	Dry Process~ Wet Process	Dry Process~ Hybrid	Dry Process~ SBS
4 ℃, 10 Hz	N	N	N
4 ℃, 1.0 Hz	N	N	N
4 ℃, 0.1 Hz	N	N	**N**
20 ℃, 10 Hz	N	N	N
20 ℃, 1.0 Hz	N	N	N
20 ℃, 0.1 Hz	N	N	N
45 ℃, 10 Hz	N	N	N
45 ℃, 1.0 Hz	N	N	N
45 ℃, 0.1 Hz	N	N	**N**
45 ℃, 0.01 Hz	N	N	N

Note: Y: P-value < α = .05 (significant difference); N: P-value > α = .05 (no significant difference).

5.4 Summary and Conclusions on Dynamic Modulus

The effect on the dynamic modulus of modifying PEM and SMA mixtures four different ways was examined and found:

1. The dynamic moduli of all PEM and SMA mixtures decreased as test temperature increased when loading frequency was constant and increased with test frequency when the temperature was constant.
2. Both PEM and SMA mixtures' phase angles increased as test temperature increased at a constant loading frequency. They decreased at 4 and 20 °C but increased at 45 °C when test frequency increased at constant temperature.
3. Dynamic moduli did not differ significantly over the entire range of frequencies for the four PEM mixtures. In other words, PEM mixes modified using dry-processed CR performed as well as those with wet-processed CR,

hybrid binders, and SBS control mixtures in terms of E*. These trends held for all the SMA mixes.

4. According to the dynamic modulus master curve, dry-processed rubberized PEM and SMA mixtures were similar to the other three PEM and SMA mixtures at higher frequency. However, their dynamic modulus values were slightly lower than those of hybrid and SBS-modified SMA mixes at lower frequency (higher temperature).

CHAPTER 6 FATIGUE LIFE OF RUBBERIZED PEM AND SMA

6.1 Introduction

Introducing crumb rubbers into asphalt mixtures has improved their fatigue performance (Huang 2002). Accurate description and prediction of fatigue resistance in rubberized asphalt mixtures are extremely important to flexible pavement design and preservation, but research was limited, and how the differences in dry and wet methods for introducing CRM affect the fatigue performance of PEM and SMA mixtures was unclear. A study comparing their fatigue performance was needed.

Fatigue tests can be classified as phenomenological or mechanistic. The phenomenological approach, such as the flexural beam fatigue test, is empirical and can introduce large errors when used to predict material performance. Mechanistic approaches, such as the simplified viscoelastic continuum damage (S-VECD) model, are more theoretically rigorous and can effectively predict the fatigue life of asphalt mixtures under different test temperatures and loading conditions.

The aims of this study were to (1) use the S-VECD model to investigate the fatigue performance of dry-processed rubberized PEM and SMA mixtures and other typical PEM and SMA mixtures, such as wet-processed, terminal blend hybrid, and SBS-modified; and (2) explore the influence on fatigue performance of introducing CRM by the wet or dry process. Figure 6-1 is a flow chart of the study's scope.

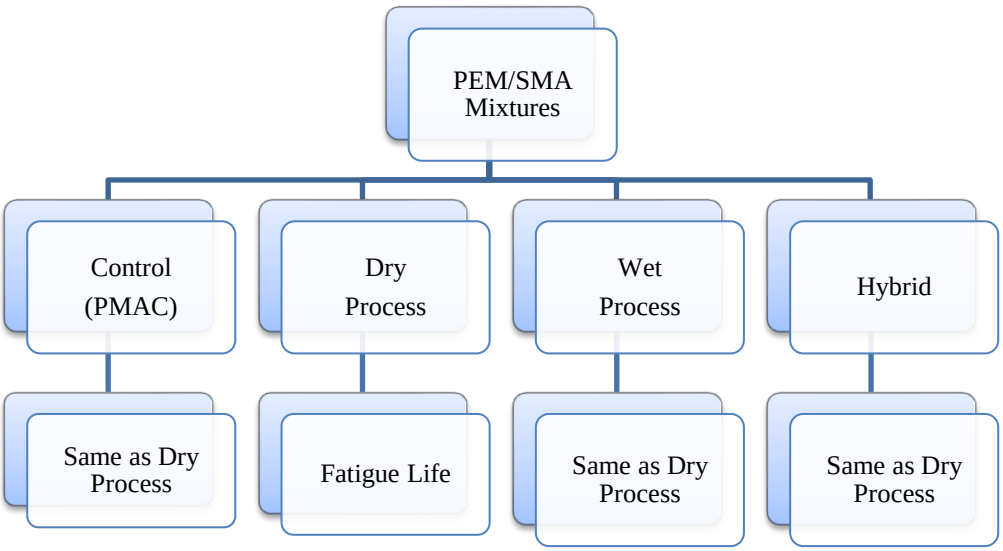

Figure 6-1. Flow chart for determining the fatigue life of rubberized PEM and SMA

6.2 Specimen Fabrication and Test Procedures

Specimen Fabrication

Specimens for the E* test were prepared as follows: Aggregates and binders were preheated in the oven for 5 hours before mixing at 165.5 ± 3 °C. The samples were placed in a forced-draft oven for 2 h ± 5 minutes before compaction to simulate short-term aging and stirred every 60 ± 5 minutes to maintain uniform conditioning. They were then gyrator-compacted at 160± 3°C.

Before proceeding to testing, each specimen's air void was measured. All PEM and SMA specimens used in this study have target air voids of 17.0 ± 0.5% and 5.0 ± 0.5%, respectively. Specimens were conditioned in an environmental chamber for 3 hours to reach the test temperature of 17 °C.

For the uniaxial constant crosshead (CX) fatigue test, specimen dimensions were 100 mm in diameter x 130 mm in height. They were glued to two end plates using a steel epoxy and a special gluing jig to eliminate any eccentricity.

Figure 6-2. Specimen fabrication

S-VECD Direct Tension Fatigue Test

This test, also called the uniaxial constant crosshead (CX) or *pull-pull* fatigue test, was performed to characterize the mixtures' fatigue performance. The machine actuator's displacement was programmed to reach a constant peak at each loading cycle. Due to machine compliance, the on-specimen strain measurements follow a power curve until failure, so the specimen does not experience a true controlled-strain or controlled-stress loading mode but rather a mixed mode. A true on-sample controlled strain or stress test using cylindrical specimens is difficult to run and can damage equipment if improperly performed (Hou 2009).

The effect of viscoplastic strain during the CX test was evident as the test temperature increased but negligible as it decreased: the softer the binder, the lower the test temperature. Sabouri and Kim (2014) suggested that a proper CX testing

temperature can be determined based on the PG of the binder (Eq. 6-1). The proper test temperature for the PG 67-22 and PG 76-22 used in this study would be lower than 19 °C, according to Eq. 6-1. However, a much lower test temperature may cause the samples to become brittle. Thus, a proper test temperature should be able to characterize viscoelastic damage when a material is not as brittle as it would be at a lower temperature and the effect of viscoplasticity is negligible (Hou 2009). Based on these considerations, 17 °C was selected as the CX test temperature in this study.

$$\mathrm{T(°C)} \leq \frac{\text{High temperature binder PG grade} + \text{low temperature binder PG binder}}{2} - 3 \leq 19°\mathrm{C} \quad (6\text{-}1)$$

Prior to the CX test, a small strain (50-75 on-specimen microstrain) was applied to determine the fingerprint dynamic modulus ($|E^*|_{Fingerprint}$), and Equation 6-2 was used to calculate the dynamic modulus ratio (DMR). A DMR value in the range of 0.9 to 1.1 guarantees that the linear viscoelastic properties obtained from the dynamic modulus tests can be used effectively in S-VECD analysis (Hou 2010). A target peak-to-peak on-specimen strain without adaptive strain control was then input to obtain the target actuator peak-to-peak strain or displacement used to control the entire fatigue test. The number of cycles at failure (N_f) was defined as the cycle at which the phase angle decreases sharply as a result of macro crack localization (Hou 2009).

$$DMR = \frac{|E^*|_{Fingerprint}}{|E^*|_{LVE}} \quad (6\text{-}2)$$

Where, $|E^*|_{LVE}$ is the linear viscoelastic dynamic modulus of the material at the particular temperature and frequency of the test.

The CX tests in this study were performed at 17 °C at a frequency of 10 Hz with an AMPT. Four to six replicate specimens at a target air void were measured at three strain amplitudes (high, medium, low) to produce a wide range of N_f (from 1,000 to 100,000). The data were analyzed using the fatigue analysis software developed at

North Carolina State University.

6.3 Results and Discussions

6.3.1 PEM Fatigue Performance

The S-VECD model can predict asphalt mixtures' fatigue life at various temperatures and strain/stress amplitudes based on the cyclic fatigue data at a single temperature and a single stress or strain amplitude. Figures 6-3 and 6-4 show the fatigue life at 5, 10, and 20 °C and 10 Hz loading frequency.

According to the strain-controlled simulation results (Figure 6-3), the difference between the fatigue life of the dry- and wet-processed CRM PEM mixtures was negligible, although the fatigue life of the dry-processed PEM mix was slightly lower than that of the wet-processed mixture as the temperature increased. However, both dry- and wet-processed CRM PEM mixtures had significantly lower fatigue life compared to hybrid and SBS-modified PEM mixtures, regardless of the temperature or strain levels. In addition, hybrid PEM mixes had a slightly longer fatigue life at lower temperatures and higher strain levels than SBS-modified PEM mixes, but this advantage disappeared as the temperature increased or the strain level decreased. Findings for the strain-controlled simulation hold true for the stress-controlled simulation (Figure 6-4).

Overall, the fatigue performance of the dry- and wet-processed CRM PEM mixes was similar but significantly worse than that of the hybrid and SBS-modified PEM mixes, which was similar.

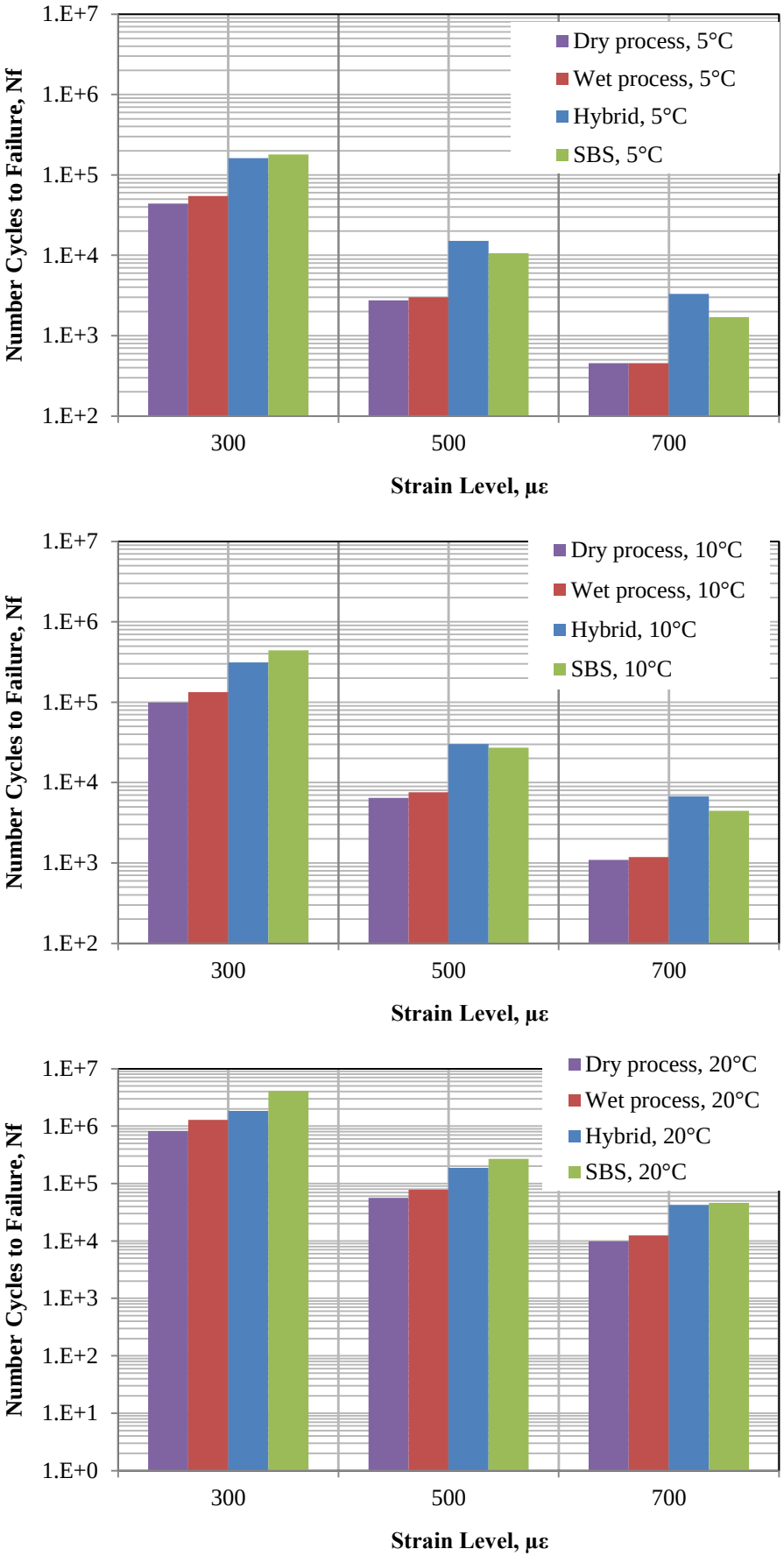

Figure 6-3. PEM fatigue life under strain control

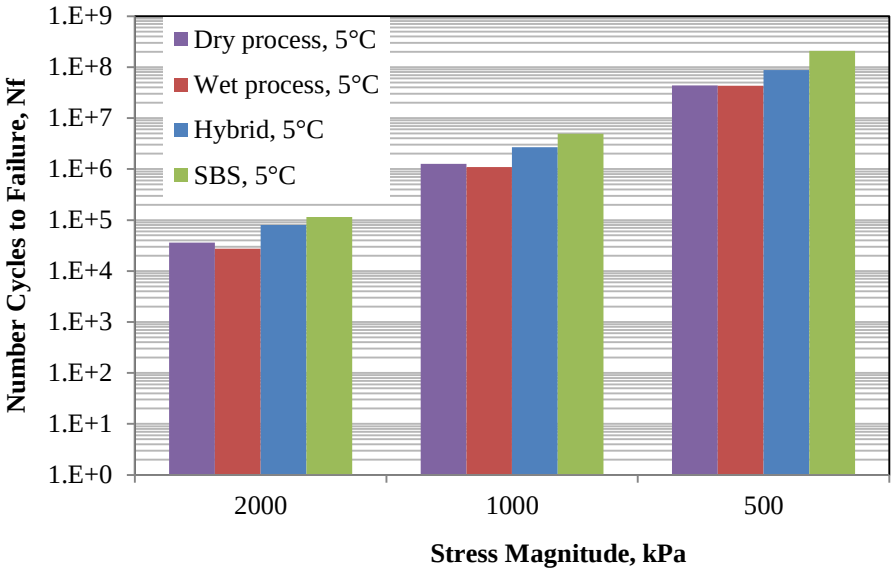

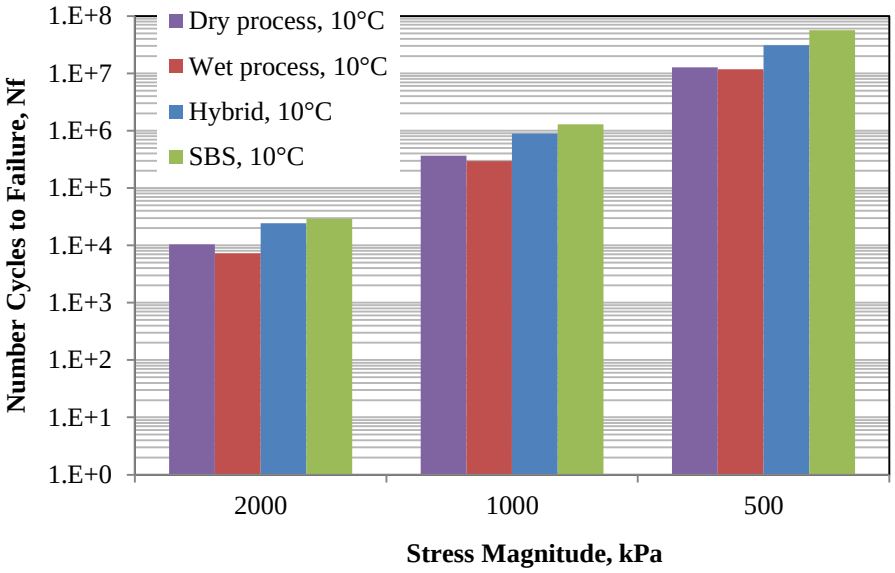

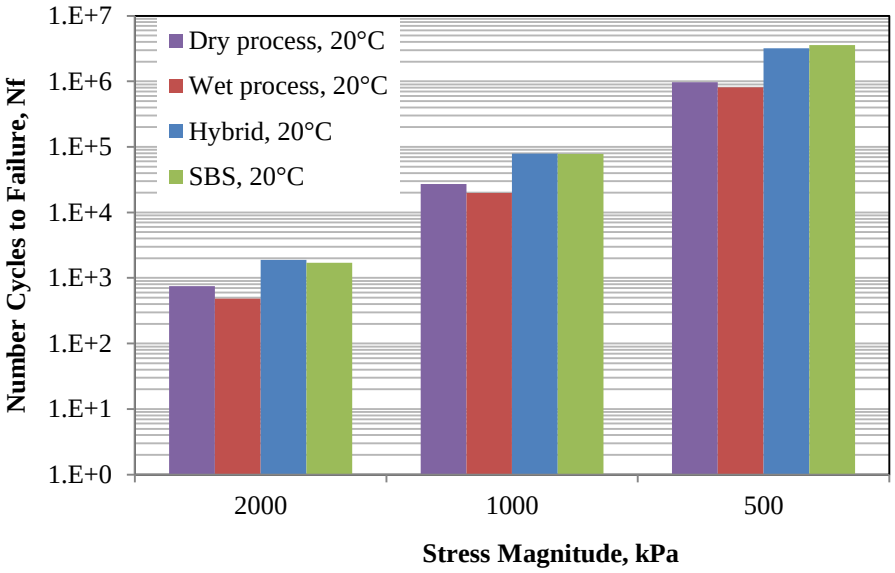

Figure 6-4. PEM fatigue life under stress control

6.3.2 SMA Fatigue Performance

Figures 6-5 and 6-6 show the fatigue life of strain- and stress-controlled samples, respectively, at 5, 10 and 20 °C and 10 Hz loading frequency. According to the strain-controlled simulation results, the fatigue life of the dry- and wet-processed CRM SMA mixtures was similar at higher strain (500 and 700με), while slightly better for the dry-processed at lower strain (300 με). Compared to the hybrid and SBS-modified SMA mixes, the dry-processed CRM SMA had a slightly higher N_f at lower strain (300 με) and a significantly lower N_f at higher strain (500 and 700με), especially at lower temperatures (5 and 10 °C).

According to the stress-controlled simulation results (Figure 6-6), the fatigue life of the dry- and wet-processed CRM SMA mixes was similar, regardless of stress level or test temperature. N_f of the dry-processed CRM SMA was similar to those of the hybrid and SBS-modified SMA mixes at 5 °C and lower as the test temperature increased (10 and 20 °C).

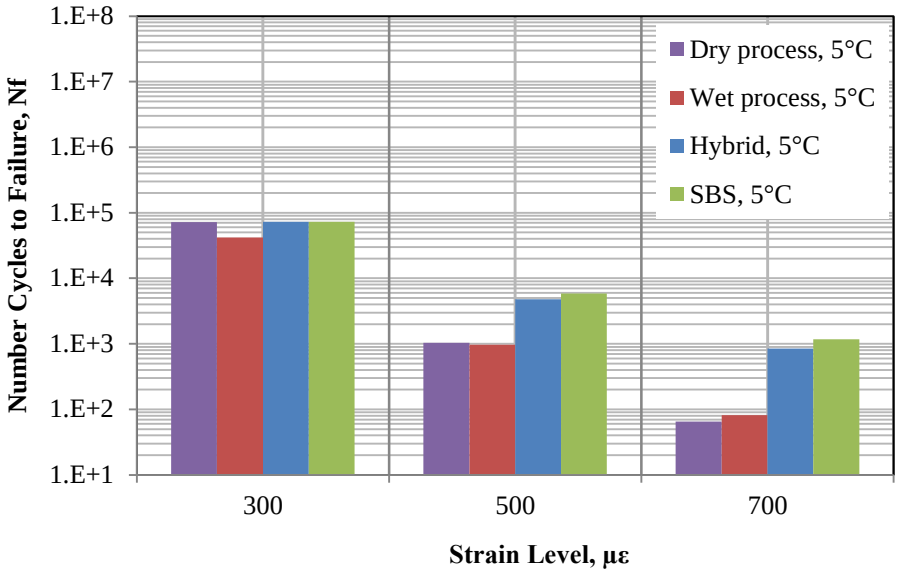

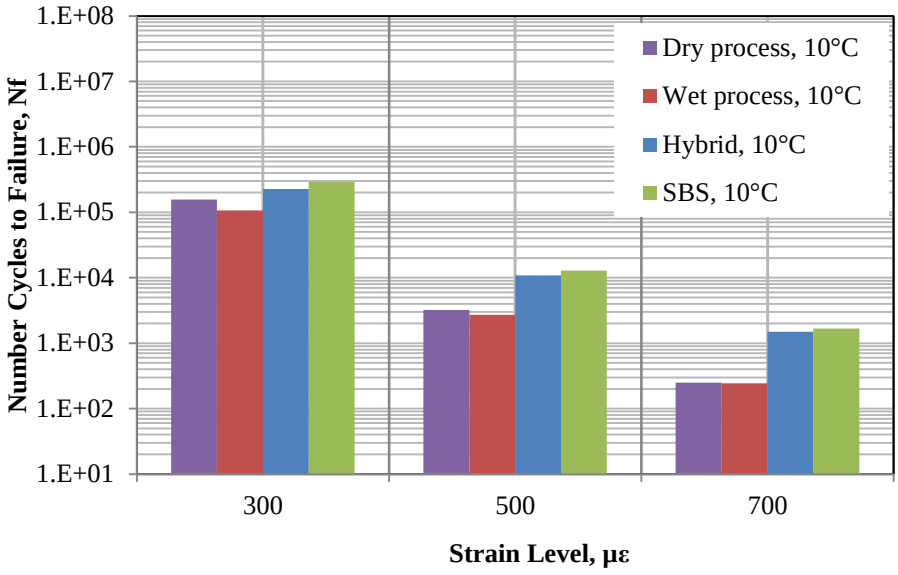

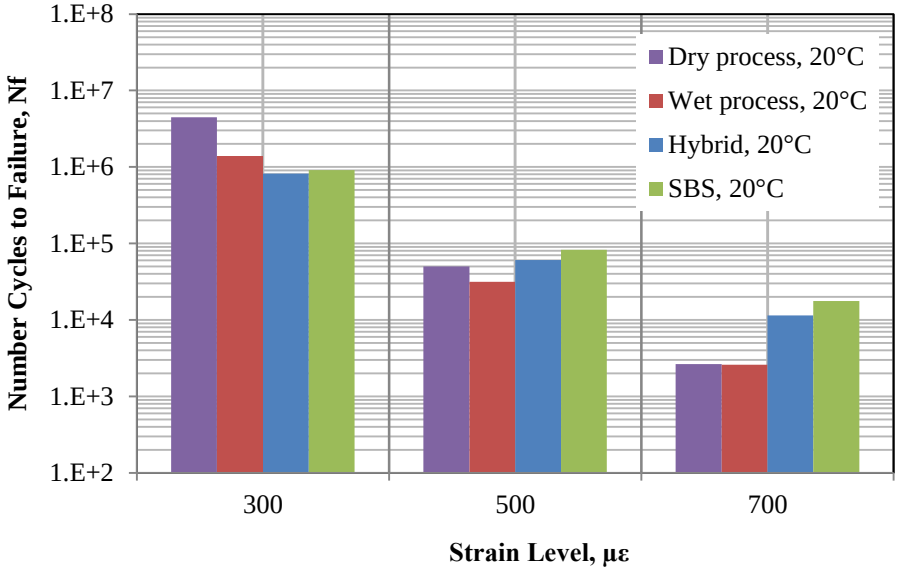

Figure 6-5. SMA fatigue life under strain control

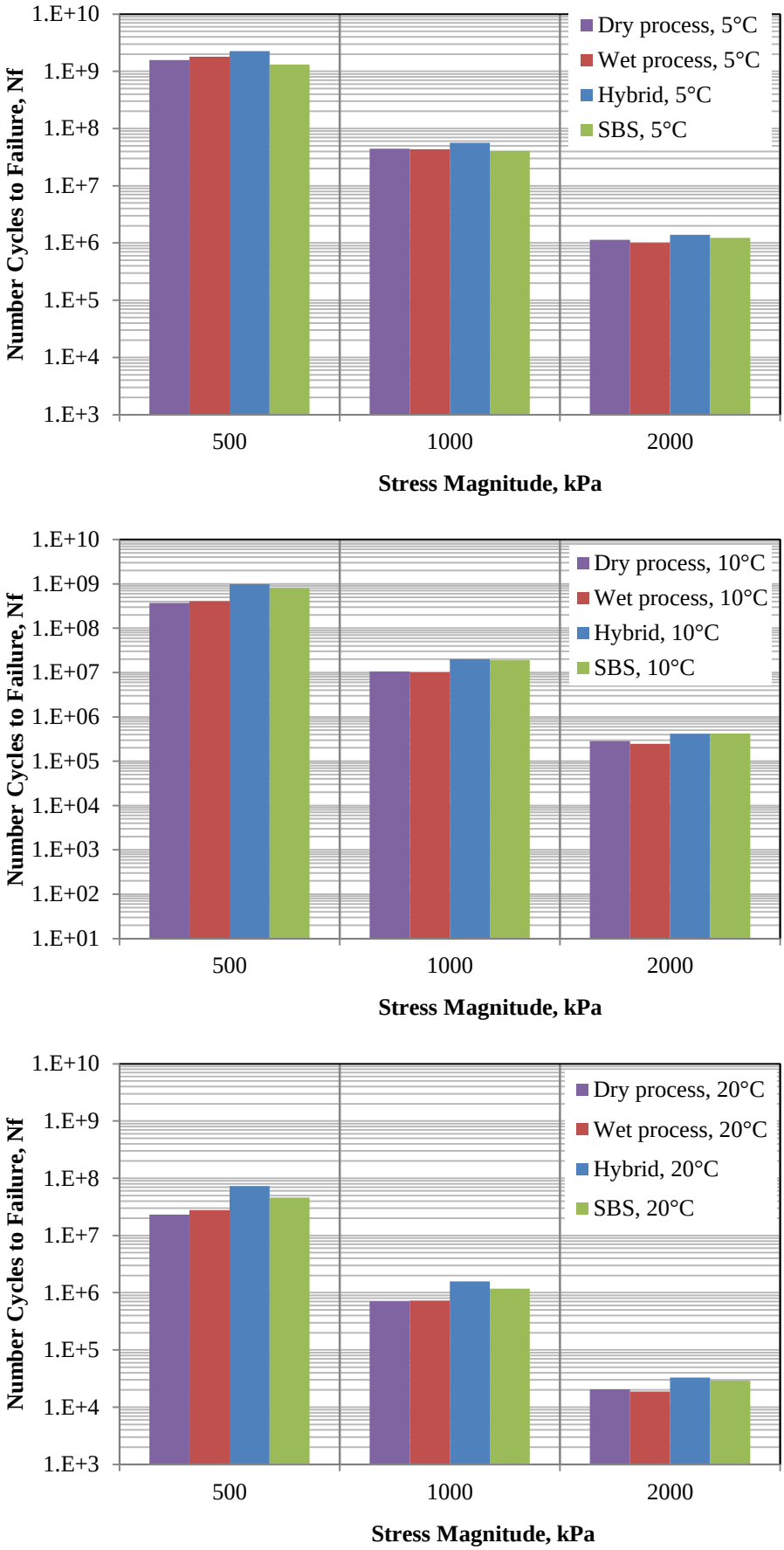

Figure 6-6. SMA fatigue life under stress control

6.4 Summary and Conclusions for Fatigue Testing of PEM and SMA Mixtures

The effect on the viscoelastic and fatigue properties of PEM and SMA mixtures with variously modified asphalt binders (dry- and wet-processed CR, hybrid, and SBS) was investigated at 17 °C and 10Hz. Results show:

1. The fatigue performance of the dry- and wet-processed CRM PEM mix was similar but significantly worse than that of hybrid and SBS-modified PEM mixes, which was similar, regardless of temperature or loading conditions.

2. Under strain-controlled loading, the fatigue life of the dry-processed CRM SMA mix was similar to that of the wet-processed at higher strain (500 and 700με) but slightly higher at lower strain (300 με). The N_f of the dry-processed CRM SMA was slightly higher at lower strain (300 με) and significantly lower at higher strain (500 and 700με), especially at lower temperature (5 and 10 °C), than that of the hybrid and SBS-modified SMA mixtures.

3. Under stress-controlled loading, N_f of the dry- and wet-processed CRM SMA was similar, regardless of stress level or test temperature. N_f of the dry-processed CRM SMA was similar to that of the hybrid and SBS-modified SMA mixes at lower temperature (5 °C) but lower as the test temperature increased (10 and 20 °C).

CHAPTER 7 EFFECT OF WEATHERING ON RUBBERIZED PEM AND SMA

7.1 Introduction

Durability is one of the primary concerns of asphalt mix design, and weathering has not been sufficiently addressed. Current laboratory methods for simulating long-term aging focus on thermal oxidation aging in an oven, but field weathering combines lights, water, and thermal cycling, which no oven or binder-aging equipment, such as the RTFO and PAV methods, can simulate. An effective way to consider all the factors that contribute to asphalt mixture aging resistance is a weathering machine that can simulate the combined effects of heat, UV, oxidation, and rain. Hagos (2008) and Grzybowski et al. (2012) reported the combined effect of environmental factors ((UV light, oxidation, and moisture) on the performance of asphalt concrete. Here, we explored the effect of weathering on the durability properties of PEM and SMA mixture samples. Figure 7-1 shows the testing plan.

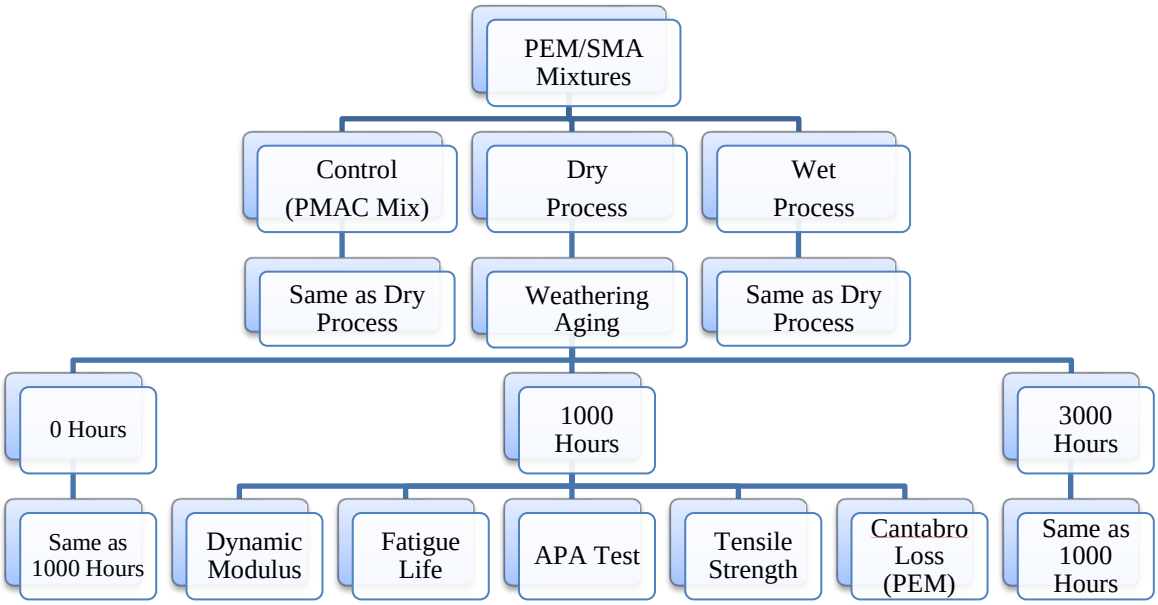

Figure 7-1. Flow chart to measure the durability properties of PEM and SMA

7.2 Materials and Test Procedures

The Georgia asphalt weathering device (GAWD) was designed to simulate the combined environmental conditions of UV light, water, and temperature. It weathers compacted asphalt mixture specimens from the top down, simulating the natural aging of in-place asphalt pavement. It consists of an environmental chamber, water-treatment system, and system controller (Fig. 7-2). Fluorescent UV-B lamps are used, as detailed in 6.1.3.3 of ASTM G154, and three 47-inch ATI Dimmable SunPower T5 lighting ballasts provide programmable intensities. It can distill and cool fresh water to 7.2 ± 3 ºC according to ASTM standard 4799. A heater in the environmental chamber ensures a constant temperature of 60 ºC. APWS testing parameters for one weathering cycle are: 51-min UV light exposure and 9-min UV light and water spray at 60 °C. These parameters come from the cycle requirements outlined in ASTM Standards 4799 and 4798.

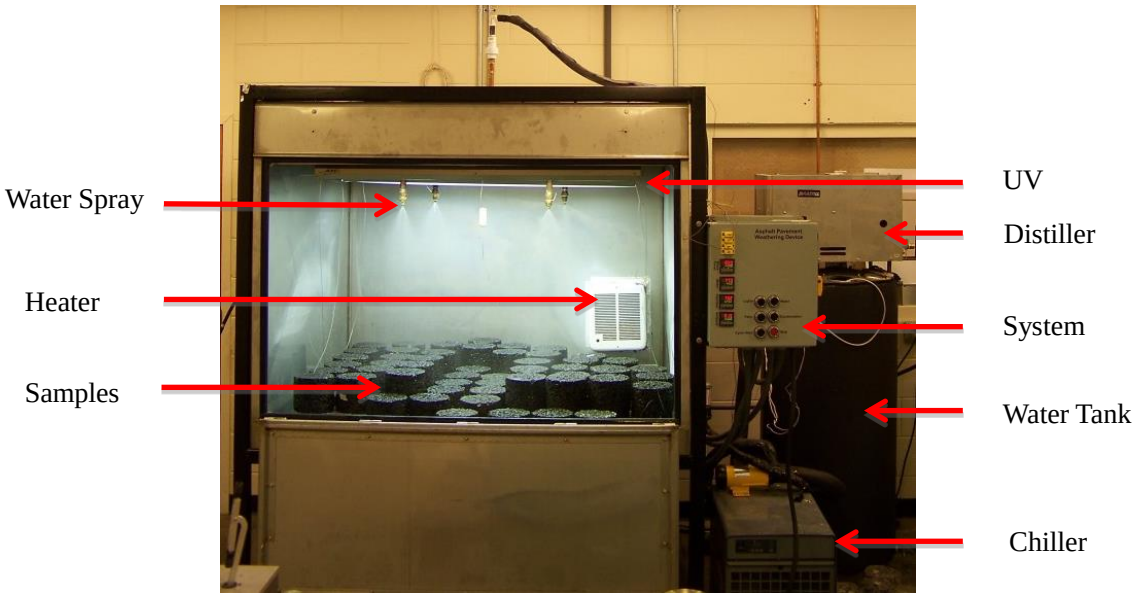

Figure 7-2. Georgia asphalt weathering device

Grzybowski et al. (2012) reported that 3,000-hours' weathering is similar to PAV aging. Therefore, Superpave gyratory compacted (SGC) PEM and SMA mixture samples were weathered in the device for 1,000 and 3,000 hours (Figure 7-2).

7.3 Results and Discussions

7.3.1 Influence of weathering on |E*| of PEM

Figure 7-3 shows the |E*| master curve of unaged and aged PEM mixture samples. A t-test ($\alpha = 0.05$) was used to determine whether the dry-processed rubberized PEM mix performed as well as the other PEM mixes. The t-test showed no significant difference, regardless of aging.

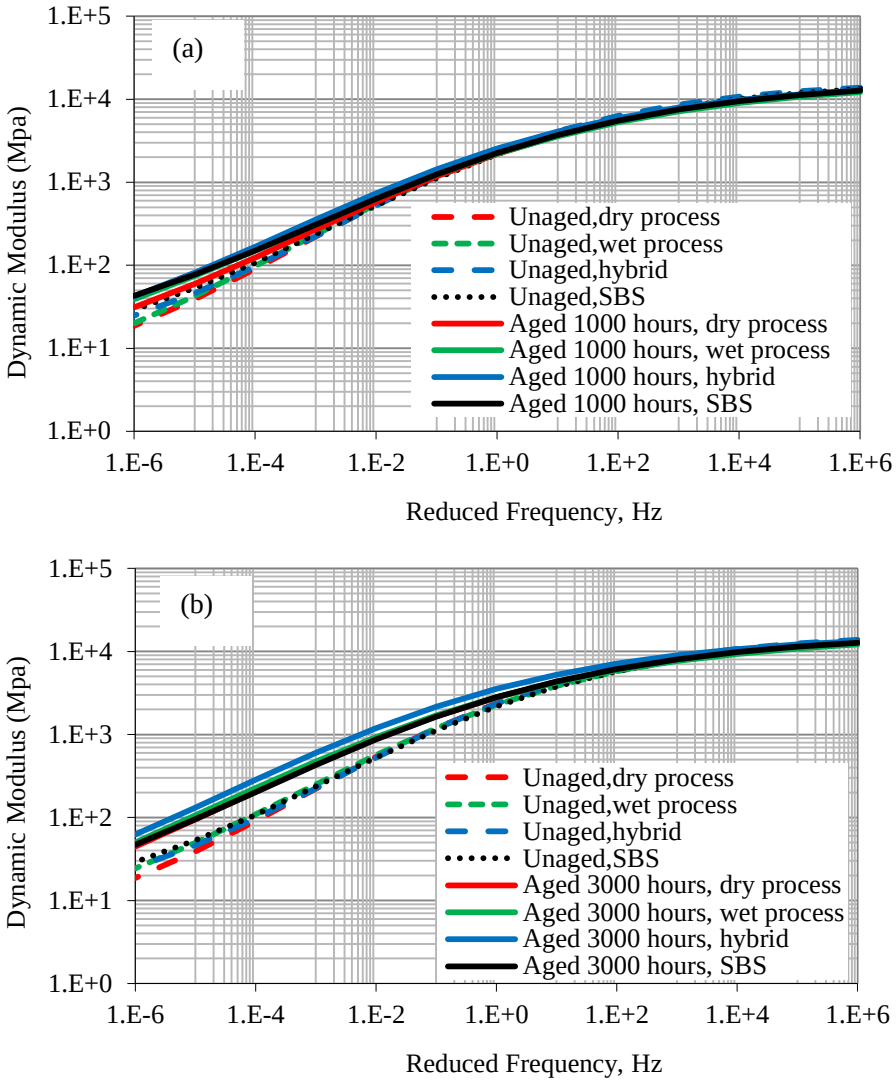

Figure 7-3. |E*| master curves: (a) unaged and 1000-hour aging; (b) unaged and 3000-hour aging

Furthermore, a t-test ($\alpha = 0.05$) was performed to compare |E*| between aging levels: unaged versus 1,000-hour aging and unaged versus 3,000-hour aging for each PEM mixture. The results showed no difference between unaged and 1,000-hour aged specimens, but statistically significant differences between unaged and 3,000-hour aged specimens at low frequency and low temperatures (0.1 Hz at 4 °C and 20 °C) or high temperature (45 °C). Weathering had more effect on |E*| at a low frequency or a high temperature than at a high frequency or a low temperature.

Many honeycomb-like structures were observed on the asphalt binder surface of

the PEM samples, indicating that it foamed due to the interaction of the environment factors (Figure 7-4).

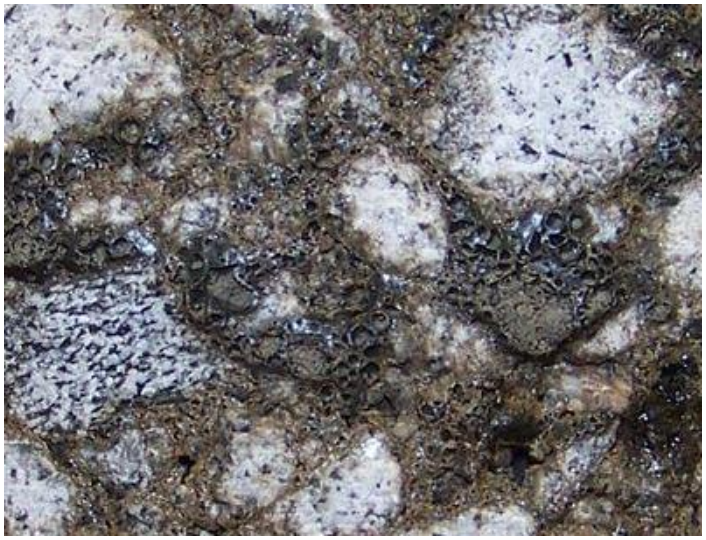

Figure 7-4. Asphalt foamed in PEM samples

The ratio of |E*| between the long-term aged and unaged specimens can elucidate the effects of aging on the mixtures' stiffness. To compare the effect of weathering on |E*|, aging ratio (AR) was calculated according to Equations 7-1 and 7-2. Figures 7-5 to 7-8 show the results of AR for all PEM mixtures. For simplicity, 1,000- and 3,000-hour aging in the weathering device were noted as long-term aging level 1 (LTA1) and long-term aging level 1 (LTA2), respectively.

$$AR1 = \frac{|E^*|_{LTA1}}{|E^*|_{unaged}} \tag{7-1}$$

$$AR2 = \frac{|E^*|_{LTA2}}{|E^*|_{unaged}} \tag{7-2}$$

where:

AR = Aging Ratio

$|E^*|_{unaged}$= |E*| value for unaged mixture

$|E^*|_{LTA1}$= |E*| value for 1,000-hour aged mixture

$|E^*|_{LTA2}$= |E*| value for 3,000-hour aged mixture

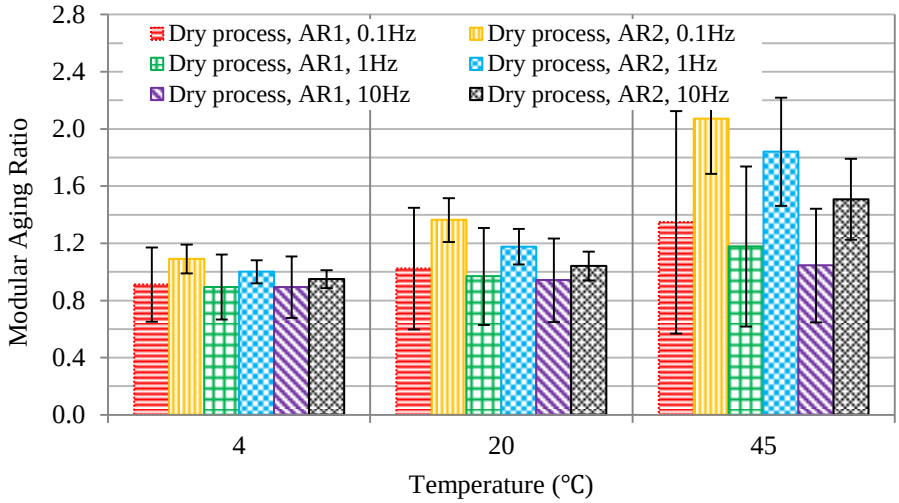

Figure 7-5. Modular aging ratio for dry-processed rubberized PEM

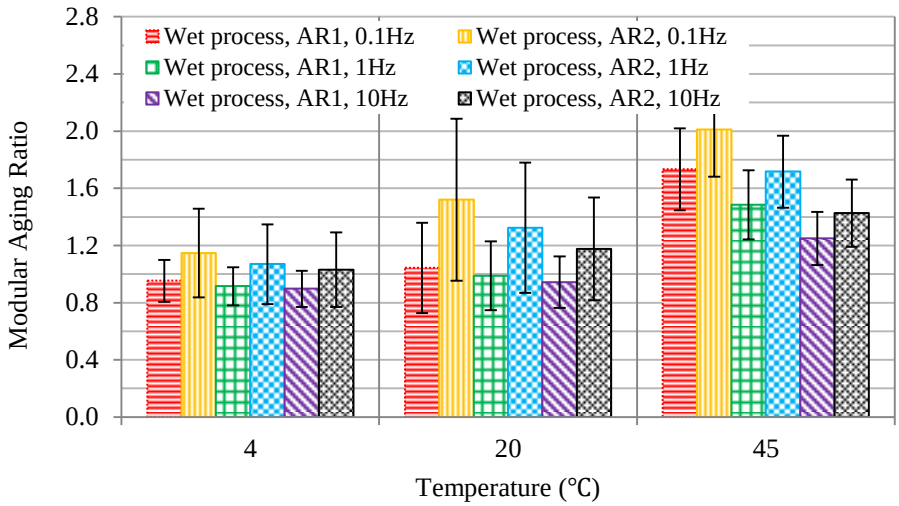

Figure 7-6. Modular aging ratio for wet-processed rubberized PEM

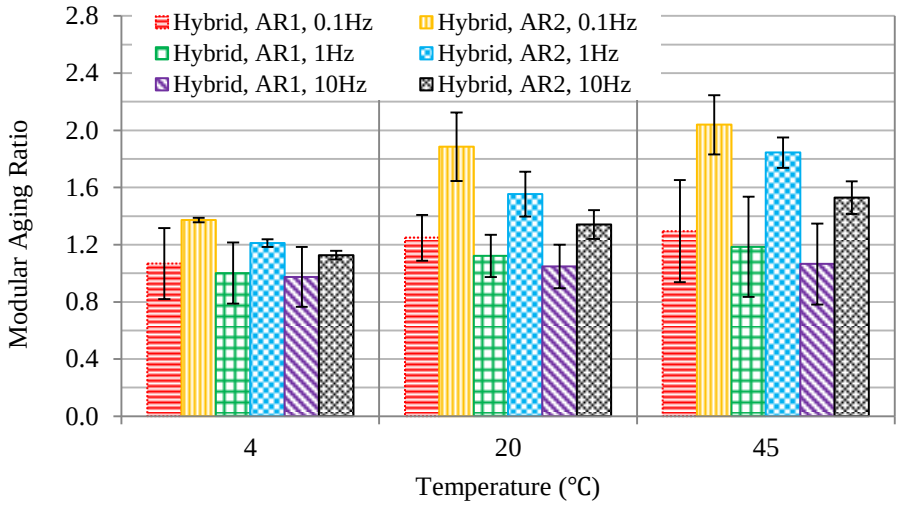

Figure 7-7. Modular aging ratio for hybrid PEM

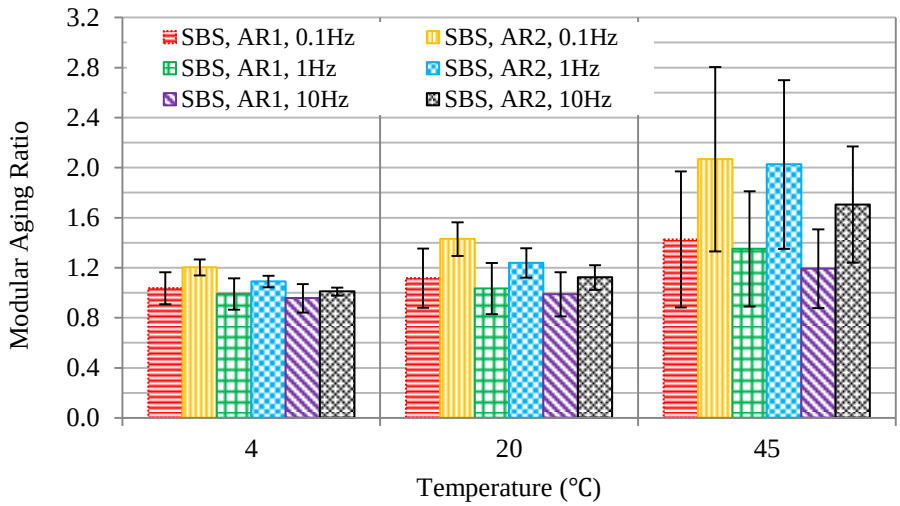

Figure 7-8. Modular aging ratio for SBS PEM

Figures 7-5 to 7-8 indicate that both AR1 and AR2 for all PEM mixtures increased with an increase in temperature, suggesting that weathering had more effect on |E*| at high temperatures than at low temperatures. Note that all AR1 at 4 °C and AR2 at 0.1 Hz and 4 °C are less than 1.0, indicating that the |E*| of all PEM mixtures at 4 °C or at 0.1 Hz and 4 °C decreased after LTA1 or LTA2. The effect of moisture on PEM samples may be responsible.

Compared to the control SBS-modified PEM specimens, both dry- and wet-processed PEM specimens had higher AR1 and AR3 values at a low frequency and a high temperature (0.01 or 0.1Hz at 45 °C), while AR1 and AR2 values for both dry- and wet-processed rubberized PEM mixes were lower at a low temperature (4 °C). Thus, both dry- and wet-processed CRM PEM mixes exhibited higher |E*| rates at a high temperature and lower at a low temperature than the control SBS-modified PEM mix after 1000- or 3000-hour weathering.

7.3.2 Influence of weathering on |E*| of SMA

Figure 7-9 shows the |E*| master curve of unaged and aged SMA samples. A t-test (α = 0.05) determined that the dry-processed CRM SMA mixture's |E*| did not differ

significantly from the others', with or without aging, indicating similar weathering resistance.

A t-test ($\alpha = 0.05$) was also performed to compare |E*| between aging levels: unaged versus 1,000-hour aging and unaged versus 3,000-hour aging for each SMA mixture. Trends were similar to those found for the PEM mixtures: no difference between unaged and 1,000-hour aging, but 3,000-hour aging had a significant effect on |E*| at lower frequency (0.1 Hz) or higher temperature (45 °C).

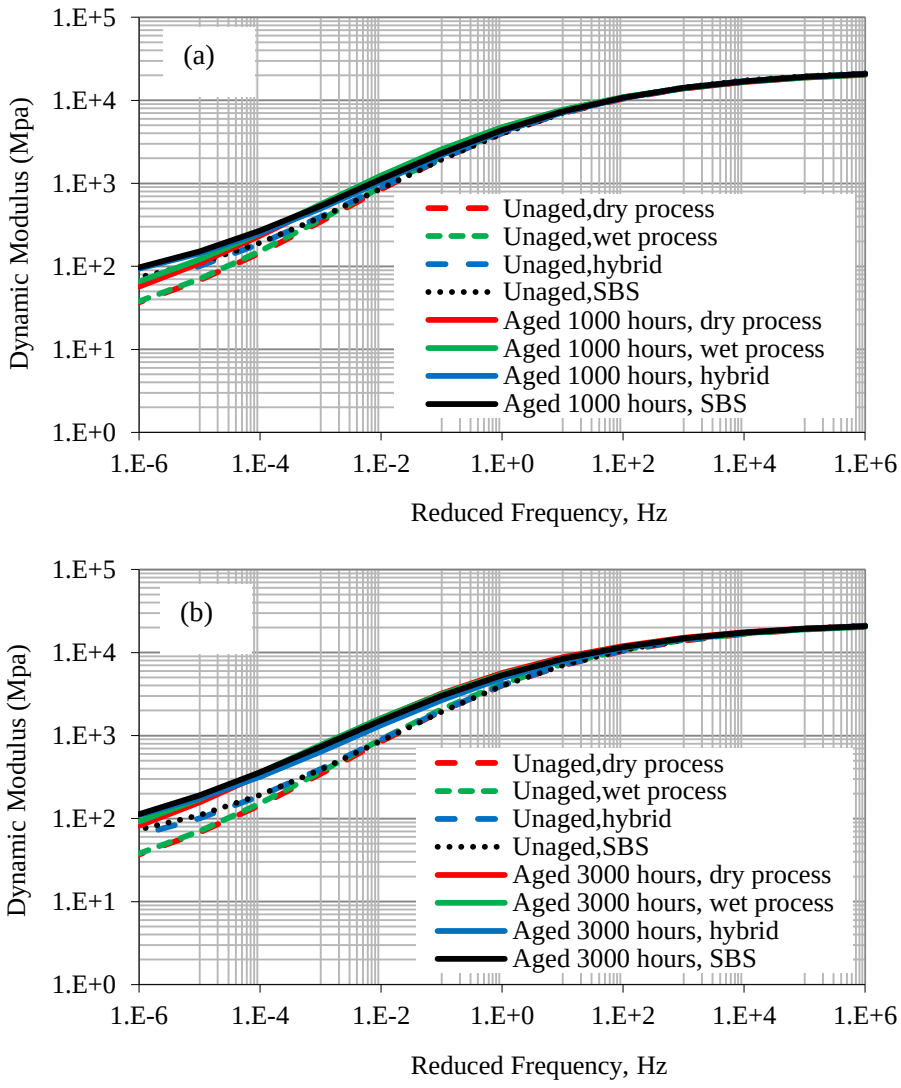

Figure 7-9. |E*| master curves for SMA: (a) unaged and 1000-hour aging; (b) unaged and 3000-hour aging

Figures 7-10 to 7-13 show aging ratio (AR) results for all SMA mixtures. Both AR1 and AR3 values at higher temperature (45 °C) or lower load frequency (0.1 Hz)

were higher than those at lower temperature or higher load frequency. The trend of AR1 and AR2 for SMA is the same as for PEM. Both dry- and wet-processed CRM SMA mixtures exhibited slightly higher AR1 and AR2 values at higher temperature than hybrid and SBS-modified SMA mixtures, indicating that at a high temperature, |E*| increases more in rubberized SMA mixes than in hybrid and SBS-modified SMA mixes after 1,000- or 3,000-hour weathering.

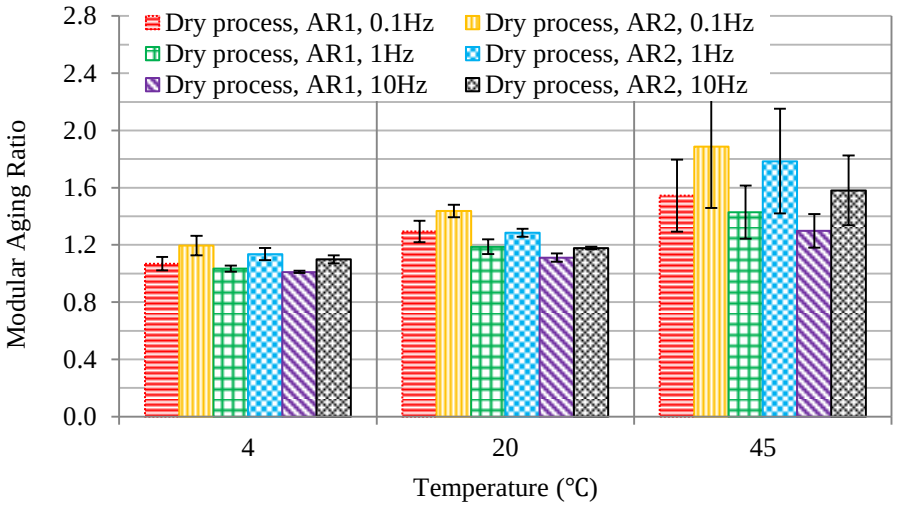

Figure 7-10. Modular aging ratio for dry-processed rubberized SMAs

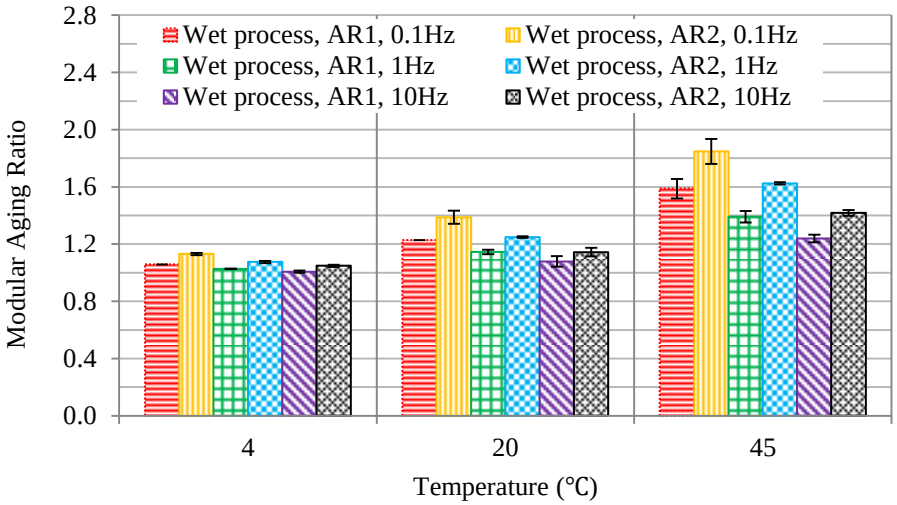

Figure 7-11. Modular aging ratio for wet-processed rubberized SMAs

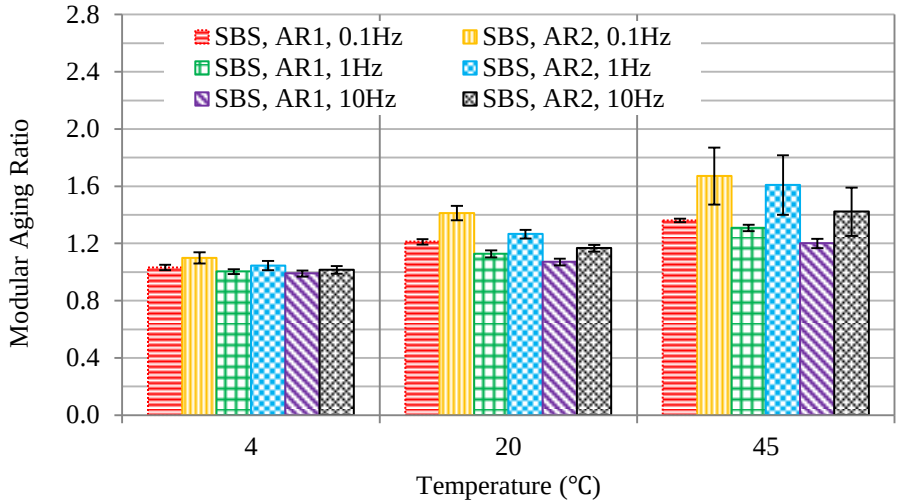

Figure 7-12. Modular aging ratio for SBS SMA

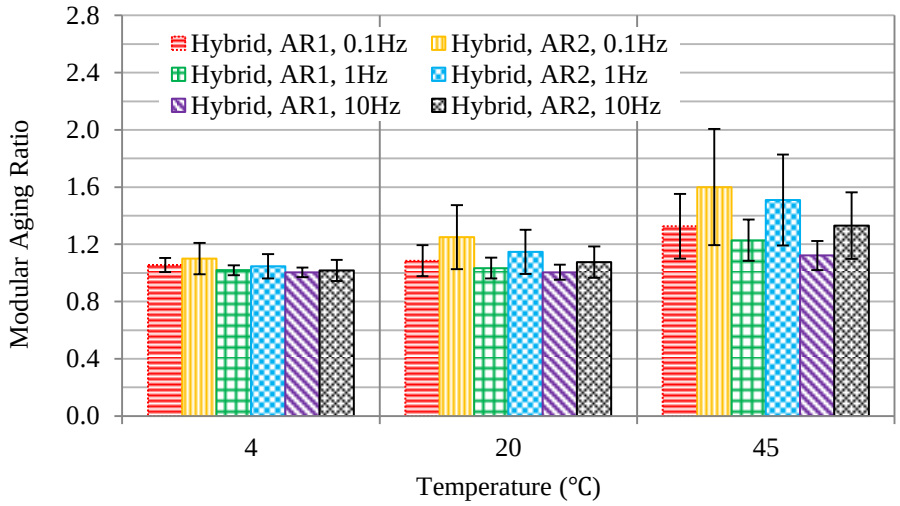

Figure 7-13. Modular aging ratio for hybrid SMA

7.3.3 Influence of weathering on fatigue life

CX tests showed two types of failure patterns for aged PEM and SMA samples. Mid-failure tests are considered good because the LVDTs are able to capture the major damage throughout the test. End-failure tests are not as good since macro-cracking localizes beyond the experimental measurement range (Hou 2009; 2010). Therefore, we consider end-failure test results invalid in this study.

Most PEM samples aged either 1,000 or 3,000 hours had top end-failures because they had higher air voids; aging at the top was worse than at the bottom, resulting in easy macro-cracking, and CX testing was not successful. Most aged SMA samples

had mid-failures; the CX test was successful. It also found that aged samples had more end-failures than unaged samples; few unaged samples had end-failures.

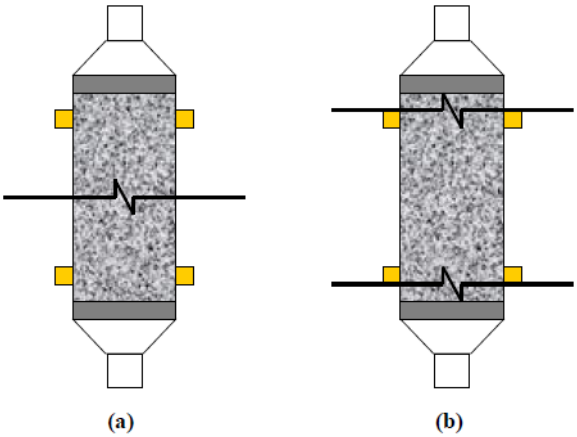

Figure 7-14. Failure locations: (a) mid-failure; (b) end-failure (Hou 2009)

Figures 7-15 and 7-16 show the fatigue life results for the 3000-hour SMA mixes. The fatigue life of the dry- and wet-processed CRM SMA mixes were similar, regardless of strain and stress level or test temperature. However, N_f of the dry-processed CRM SMA mix was lower than that of hybrid and SBS-modified SMA mixtures, regardless of strain and stress level or test temperature.

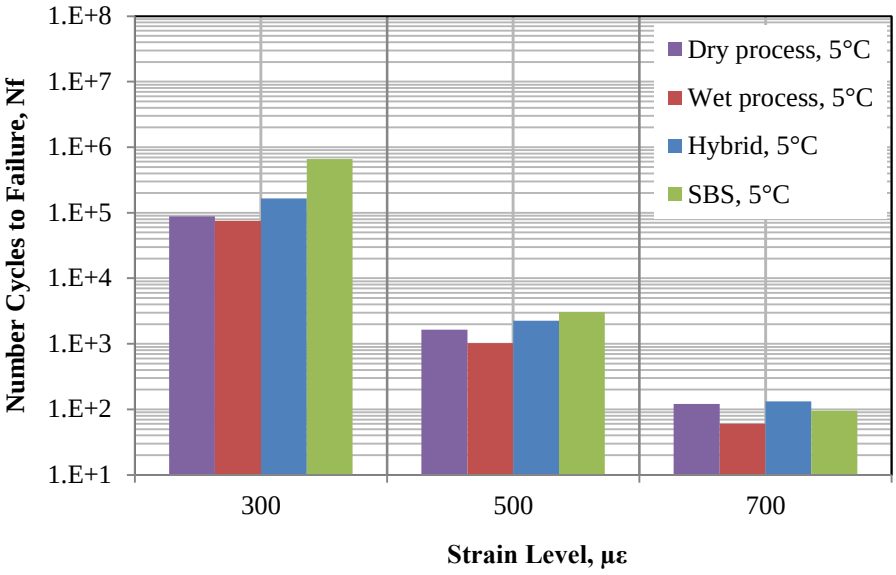

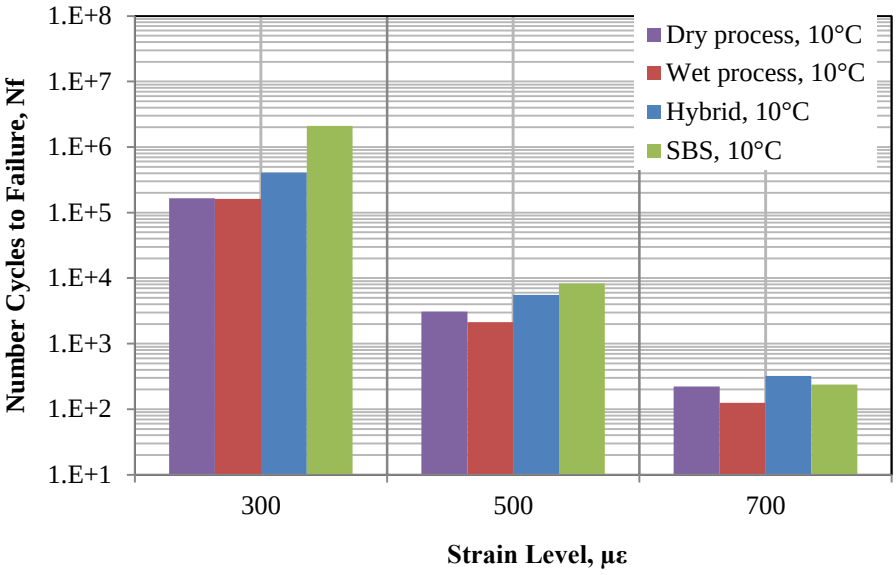

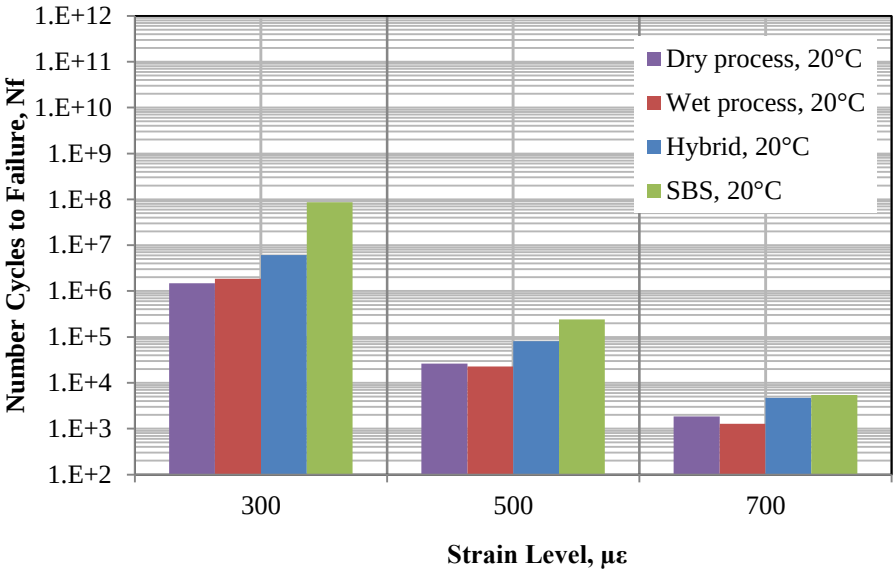

Figure 7-15. SMA fatigue life under strain control after 3,000-hour aging

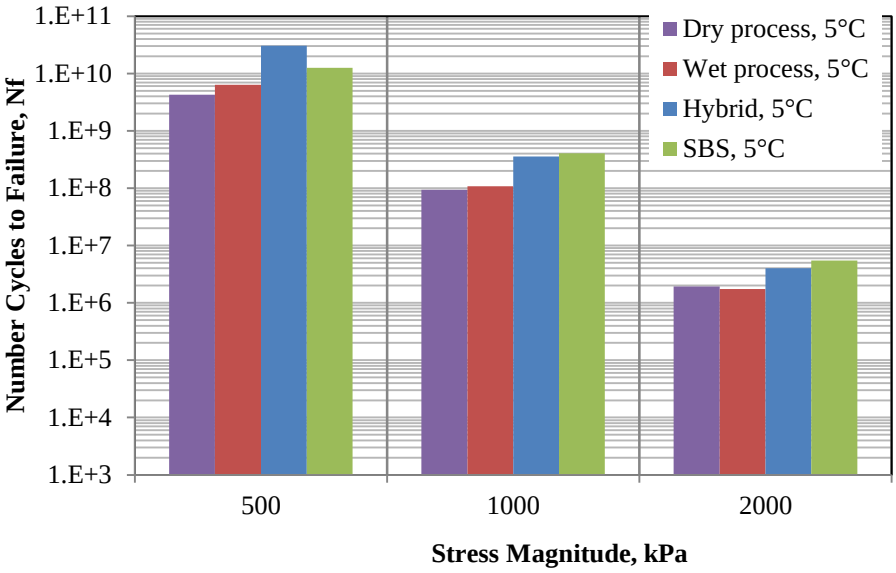

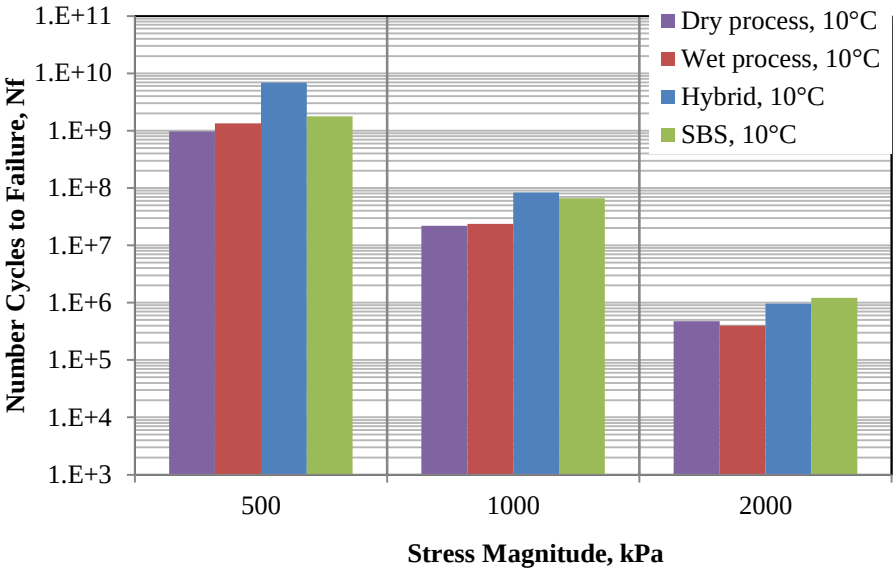

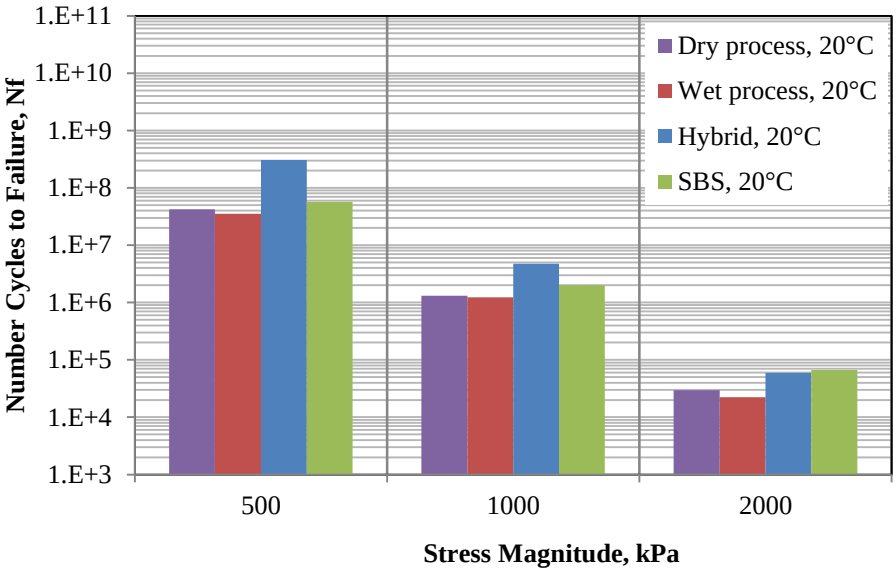

Figure 7-16. SMA fatigue life under stress control after 3,000-hour aging

7.3.4 Influence of weathering on rutting resistance

Figure 7-17 shows the rutting depth results for unaged and aged PEM mixtures. As expected, rutting depth decreased as weathering time increased. For unaged samples, the rutting depth of dry-processed CRM PEM (2.6 mm) was similar to that of SBS-modified PEM (2.7 mm); less than that of the wet-processed CRM mixture (3.2 mm); and more than that of the hybrid PEM mix (2.1 mm). After 1,000-hours aging, the rutting depth of the dry-processed CRM PEM mix was higher than that of the other three PEM mixtures. After 3,000-hour aging, the rutting depth of the dry- and wet-processed CRM PEM mixtures was similar but higher than that of the hybrid and SBS-modified PEM mixtures. Furthermore, hybrid PEM mix had the lowest rutting depth, regardless of aging.

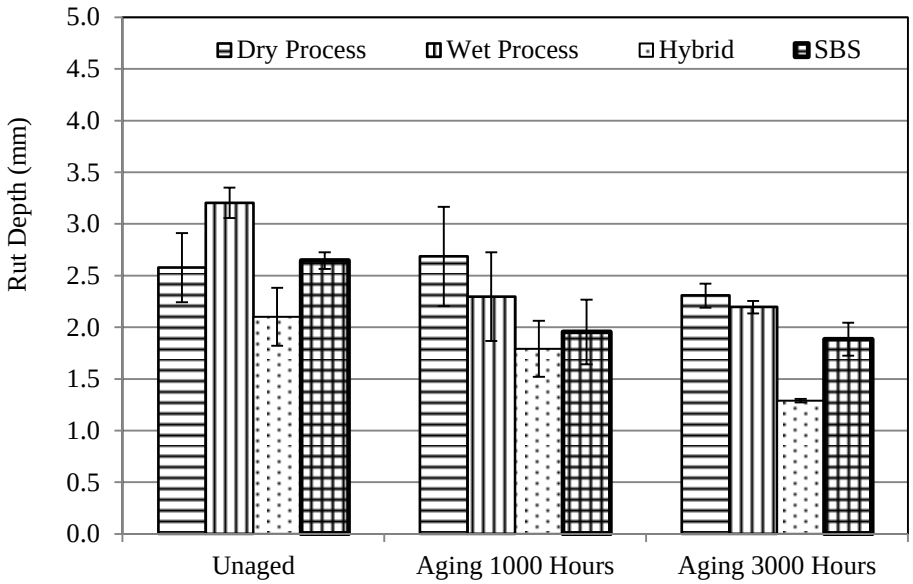

Figure 7-17. PEM rut depth

Figure 7-18 shows the rutting depth results for unaged and aged SMA mixtures. As for PEM, rutting depth decreased as weathering time increased. For the unaged samples, dry-processed CRM SMA had the deepest rutting followed by SBS-modified SMA and wet-processed CRM SMA. Dry- and wet-processed CRM SMA rutting was

similar and deeper than that of hybrid and SBS SMA, regardless of aging time. Hybrid SMA, like hybrid PEM, had the least rutting, regardless of aging.

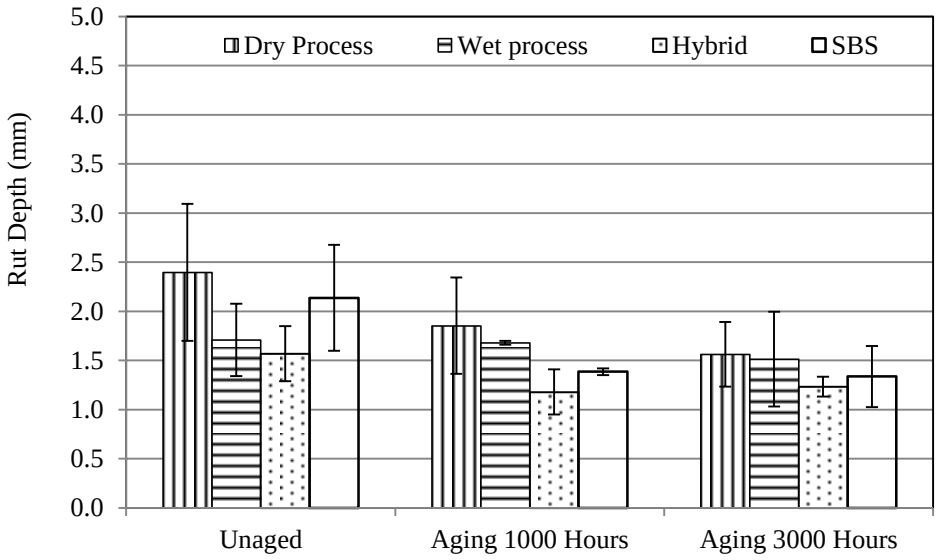

Figure 7-18. SMA rut depth

7.3.5 Influence of weathering on Cantabro loss

The raveling resistance of PEM mixtures is generally investigated using the Cantabro loss test, which evaluates the bonding between aggregate particles and asphalt binders based on abrasion and impact. In this test, the gyration samples with a diameter of 150 mm and a height of 130 mm are weighed and placed in a Los Angeles Abrasion Tester without the steel ball, and the drum is turned for 300 revolutions. The percentage of mass lost during this process is used to evaluate the raveling resistance of PEMs.

Figure 7-19 shows the Cantabro loss results for unaged and aged PEM mixtures. Hybrid PEM had the highest loss (18.4%); dry- and wet-processed CRM PEM mixtures had similar losses (17.7% and 17.4%, respectively); SBS-modified PEM had the least loss at 14.9%. After 1,000 and 3,000 hours of aging, Cantabro loss was similar in dry- and wet-processed CRM PEM samples but higher in the hybrid and SBS-modified PEM. SBS-modified PEM had the least Cantabro loss, regardless of aging.

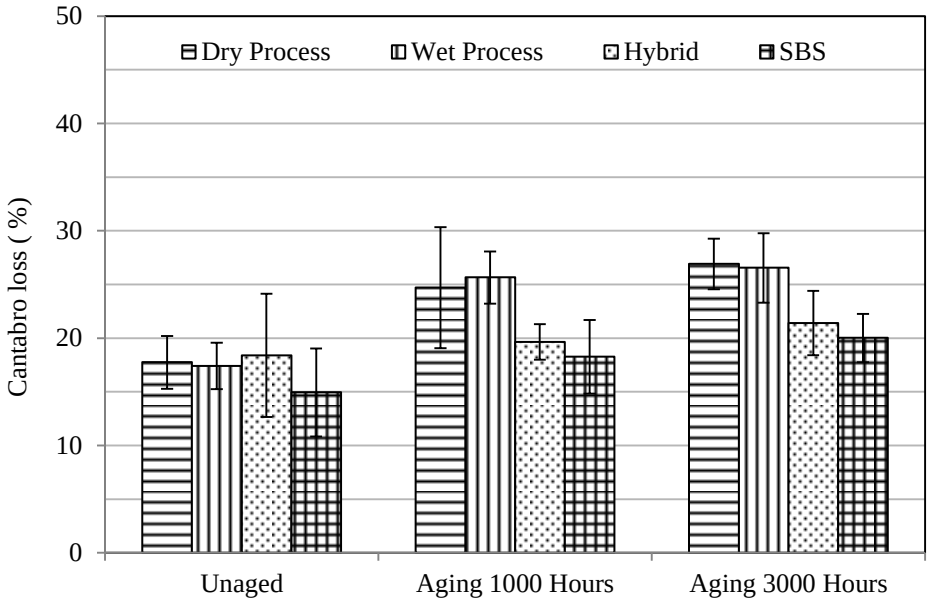

Figure 7-19. Cantabro loss results

7.3.6 Influence of weathering on indirect tensile strength

The indirect tensile strength test (IDT) is used to determine asphalt concrete mixtures' strength and resistance to fatigue, temperature cracking, and rutting. Testing was conducted according to ASTM D 6931–12.

Prior to the IDT test, the specimens were placed in a water bath for ≥30<120 minutes. During testing, 13-mm-wide strip loading was used for a 101-mm-diameter specimen to provide uniform loading at a loading rate of 51 mm/minute. Peak load was recorded, and the split tensile strength calculated using Equation 7-3.

$$S_t = \frac{2000P}{\pi tD} \quad (7\text{-}3)$$

where St=IDT strength, kPa

P=maximum load, N

t=specimen height, mm

D=specimen diameter, mm.

Figure 7-20. Water bath

Figure 7-21. Indirect tensile strength test

Figures 7-22 and 7-23 illustrate the IDT results for unaged and aged PEM and SMA mixtures. IDT values increased after 1,000 hours then decreased after 3,000 hours for all mixtures except those with dry-processed CRM, which increased continually after both aging conditions. For PEM mixtures, the IDT value of the

unaged, dry-processed CRM mix was lowest followed by wet-processed CRM mix; it was significantly higher for the hybrid and SBS-modified mixtures. However, after 3,000 hours, the IDT values for the dry- and wet-processed CRM PEM were similar and higher than that of the hybrid and SBS-modified PEM. Among the SMA mixtures, unaged, dry-processed CRM had a slightly lower IDT than the others, but after 3,000 hours, the IDT of both dry- and wet-processed CRM mixes was higher than that of the hybrid and SBS-modified mixtures.

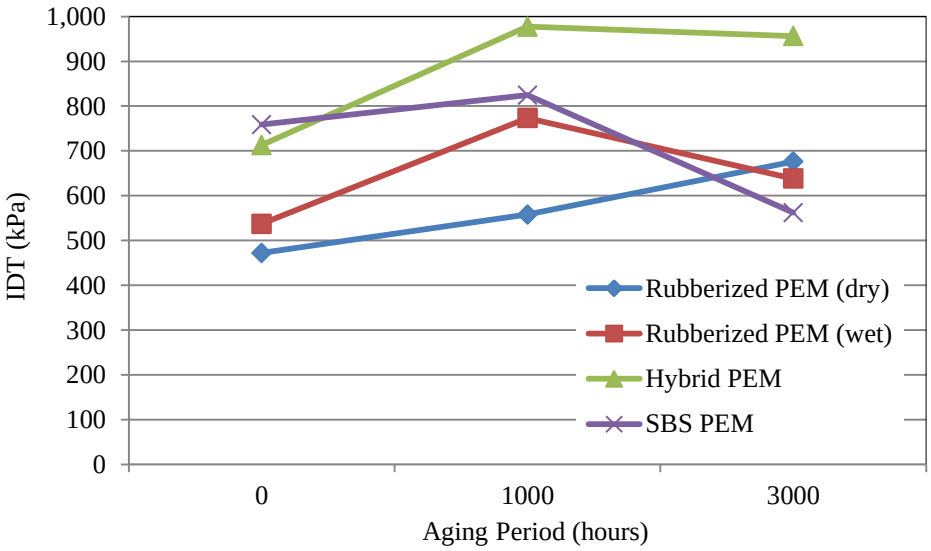

Figure 7-22. Indirect tensile strength results for PEM

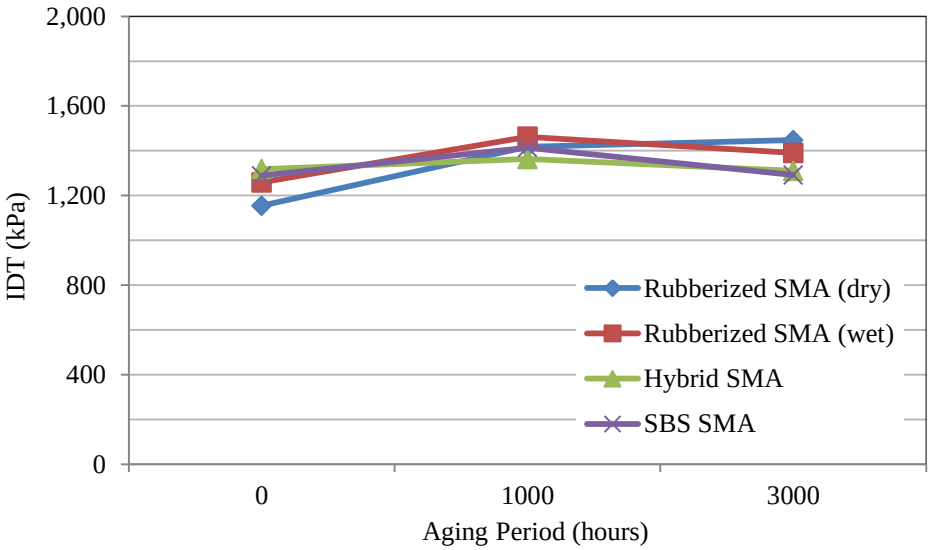

Figure 7-23. Indirect tensile strength results for SMA

7.4 Summary and Conclusions on Weathering Effects

The effect of weathering on the performance of CRM, hybrid, and SBS-modified asphalt binders mixed with PEM and SMA was tested and the following conclusions can be drawn:

1. The |E*| of dry-processed CRM PEM and SMA mixes did not differ significantly from the other samples', regardless of aging duration (unaged, 1,000, or 3,000 hours).
2. The |E*| for each PEM and SMA mixture did not differ significantly between unaged and 1,000 hours of aging. However, they were all significantly hardened after 3,000 hours of aging.
3. After 3000-hours' aging, the fatigue life of dry-processed CRM SMA mix was similar to that of wet-processed but shorter than that of hybrid and SBS-modified SMA mixes, regardless of strain and stress levels and test temperatures.
4. After 3,000 hours' aging, the test could not measure the fatigue life of PEM mixtures.
5. Rutting and Cantabro loss were higher in dry- and wet-processed CRM PEM mixes than in control hybrid and SBS-modified PEM, regardless of aging.
6. After 3,000 hours, IDT values were higher for dry-processed CRM PEM and SMA than for controls.

CHAPTER 8 INTERACTION BETWEEN CRM AND ASPHALT

8.1 Introduction

The interaction between CRM and asphalt binder in the dry process has received much less attention than wet processing. A prevailing assumption is that in the dry process, CRM is added to replace some of the fine aggregates, so its effects on asphalt are negligible.

This study focused on the interaction between CRM and asphalt binder in dry-processed rubberized PEM and SMA mixes during and after the mixing process, including silo storage time prior to paving. A series of tests on rheological properties and chemical analyses were conducted on samples stored in the oven for 30, 60, and 90 minutes at 160°C using such tools as the dynamic shear rheometer (DSR), high-pressure gel permeation chromatography (HP-GPC), and Fourier-transform infrared spectroscopy (FTIR). Atomic force microscopy (AFM) was used to explore nano-structure characteristics. Figure 8-1 shows the experimental design.

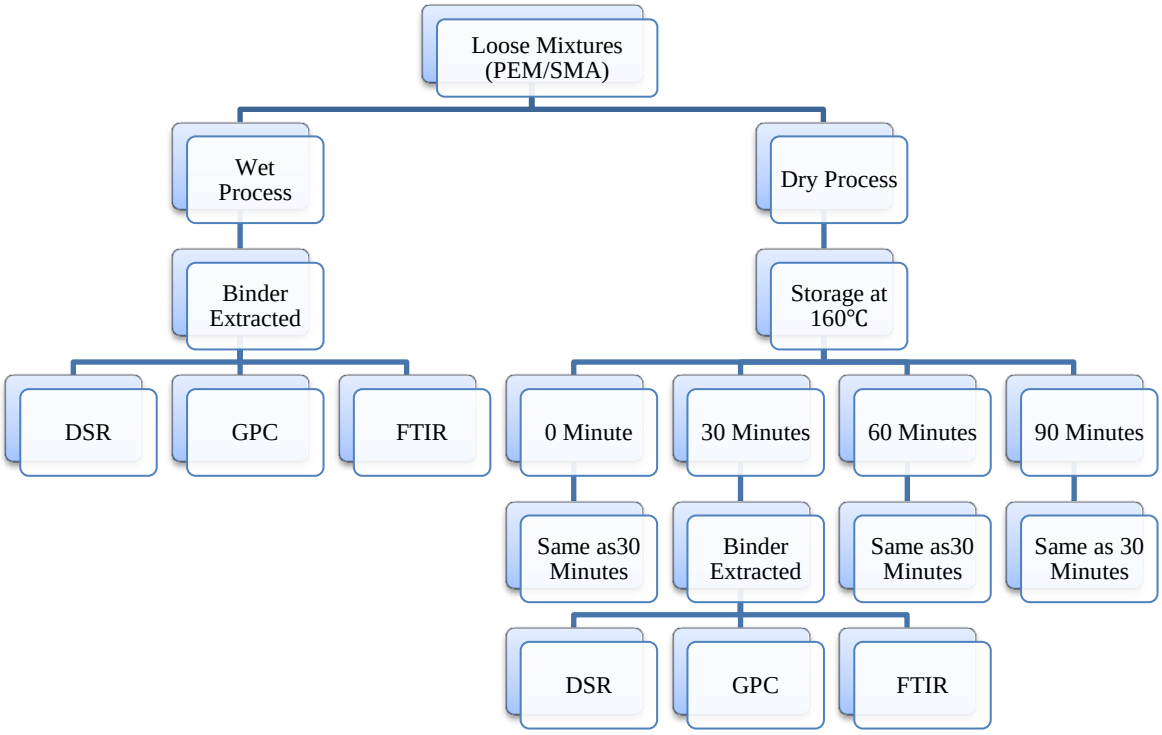

Figure 8-1. Flow chart of the experimental design

8.2 Materials and Test Methods

Materials and mixture preparation

Aggregate types, PEM and SMA mixture gradations, fibers, mineral fillers (fly ash), hydrated lime, asphalt PG grade, and CRM were identical to those listed in Chapter 4 (Tables 4-1 to 4-4). A wet-processed CRM binder was used as a control. Chapter 4 (section on materials and test procedures) also defines the production of the CRM binder and how the wet-processed rubberized mixtures were mixed. Storage temperature was set at 160 ℃ for 30, 60, and 90 minutes to investigate the interaction between CRM and asphalt over time.

Extract of asphalt binder

ASTM D1856, Abson recovery, has been the major method for recovering asphalt binder since 1933. Recently, ASTM D5404, Recovery of Asphalt Using the Rotavapor Apparatus, has become more widely used. Here, the CRM asphalt binders were extracted from the produced HMA mixture based on the ASTM D2172 procedure, using the centrifuge extractor and tetrahydrofuran (THF) as the solvent.

Figure 8-2. Asphalt binder extracted from mixture dissolved in THF

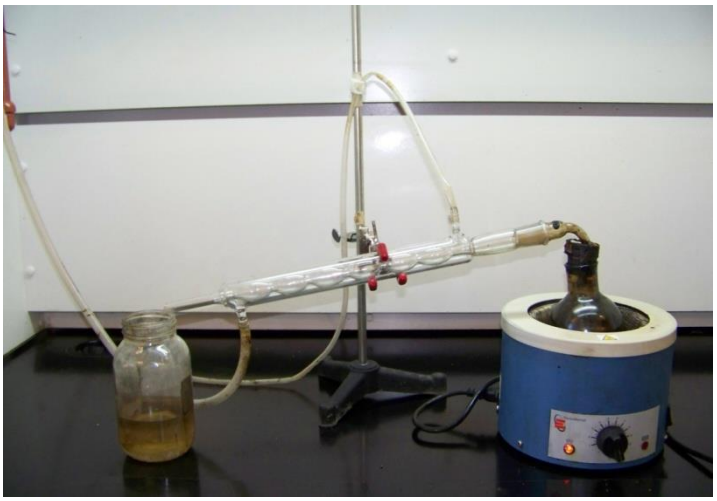

Figure 8-3. Separated asphalt binder and THF

Gel Permeation Chromatography

Waters GPC equipment and software (Milford, MA) were used for the chromatographic analysis of binders (Fig. 8-4). A differential refractive index meter (Waters 410) was used as a detector, and two columns (Waters HR 4E and HR 3) were used to separate binder constituents by molecular size. Table 8-3 shows the column specifications. Throughout testing, the binder constituents were kept at 35 °C in a column oven. In the mobile phase, THF flowed at a rate of 1 ml/min. The concentration rate was 0.5% by weight of binder as recommended by the equipment manufacturer.

Figure 8-4. GPC system used in this study

Each binder sample, dissolved in THF, went through a 0.45-μm syringe filter prior

to the injection module. A sample volume of 50 µl was injected for each test, which took 30 minutes; elution started approximately 11 minutes after injection and ended at approximately 21 minutes (Fig. 8-5). Each sample was tested three times, and the average value of the large molecular size (LMS) portion was reported.

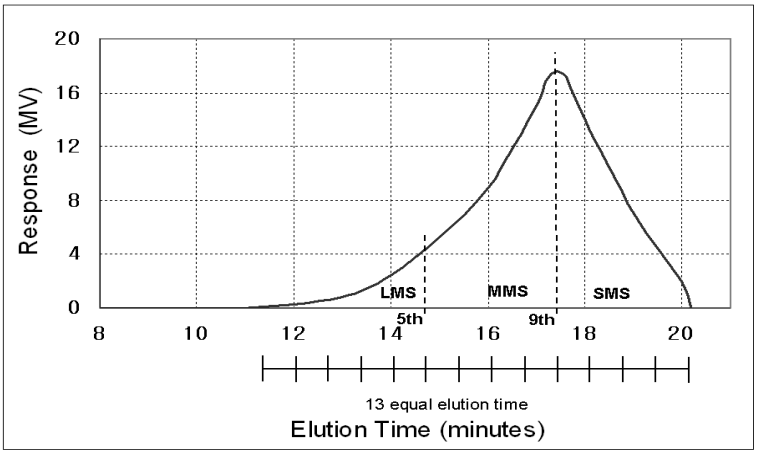

Figure 8-5. A typical chromatogram of an asphalt binder

In Figure 8-5, the area under the curve represents 100% of the binder molecules injected into the GPC system. Asphalt binder constituents are generally classified into several groups. In this study, the chromatogram profile was partitioned into 13 slices and three parts: large molecular size (LMS; slices 1-5), medium molecular size (MMS; 6-9), and small molecular size (SMS; 10-13). Only the LMS value was used to characterize binder properties. Research has shown that LMS correlates best with asphalt binder properties.

Fourier-transform infrared spectroscopy (FTIR) Test

FTIR can measure the infrared absorbance spectrum of a solid, liquid, or gas. Bonding in the test material is detected according to the assignments of the wave numbers of the main bands (Table 8-4).

Table 8-1. Assignments of the main bands of asphalt binder in FTIR spectra

Wave number(cm^{-1})	Assignment [a]
3594,3735	νO-H
2924, 2853	νC-H aliphatic
1735	νC=O
1700	νC=O conjugated
1600	νC=C AROMATIC
1460	νC-H of –(CH2)n-(aliphatic index)
1376	νC-H of –CH3 (aliphatic branched)
1030	νS=O sulfoxide
966	νC-H trans disubstituted –CH=CH-(butadiene block)
748,690	νC-H aromatic monosubstitued (styrene block)

[a]ν=Stretching, δ=bending

We used a NICOLET iD7 ATR FTIR spectrometer (Fig. 8-6; Thermo Scientific) with 4-cm^{-1} resolution, scanning frequency of 16 times, and test range of 500-4000 cm^{-1}. The main result range, 500-2000 cm^{-1}, was observed to determine the change in index (S=O, C=O).

Figure 8-6. FTIR system used in this study

After determining the characteristic absorption bands of asphalt, the functional and structural indices were calculated from valley to valley rather than band heights because this approach accounts for several vibrations of the same type simultaneously (e.g., C=O ester, acid, and ketone vibrations between 1753 and 1635 cm-1). Equation

8-1 shows ratio changes in CRM asphalt binders after storage:

$$I_{C=O} = \frac{\text{Area of the carbonyl band centered around } 1690\ cm^{-1}}{\sum \text{Area of the spectral bands between } 2000\ cm^{-1} \text{ and } 600\ cm^{-1}} \quad (8\text{-}1)$$

8.3 Results and Discussion

8.3.1 Results for rubberized PEM

DSR results

Figure 8-7 shows the complex shear modulus (G*) values of binders extracted from dry-processed rubberized PEM at different storage times. Longer storage time increased their G*, and binder extracted from 90-minute aged mixtures had the highest value. Binders extracted from mixtures stored for 30 minutes had the same G* as wet-processed CRM asphalt mixtures.

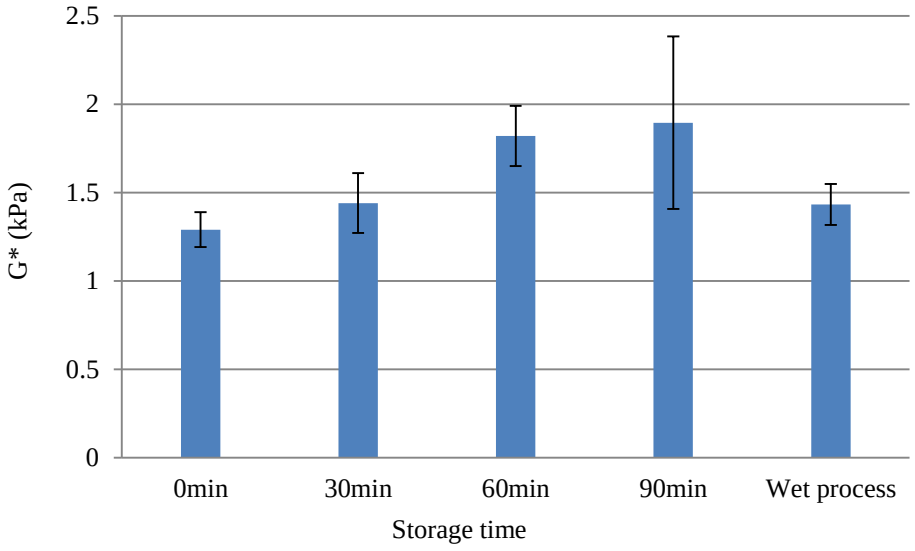

Figure 8-7. G* of asphalt binder extracted from rubberized PEM

Table 8-2 shows the results of a one-way analysis of variance, which found no difference at the $\alpha = 0.05$ significance level between the G* values of asphalt binder extracted from dry-processed PEM stored for 30 minutes and wet-processed

PEM.

Table 8-2. Statistical analysis of G* of asphalt binder from rubberized PEM

	30	60	90	Wet
30	-	S	S	N
60		-	S	S
90			-	S
Wet				-

Note: S=significant difference; N=no significant difference; significance level=0.05

All binders were tested at 76 ℃ and thus exhibit viscoelasitc properties. As Figure 8-8 shows, the phase angles of all binders extracted from dry-processed rubberized PEM decreased as storage time increased from 30 to 90 minutes. As expected, the phase-angle values of wet-processed binders at 76 ℃ were greater than those of dry-processed recovered binders but the same as those of dry-processed recovered binders stored for 30 minutes, indicating that their elasticity is equivalent.

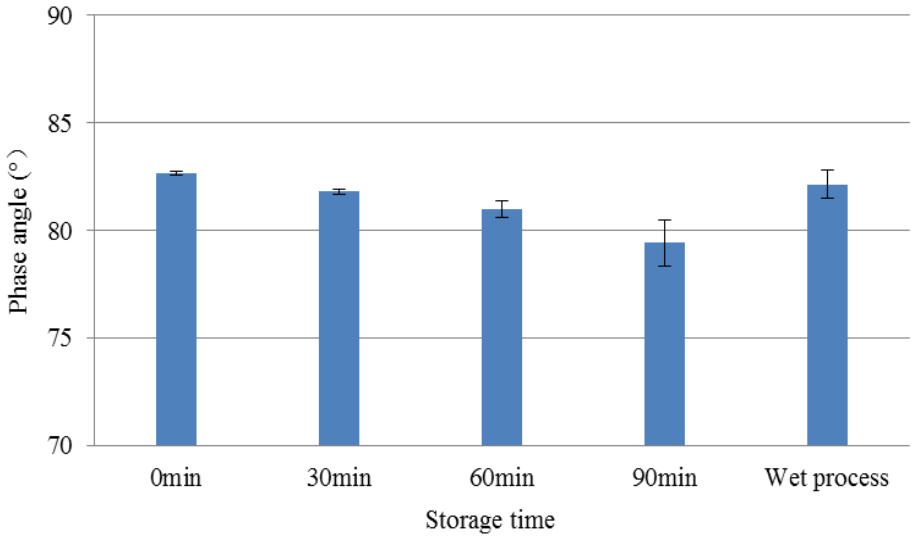

Figure 8-8. Phase angle of asphalt binders extracted from rubberized PEM

Table 8-3 shows that storage time significantly affected phase angle. The phase angles of binders extracted from dry-processed rubberized PEM after 30 and 60 minutes' storage did not differ significantly from those of wet-processed PEM.

Table 8-3. Statistical analysis of phase angles of binders from rubberized PEM

	30	60	90	Wet
30	-	S	S	N
60		-	S	N
90			-	S
Wet				-

Note: S=significant difference; N=no significant difference; significance level=0.05

Figure 8-9 shows that the G*/sinδ value of binders extracted from dry-processed rubberized PEM increases with storage time. Binders extracted from dry-processed rubberized PEM stored for 30 minutes had the same value as the wet-processed and thus, their rutting resistance is equivalent.

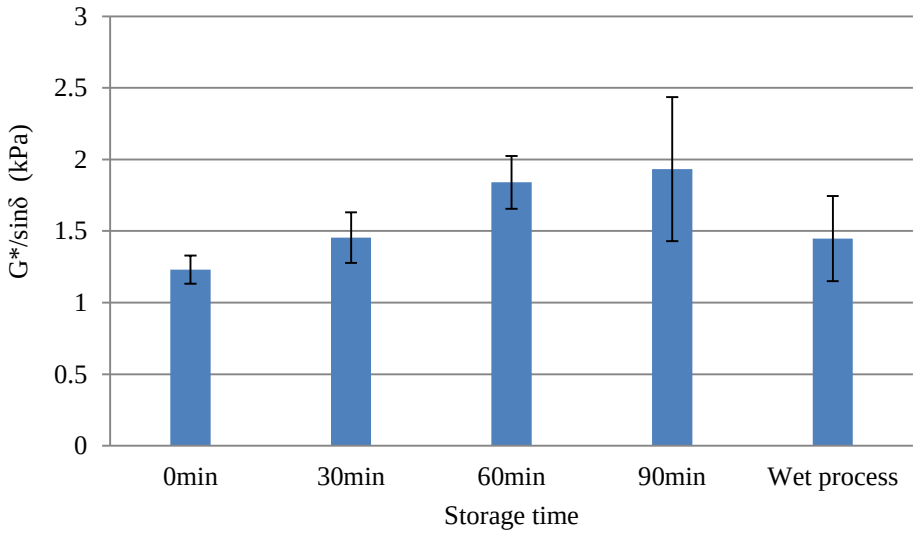

Figure 8-9. Rutting resistance of asphalt binders extracted from rubberized PEM

Table 8-4 reports the statistical analysis showing that the change in rutting

resistance factor between extracts from dry-processed rubberized PEM stored for 30 minutes and wet-processed PEM was not significant. In addition, for each asphalt binder extracted from dry-processed rubberized PEM, differences between storage periods were statistically significant. Obviously, longer storage time improves the rutting resistance of dry-processed rubberized PEM. The interaction between CRM and binder results in a stiffer asphalt binder due to dry-process mixing and aging.

Table 8-4. Statistical analysis of asphalt binder rutting resistance

	30	60	90	Wet
30	-	S	S	N
60		-	S	S
90			-	S
Wet				-

GPC results

Figure 8-10 shows the LMS values for control and binders extracted from loosely mixed PEM based on the GPC test as a function of aging times. In general, the LMS values of both dry-processed binders increased over time. Wet- and approximately 45-minute aged dry-processed CRM asphalt binder have the same molecular size distribution.

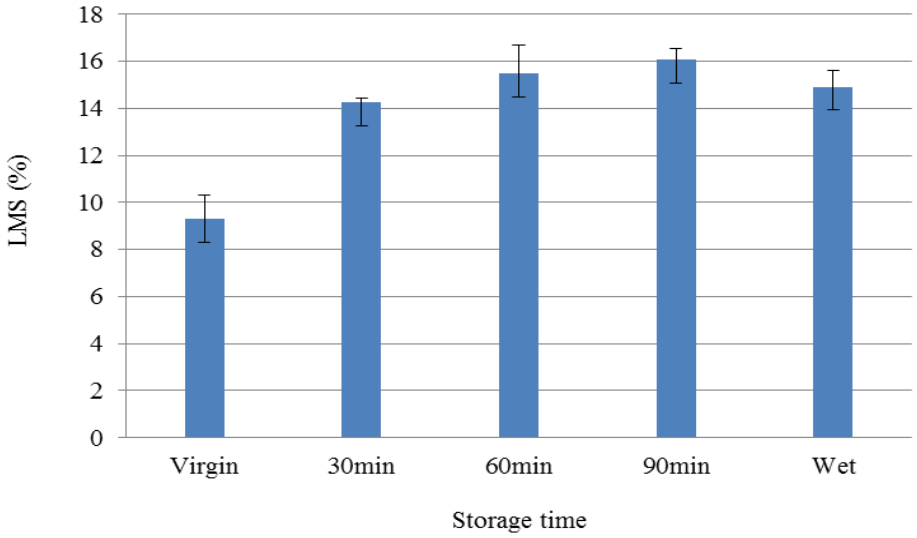

Figure 8-10. LMS of asphalt binder extracted from rubberized PEM

FTIR results

Figure 8-11 shows infrared (IR) spectrum analysis images of four asphalt binders extracted from PEM. Storage time changed their chemical bonding. The asphalt binder aging process is an oxidation reaction. Asphalt is composed of hydrocarbons and small amounts of metals. Under atmospheric conditions, the oxygen attacks the weak molecular bonding in the asphalt, yielding carbon dioxide and water. Nitrogen and sulfur may become nitrogen and sulfur dioxide and escape the asphalt binder. The absorbance at 1,700 cm^{-1} and 1,030 cm^{-1} characterizes the carbonyl index (C=O) and the sulfoxide index (S=O), respectively.

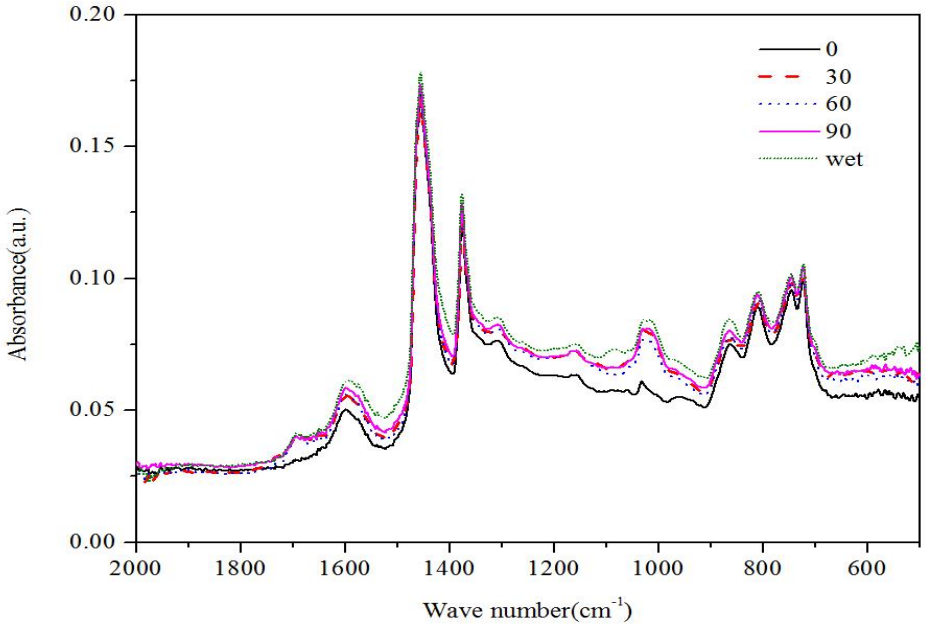

Figure 8-11. FTIR spectra of CRM asphalt extracted from rubberized PEM

Figure 8-12 shows the ratio changes in the carbonyl index (C=O) of CRM asphalt binders after different storage times. In dry-processed rubberized PEM, it increased after 30 minutes and decreased slightly after 90 minutes. Results were similar for asphalt binder extracted from wet-processed rubberized PEM.

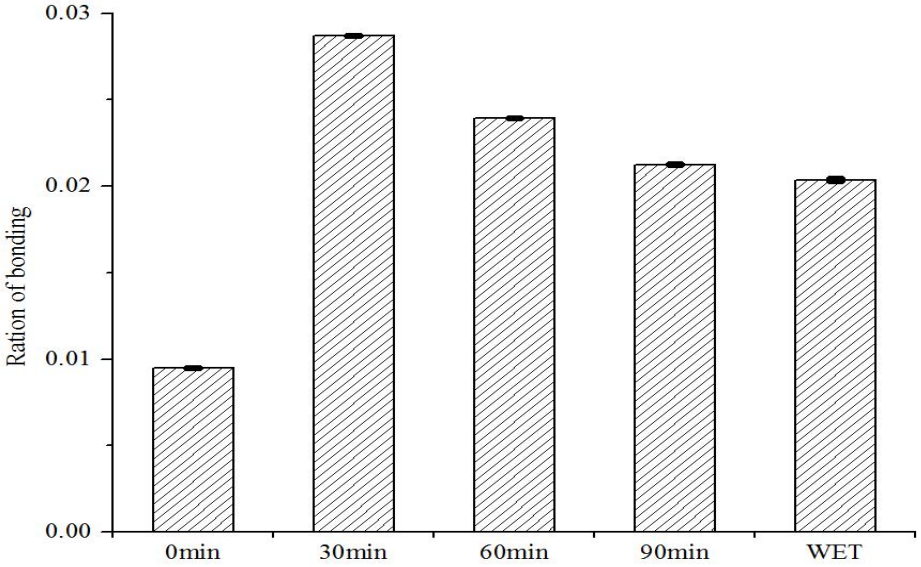

Figure 8-12. Bonding ratio (C=O) in CRM asphalt extracted from PEM

8.3.2 Results for rubberized SMA

DSR results

Figure 8-13 shows the G* values of asphalt binder extracted from dry-processed rubberized SMA after different storage times. Overall, G* increased with storage time. G* for the sample stored for 30 minutes was less than that of wet-processed CRM asphalt binder, but after 60 and 90 minutes, they seem equal. These results indicate that the G* of asphalt binder in dry- and wet-processed rubberized SMA can reach the same level.

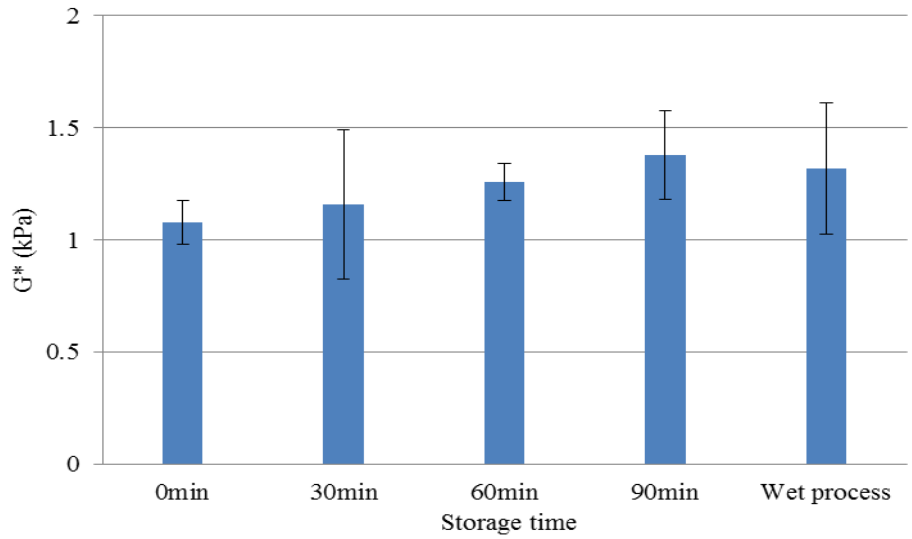

Figure 8-13. G* of asphalt binder extracted from rubberized SMA

Table 8-5 shows the results of a one-way analysis of variance of the significance of the change in G* with increased storage. No significant difference at the $\alpha = 0.05$ level between the G* of asphalt binder extracted from dry-processed rubberized SMA after 90 minutes' storage and wet-processed SMA was found.

Table 8-5. Statistical analysis of the G* of asphalt binder from rubberized SMA

	30	60	90	wet
30	-	S	S	S

60		-	N	S
90			-	N
Wet				-

Note: S=significant difference; N=no significant difference; significance level=0.05

Figure 8-14 shows that the phase angles of all binders extracted from dry-processed rubberized SMA decreased as storage time increased from 30 to 90 minutes. As expected, the phase angle values of asphalt binder extracted from wet-processed rubberized SMA at 76 ℃ were greater than those of dry-processed binder. The phase angle of binders extracted from dry-processed rubberized SMA after 90 minutes' storage was lowest. For the binders tested, longer storage increases elasticity.

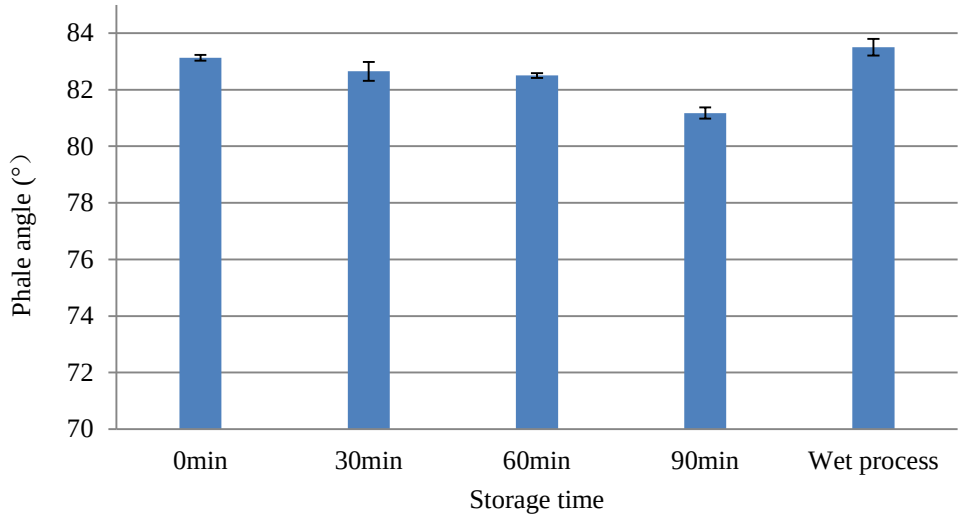

Figure 8-14. Phase angle of asphalt binder extracted from SMA

Table 8-6 indicates no significant difference between asphalt binders extracted from dry-processed rubberized SMA stored for 30 minutes and wet-processed SMA.

Table 8-6. Statistical analysis of phase angle of binder from rubberized SMA

	30	60	90	wet

30	-	S	S	N
60		-	S	S
90			-	S
Wet				-

Note: S=significant difference; N=no significant difference; significance level=0.05

Figure 8-15 shows that the G*/sinδ value of binders extracted from dry-processed rubberized SMA increased with aging; it was over 1kPa for samples stored 30 minutes. Thus, storage can improve a binder's pavement performance grade. Binders extracted from wet-processed rubberized SMA had a G*/sinδ value larger than that of dry-processed stored for 60 minutes and smaller than that of dry-processed stored for 90 minutes. We conclude that over 60 minutes of storage can make the asphalt binder in dry-processed rubberized SMA reach a level similar to that of wet-processed.

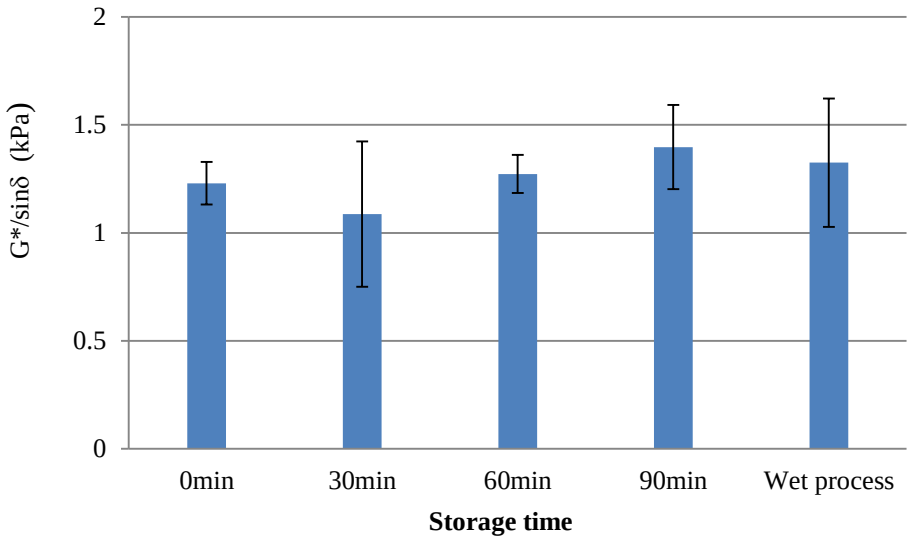

Figure 8-15. Rutting resistance of binder extracted from rubberized SMA

Table 8-7 shows that storage times made statistically significant differences in the rutting resistance of all asphalt binders extracted from dry-processed rubberized SMA. The rutting resistance of those stored for 60 and 90 minutes did not differ from that of those extracted from wet-processed SMA.

Table 8-7. Statistical analysis of asphalt binder rutting resistance

	30	60	90	wet
30	-	S	S	S
60		-	S	N
90			-	N
Wet				-

Note: S=significant difference; N=no significant difference; significance level=0.05

GPC results

Figure 8-16 shows the LMS values of control and binders extracted from a loose, dry-processed rubberized SMA based on the GPC test as a function of aging time.

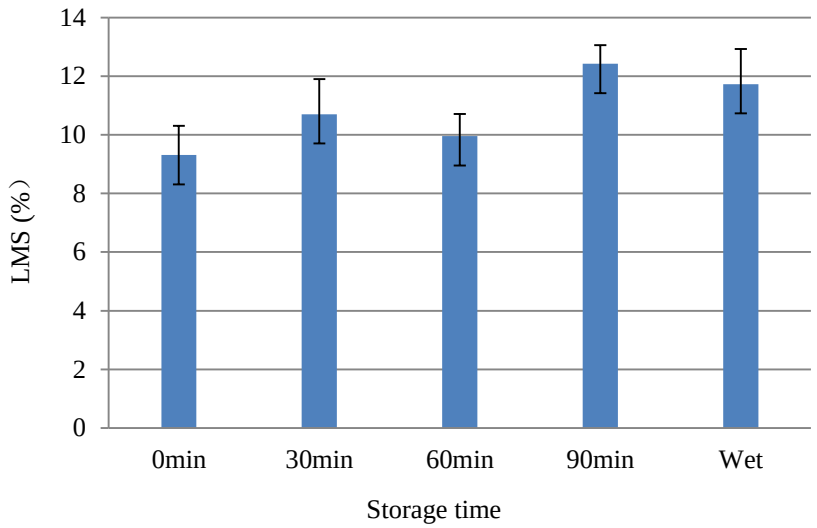

Figure 8-16. LMS of asphalt binder extracted from rubberized SMA

FTIR results

Figure 8-17 shows the infrared (IR) spectrum analysis of four asphalt binders extracted from SMA mixtures. Peaks appear at 1700 cm^{-1}, 1600 cm^{-1}, and 1065 cm^{-1}, indicating that the asphalt has aged in the storage process.

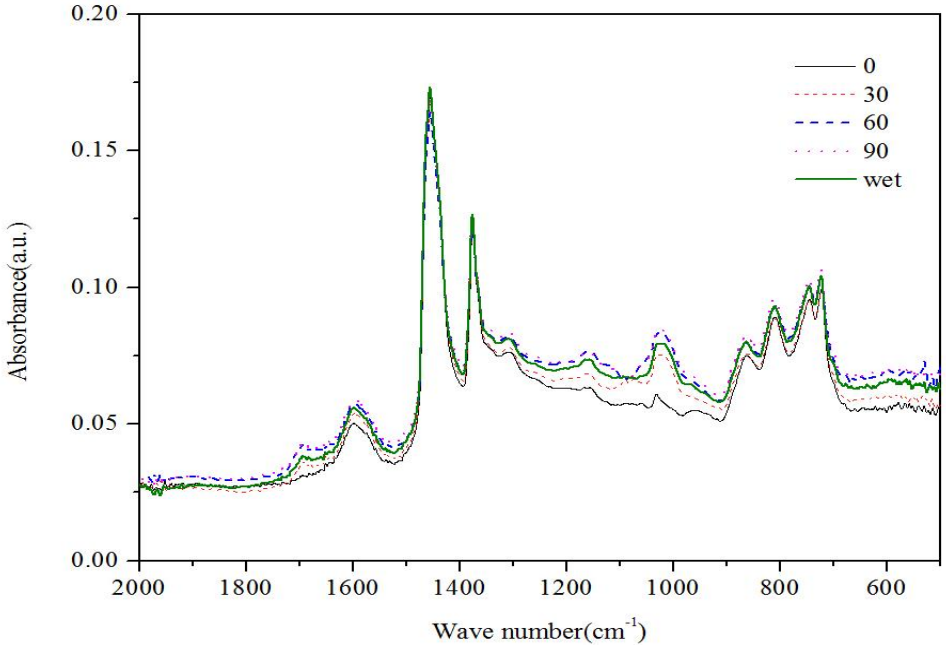

Figure 8-17. FTIR spectra of CRM asphalt extracted from rubberized SMA

Figure 8-18 shows that the carbonyl index (C=O) of asphalt binder extracted from a dry-processed CRM SMA mixture increases with storage. After 30 minutes, it is close to that of wet-processed SMA.

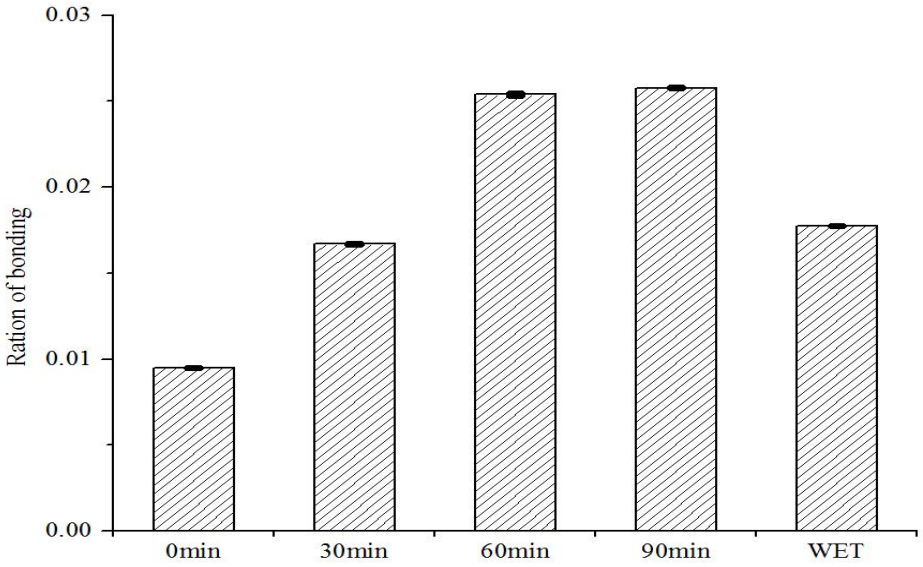

Figure 8-18. Bonding ratio (C=O) in CRM asphalt extracted from dry- and wet-processed rubberized SMA

8.3.3 Nanoscale evaluation of asphalt/CRM interaction

Atomic force microscopy (AFM; Fig. 8-19) was used to determine how asphalt interacts with the crumb rubbers added in the dry process and to compare the microstructural properties of asphalt modified in the wet and dry processes. The aim was to determine whether the rubbers modify the binder or the mixture. ACLA probes were used in the AFM tapping mode to avoid damaging the asphalt binder surface and/or the tip and to reduce tip contamination.

Figure 8-19. Nanosurf AFM

Wet-processed rubberized asphalt binder was produced by mixing -30 mesh CRM at 10% of the weight of the asphalt binder with a base binder of PG 67-22 at 170 °C and 700 RPM for 45 minutes. Dry-processed rubberized asphalt binder was produced by mixing PG 67-22 asphalt with CRM at 10% of the weight of the asphalt binder and TOR at 4.5% of the weight of CRM for 2 minutes at 160 °C. Prior to AFM, an 80-mesh sieve was used to remove the CRM in the unaged and short-term aged rubberized asphalt binders to avoid the effect of CRM particles on measurements. The filtered hot asphalt was poured onto a clean glass substrate, then placed in the oven (130 °C) for 5 minutes to form the smooth surface critical to successful AFM testing.

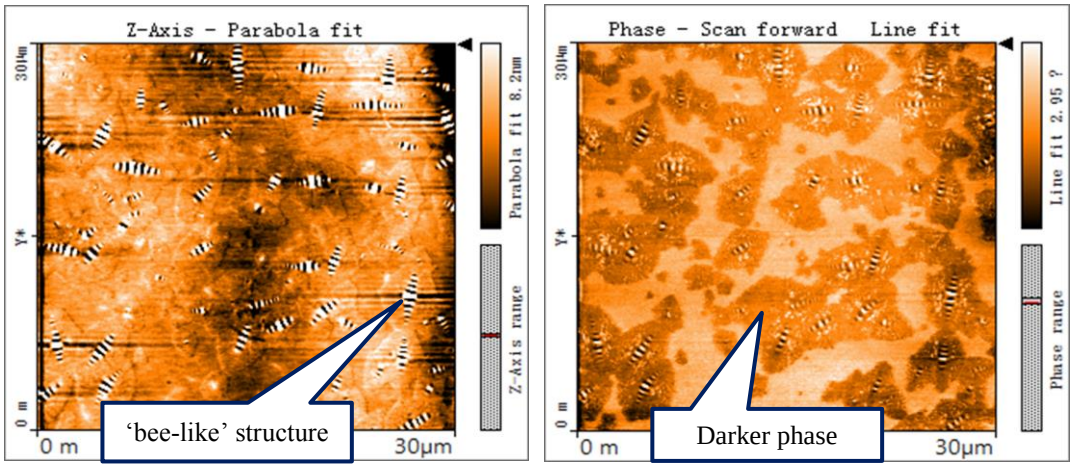

Figure 8-20. Topographic and phase images of PG 67-22

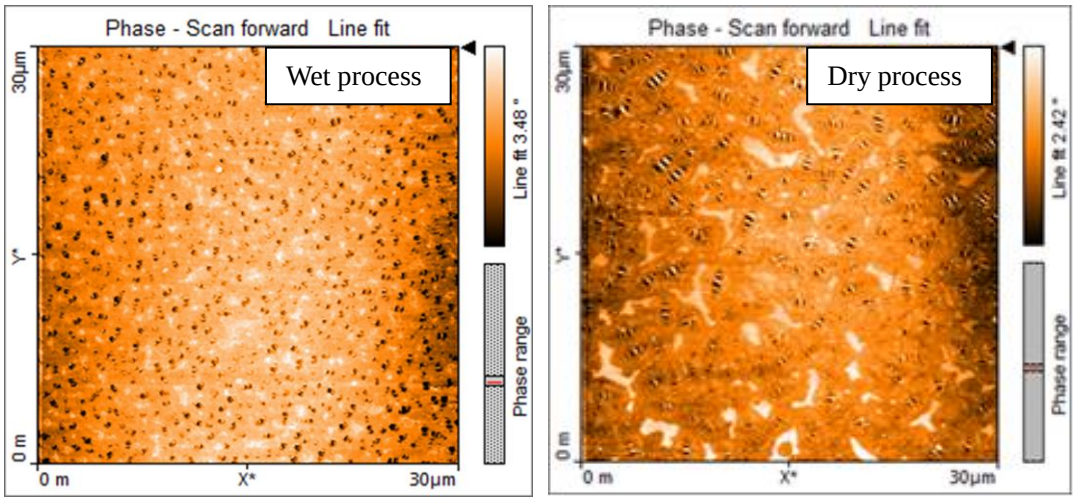

Figure 8-21. Phase images of unaged rubberized asphalt binders

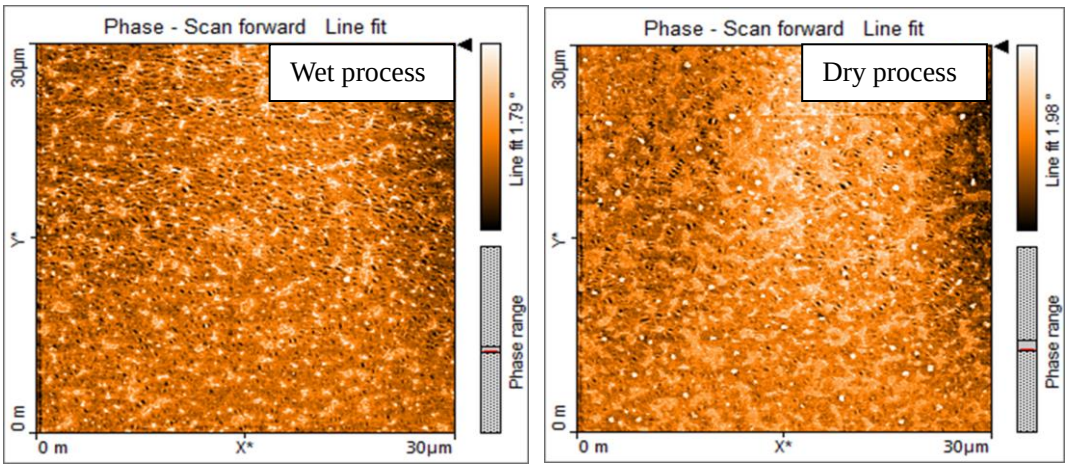

Figure 8-22. Phase images of short-term aged rubberized asphalt binders

Bee-like structures and the darker phases around them, which represent the parts

with higher modulus, can be seen in all asphalt binders (Figs. 8-20 to 8-22), but their concentration in dry- and wet-processed rubberized asphalt differs obviously from each other before aging and slightly after short-term aging. Furthermore, we calculated the roughness of the topographical images of rubberized asphalt binder, and results showed that it was 21nm and 14nm before aging and 3.2 nm and 3.3 nm after short-term aging for the dry- and wet-processed binders, respectively. This finding indicates that the short-term aging during storage and paving decreases the difference in the microstructures of dry- and wet-processed rubberized binders.

Additionally, the concentration of bee-like structures and the area of darker phases were significantly higher in rubberized asphalt binders than the base asphalt of PG 67-22, regardless of dry or wet processing.

8.3.4 Rheological properties of dry- and wet-processed rubberized binders

To determine the difference in the rheological properties of dry- and wet-processed rubberized binders, we performed frequency sweep tests using a DSR according to AASHTO T 240. They were run with the 25-mm diameter plate and 1-mm testing gap geometry at 50 °C. Dry- and wet-processed rubberized binder samples were fabricated as for the AFM test, but the CRM was not removed.

Figure 8-23 shows the frequency sweep results for virgin asphalt and dry- and wet-processed rubberized binders in terms of: (a) elastic modulus (G’), viscous modulus (G’’), and complex viscosity (|η*|); and (b) complex modulus (|G*|) and phase angle (δ). All dry-processed rubberized binders, regardless of aging, had similar results. In addition, compared to virgin asphalt, both dry- and wet-processed rubberized binders had significantly higher modulus (G’, G’’, and |G*|) and complex

viscosity (|η*|) but lower phase angle (σ). Thus, the dry and wet processes equally improved the high-temperature properties of asphalt binder.

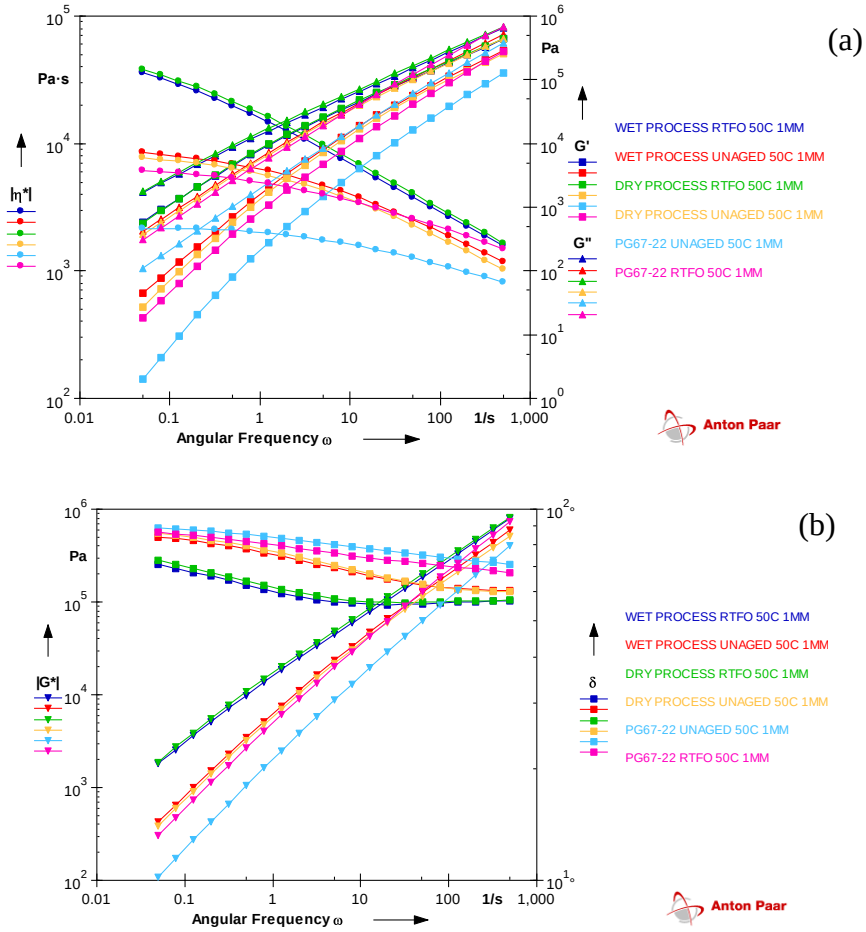

Figure 8-23. Frequency sweep results

8.4 Summary and Conclusions on CRM-Asphalt Interaction

A series of rheological property tests and chemical analyses were conducted on dry-processed rubberized mixtures stored in an oven at 160 ℃ for 30, 60, and 90 minutes to evaluate the interaction of CRM and asphalt. Based on the DSR, GPC, and FTIR results, interaction is significant during the production and paving stages, regardless of mixture type. Other conclusions include:

1. At compaction temperature, the G*/sin(delta) of rubberized CRM in a dry-processed asphalt mixture increased with mixture storage time for both PEM and SMA.

2. The LMS of extracted asphalt binder increased with storage time and corresponded with the DSR results for both rubberized PEM and SMA.

3. Differences in carbonyl index (C=O) between binder extracted from dry- and wet-processed rubberized PEM were insignificant at some storage times, indicating that these periods of aging made no obvious difference.

4. GPC and G* changes in LMS in DSR tests explained the interaction between CRM and asphalt during storage of dry-processed rubberized PEM.

5. Dry-processed rubberized binders had similar moduli (|G*|, G', and G''), phase angles (σ), and complex viscosity (|η*|), whether they were aged a short time or not.

6. Based on AFM testing, unaged, dry-processed rubberized asphalt has less surface roughness than wet-processed rubberized asphalt. However, after short-term aging, their roughness was similar.

CHAPTER 9 EFFECT OF WEATHERING ON CRM AND BINDER INTERACTION

9.1 Introduction

Any adverse effect of weathering on the interaction of CRM and asphalt would severely limit the usefulness of asphalt rubber as a paving material, but experimental data are lacking. We used rheological testing, GPC, and FTIR to determine the effects, with SBS binder as the control.

9.2 Materials and Test Methods

Aggregate type, PEM and SMA gradation, fibers, mineral fillers (fly ash), hydrated lime, asphalt PG grade, and CRM were identical to those listed in Chapter 4 (Tables 4-1, 4-2, 4-3, 4-4). Production of the CRM binder, mixture preparation, and extraction of the asphalt were also the same. PEM and SMA mixed with different asphalt binders (dry processed, wet processed, SBS, and hybrid) were aged for 1,000 and 3,000 hours in the Asphalt Pavement Weathering System (APWS). Test procedures, including GPC and FTIR, were the same as indicated in Chapter 4, section 4.2 Materials and Test Procedures. The PAV method was used to determine the fatigue factor ($G^*\sin(\delta)$) of asphalt binder extracted from the mixtures to characterize its rheological properties.

9.3 Results and Discussions

9.3.1 Effect of weathering on asphalt binder in PEM

Rheological characteristics

Figure 9-1 shows the $G^*\sin(\delta)$ of four asphalt binders extracted from PEM weathered for 1,000 or 3,000 hours. After 1,000 hours, the $G^*\sin(\delta)$ of dry-processed rubberized

CRM asphalt binder was almost equivalent to that of the SBS and hybrid binders and less than that of wet-processed rubberized CRM binder. After 3,000 hours, the G*sin(δ) of dry- and wet-processed rubberized CRM asphalt binder were almost equivalent and larger than that of SBS and hybrid. G*sin(δ) increased most in dry-processed rubberized CRM asphalt binder and least in SBS asphalt binder.

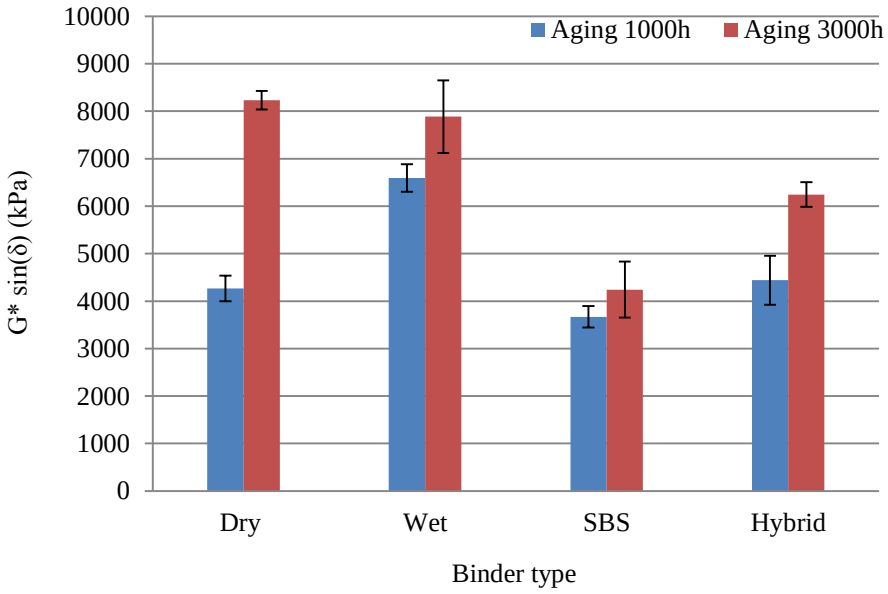

Figure 9-1. G*sinδ (at 19 ℃) of asphalt binder extracted from PEM

GPC results

Figure 9-2 shows the LMS results for asphalt binder extracted from the four PEM mixtures after weathering for 1,000 or 3,000 hours. Weathering for 1,000 hours significantly increased LMS; wet-processed binders had the least increase, and hybrid the most. In general, the effect of weathering for 3,000 hours differed by binder type. The increase was smaller for CRM asphalt binder than SBS and hybrid; hybrid had the highest increase in LMS value (over 5.6% more than the 1,000-hour value), and wet-processed binder the least (almost identical).

Hybrid binder proved most susceptible to weathering, and both dry- and wet-processed CRM binder were least. Aging time seems to have little influence on

the increase in LMS in CRM asphalt binder because of the carbon black in the CRM particles. Aging in asphalt binder is an oxidation reaction. Asphalt is composed of hydrocarbons and small amounts of metals. During the aging process, the natural resins and asphaltenes, which are soluble in aromatics, react with oxygen. In the CRM asphalt binder production process, the rubbers absorb the asphalt binder's resin, oil, and lightweight elements, reducing the LMS value change.

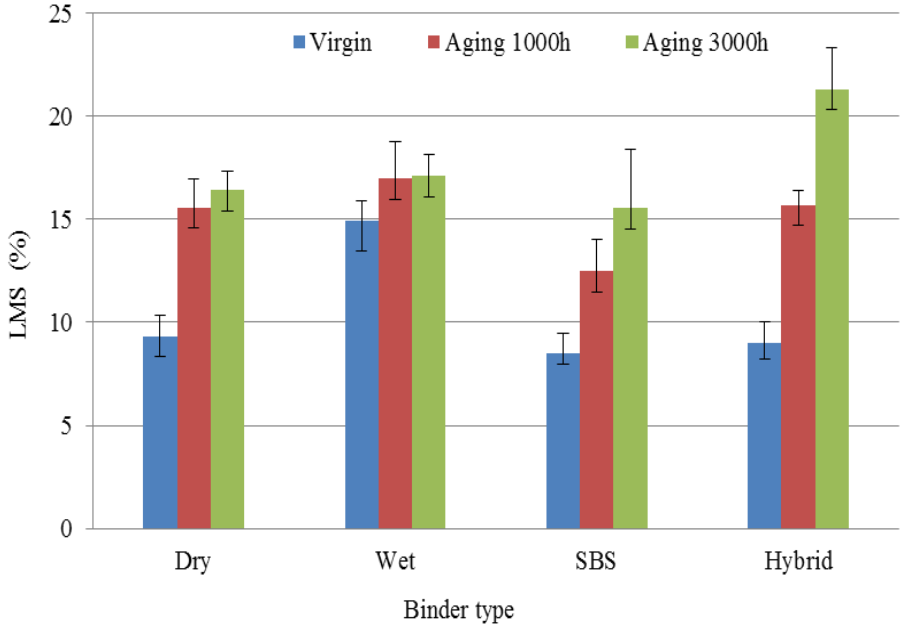

Figure 9-2. LMS of asphalt binder extracted from PEM

FTIR results

Figure 9-3 shows the infrared (IR) spectrum analysis of four asphalt binders extracted from PEM mixtures. The chemical bonding changed after weathering 1,000 or 3,000 hours, with peaks at 1,700 cm^{-1}, 1,600 cm^{-1}, and 1,065 cm^{-1}, indicating a dehydrogenated type of oxidation and generation of new, unsaturated bonds.

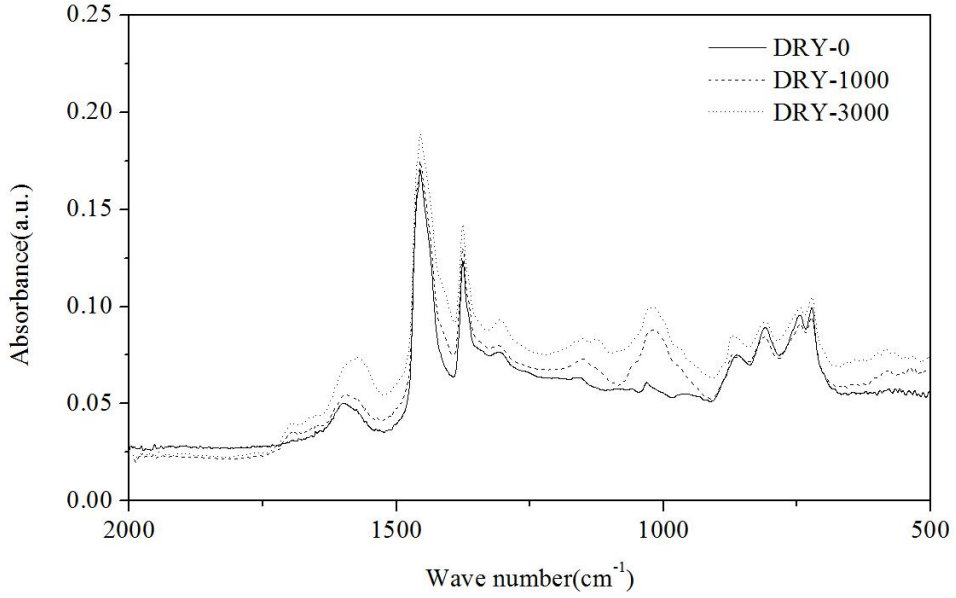

a) Dry process

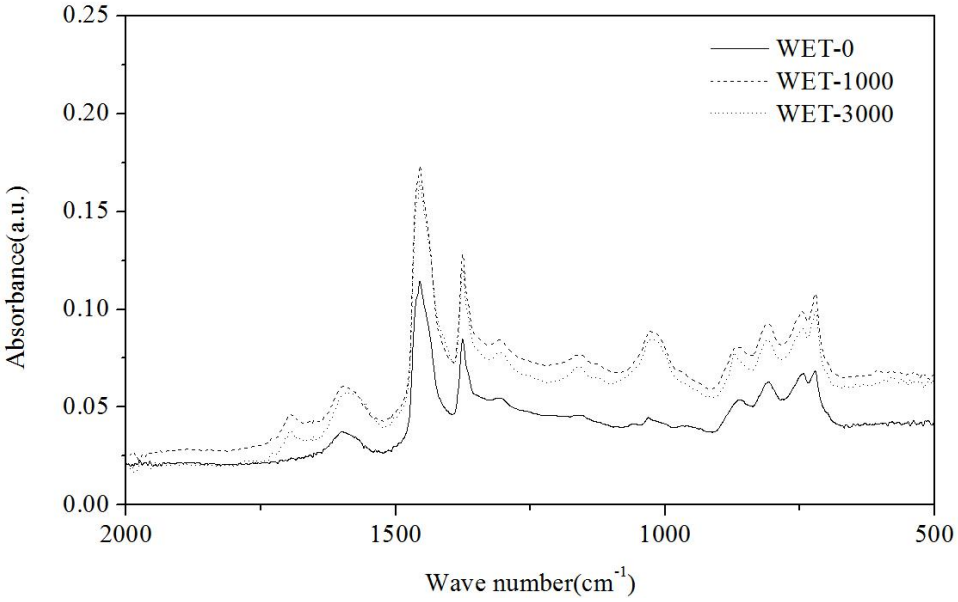

b) Wet process

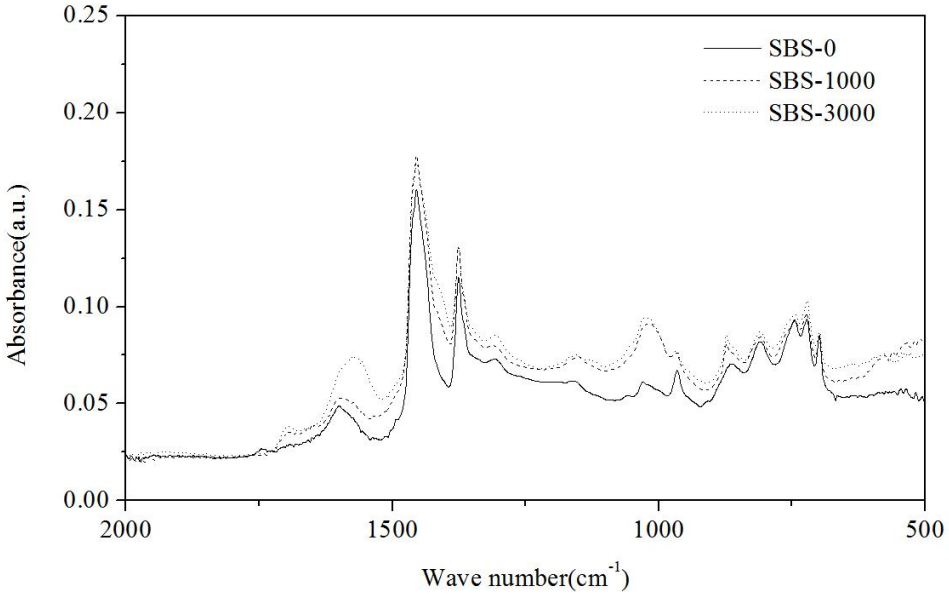

c) SBS

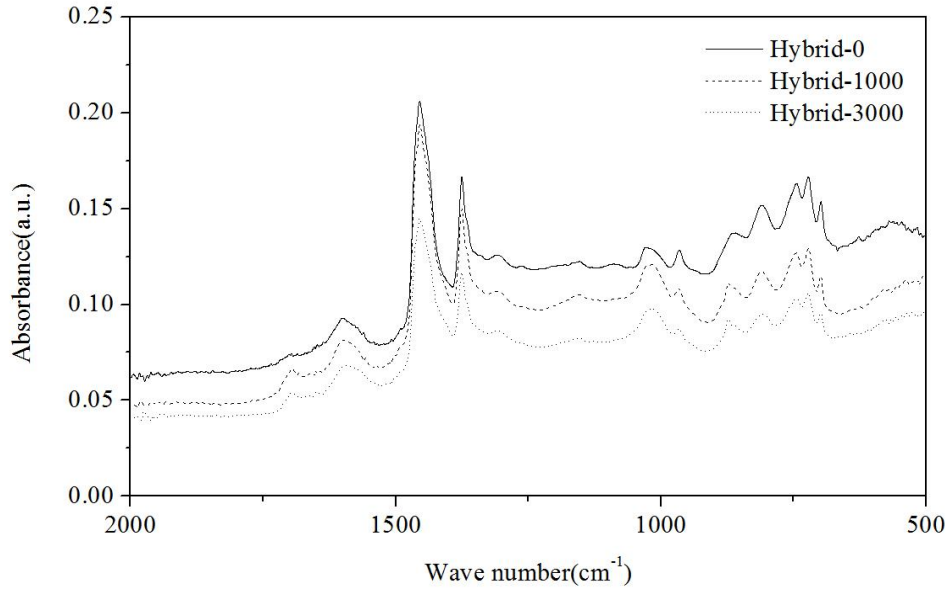

d) Hybrid

Figure 9-3. FTIR spectra of asphalt binder extracted from PEM

Figure 9-4 shows the ratio change（C=O）in the asphalt binder extracted from the four PEM mixtures after weathering 1,000 or 3,000 hours. The chemical bonding changed with aging, with a characteristic peak at 1,700 cm^{-1}, corresponding to a C=O bond. After 1,000 hours, the carbonyl function rate (carbonyl index) increased to become almost the same for asphalt binders extracted from the four PEM mixtures but

at different rates. The increasing value of the C=O ratio was highest for hybrid asphalt binder and lowest for SBS.

Up to 1,000 hours, the samples evolved significantly but then became less reactive. While the carbonyl index increased regularly up to 1,000 hours, it then decreased depending on weathering time and asphalt binder type. Evaporation, leaching, photo-oxidation, and other uncontrolled natural phenomena influence the nature and amount of each asphalt compound.

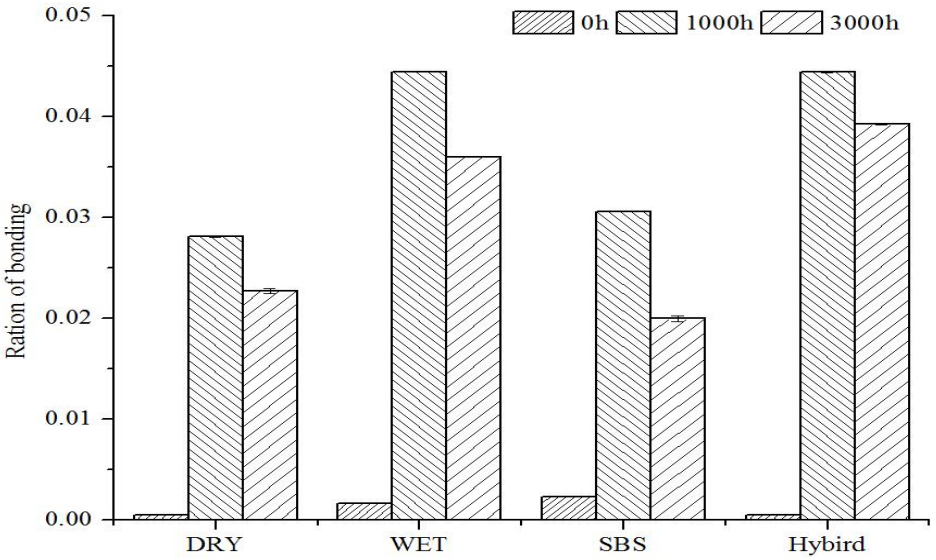

Figure 9-4. Bonding ratio (C=O) of asphalt binder extracted from rubberized PEM

9.3.2 Effect of weathering on asphalt binder in SMA

Rheological characteristics

Figure 9-5 shows the G*sin(δ) of four asphalt binders extracted from SMA mixtures after weathering 1,000 or 3,000 hours. Generally, it was almost the same for wet- and dry-processed CRM asphalt binder and less for hybrid and SBS asphalt binders. SBS was the lowest, and it increased less for asphalt binders extracted from SMA mixtures than PEM mixtures. It increased least in hybrid asphalt binder, but the increase in dry-

and wet-processed rubberized CRM asphalt binder was almost identical.

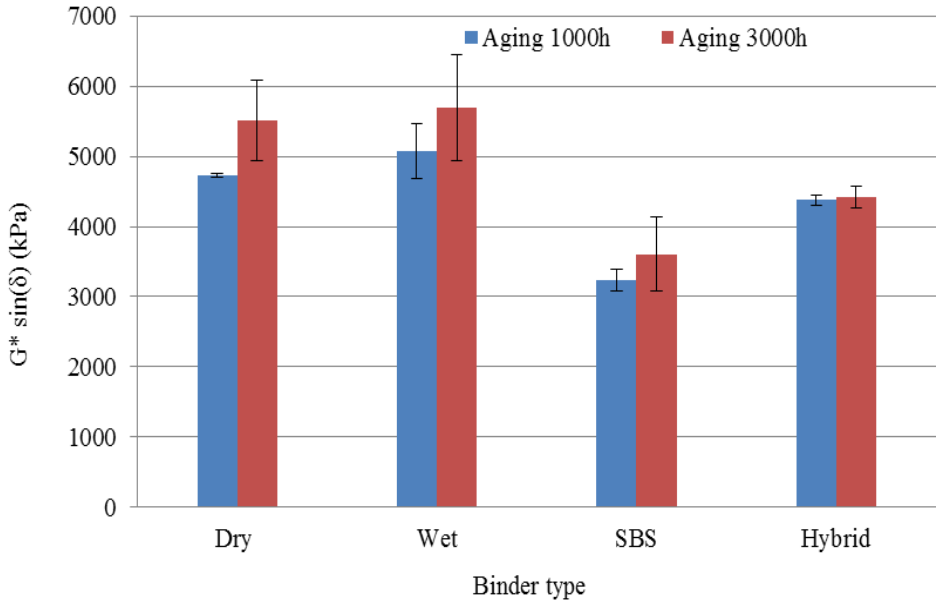

Figure 9-5. G*sin(δ) (at 19 ℃) of asphalt binder extracted from SMA

GPC results

Figure 9-6 shows LMS results for asphalt binder extracted from the four SMA mixtures weathered for 1,000 or 3,000 hours. Weathering for 1,000 hours increased LMS, as it did in PEM mixtures. The increase was least in wet-processed binder but almost the same for the others and the same as that in PEM mixtures.

For the samples weathered 3,000 hours, the general trend is similar to the findings for PEM. The increase in LMS value was still highest in hybrid binder and least in CRM asphalt binder, but dry-processed was less than wet-processed. SBS asphalt binder behaved as it did in the PEM mixture, and the increase in LMS value was the same as that for wet-processed asphalt binder.

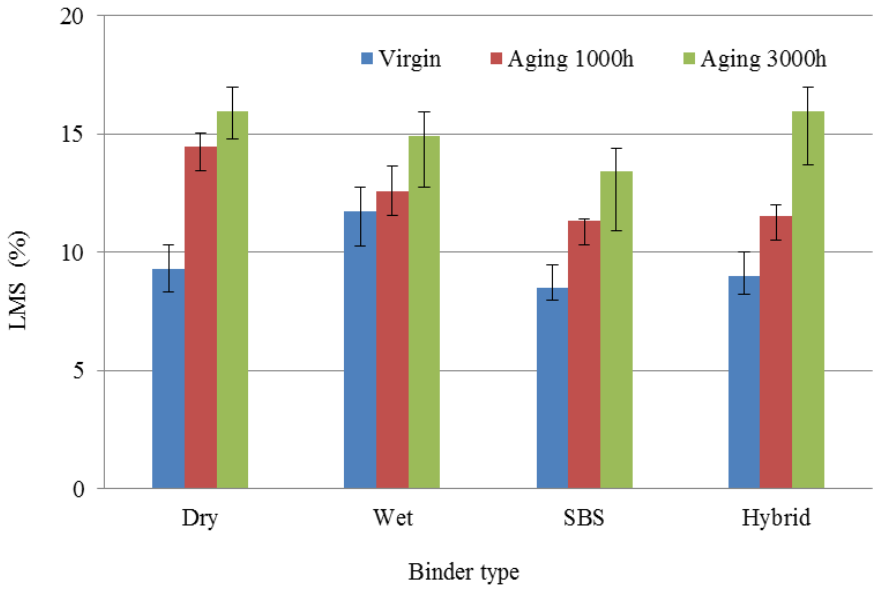

Figure 9-6. LMS of asphalt binder extracted from SMA

FTIR results

Figure 9-7 shows the infrared (IR) spectrum analysis of the four asphalt binders extracted from SMA. Peaks at 1,700 cm^{-1}, 1,600 cm^{-1}, and 1065 cm^{-1} show enhancement after weathering 1,000 hours.

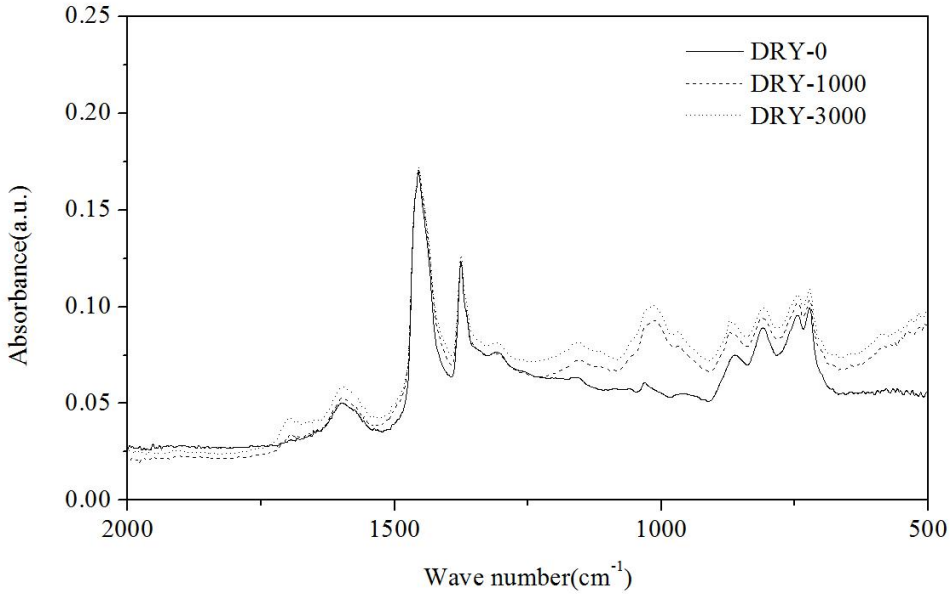

a) Dry process

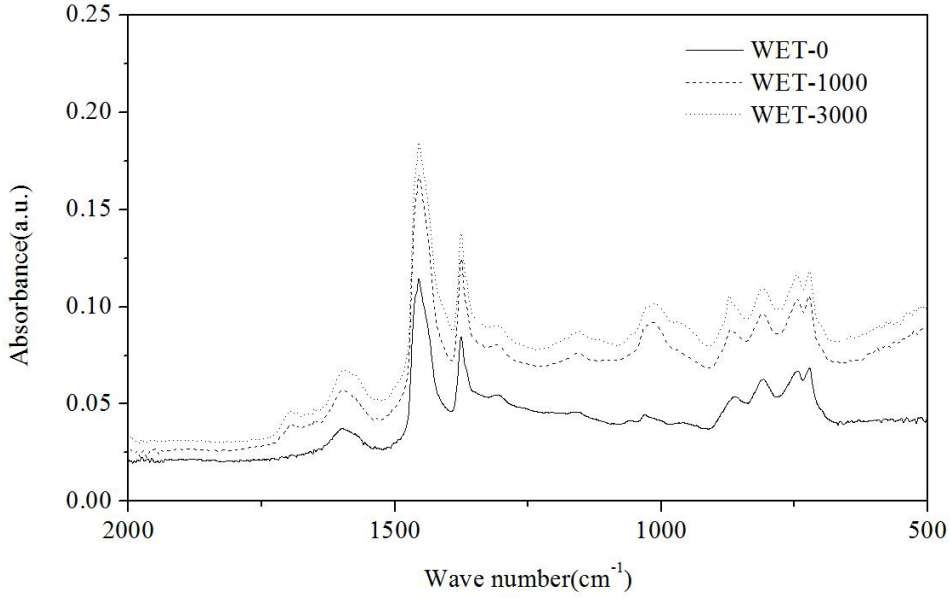

b) Wet process

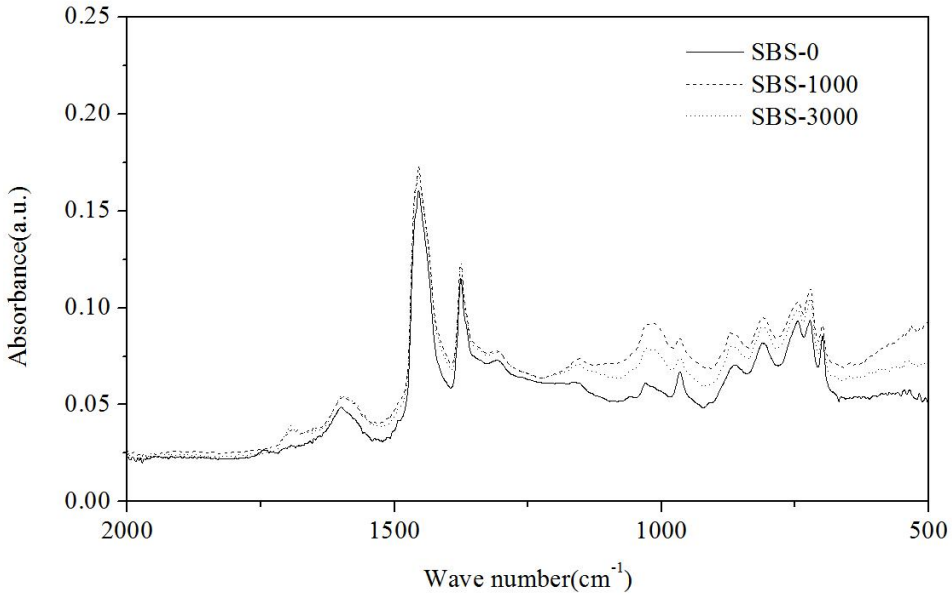

c) SBS

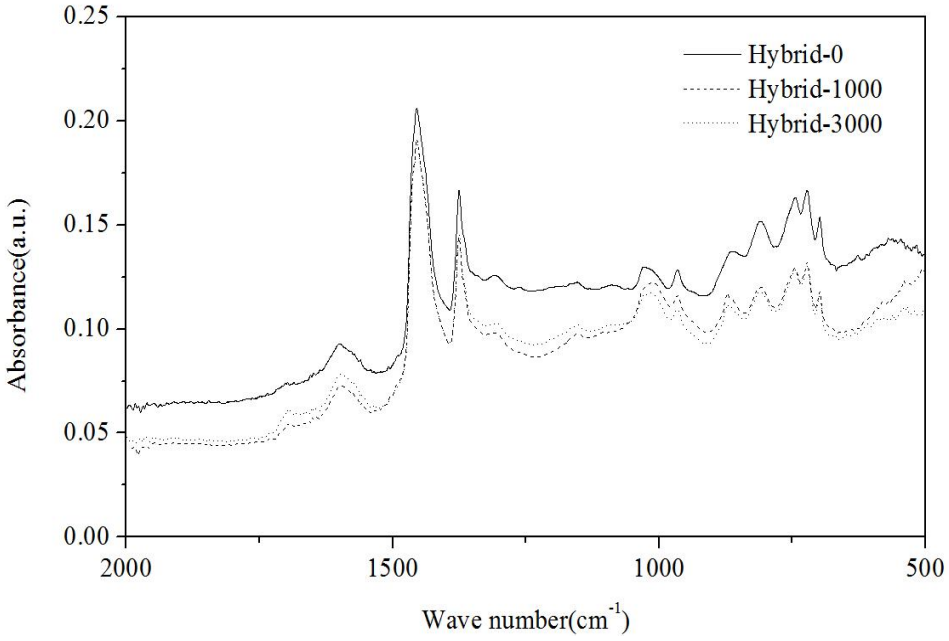

d) Hybrid

Figure 9-6. FTIR spectra of asphalt binder extracted from SMA

Figure 9-7 shows the ratio change (C=O) in the asphalt binder extracted from four SMA mixtures weathered for 1,000 or 3,000 hours. It increased regularly with weathering for 1,000 hours, least in SBS, indicating that SBS asphalt binder ages least to this stage. After 3,000 hours, the hybrid binder showed the highest increase in C=O bonding, and wet-processed CRM asphalt binder the least. The trend of these FTIR results reflects GPC results. Wet-processed asphalt binder is most resistant to aging, and hybrid the least.

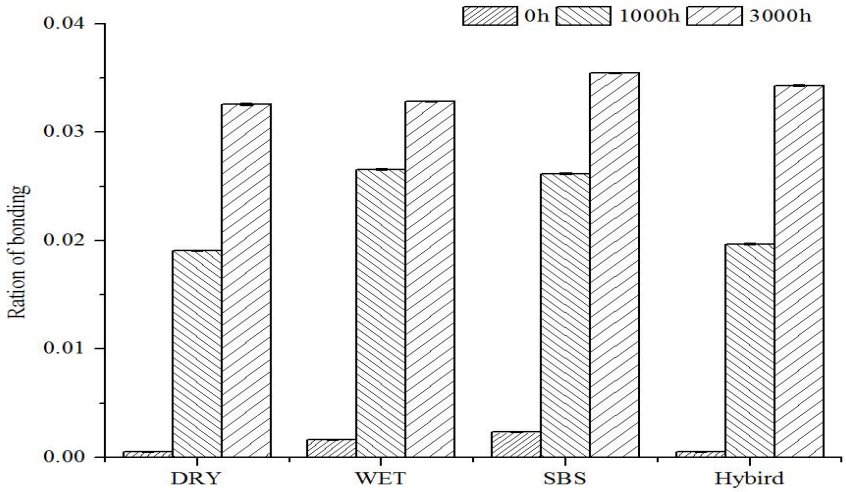

Figure 9-7. Ratio of bonding (C=O) of asphalt binder extracted from SMA

9.4 Summary and Conclusions on Effect of Weathering on CRM and Asphalt Interaction

This chapter examined the influence of weathering on the interaction of CRM with binders. The following conclusions can be drawn:

1. The values of G*sin(delta) differ significantly among the four asphalt binders extracted from PEM and SMA after weathering 1,000 or 3,000 hours. After 3,000 hours, the fatigue factor of dry- and wet-processed rubberized asphalt binders was equivalent and larger than that of SBS and hybrid asphalt binders.

2. The LMS of asphalt binders extracted from PEM and SMA increases significantly to 1,000 hours and slowly from 1,000 to 3,000 hours. The value of wet-processed asphalt binder was close to that of SBS and hybrid.

3. For SMA mixtures, the ratio of C=O bonding in dry-processed rubberized asphalt binder was equivalent to the others' after weathering for 3,000 hours. However, it was larger than that of wet-processed binders from PEM. Overall, the degree of aging of rubberized asphalt binder was almost the same.

CHAPTER 10 FIELD INSPECTION OF PAVEMENT PERFORMANCE

10.1 Visual Investigation of Test Section

We compared the performance of dry- and wet-processed rubberized open-graded friction course (OGFC) pavements to control OGFC pavements on State Route 247 near Macon. Traffic control closed the lane for the inspection, according to the requirement of the FHWA's Manual on Uniform Traffic Control Devices (MUTCD). Field inspection includes drilling core samples and investigating for evidence of distress: measuring rut depth and the amount and severity of cracking, raveling, bleeding, pushing, and potholes.

Rut depth was measured in both sample areas' wheel paths and recorded in units of 1/16 inch (Fig. 10-1). Rutting measurements were taken by "blocking" up the stringline using a hollow steel pipe (Fig. 10-2).

Figure 10-1. Rut-depth ruler

Figure 10-2. Rut measurement

Table 10-1 summarizes SR 247 pavement performance. After three years' service, we found no cracking, raveling, bleeding, pushing, or potholes (Figs. 10-3, 10-4, and 10-5), and all OGFC pavements showed only minor rutting at a depth of 1/16 inch.

Table 10-1. Field inspection test results

Item		Control OGFC	Rubberized OGFC (dry)	Rubberized OGFC (wet)
Rut Depth (1/16 inch)	section 1	2	3	2
	section 2	2	2	3
	section 3	3	2	2
	section 4	2	3	3
	section 5	2	N/A	0
Cracking (%)		0	0	0
Raveling (%)		0	0	0
Bleeding (%)		0	0	0
Pushing (%)		0	0	0

Figure 10-3. Wet-processed rubberized OGFC surface

Figure 10-4. Dry-processed rubberized OGFC surface

Figure 10-5. Control OGFC surface

10.2 Performance Evaluation of Core Samples

Cores were drilled from the wheel paths and lane centers of each test section to determine the influence of traffic loading on pavement physical properties and durability (Figs. 10-6; 10-7). Of the 28 samples, 8 were wet-processed; 10

dry-processed; and 10 were control OGFC.

Figure 10-6. Core sample drilling

Figure 10-7. Core samples

The Hamburg test using a retrofitted APA was performed on the core samples based on AASHTO T-324. Test specimens, 6 inches in diameter, were obtained by cutting the field core samples to a height of 2.5 inches. Each specimen consisted of two layers of HMA: a 1-inch top layer of OGFC and a 1.5-inch underlayer of Superpave asphalt mixture (Fig. 10-8). Four core samples for each OGFC test section were measured by retrofitted APA testing: two samples were from the wheel path, and another two were from the center path. Prior to the test, the specimens were

submerged in hot water (50 °C) for 30 minutes to reach the required temperature. The APA automatically ends the test when the steel wheels pass over the specimens 20,000 times, or a 0.8-inch deformation is reached.

Figure 10-8. Field core specimens for APA Hamburg testing

Mixtures showing excessive susceptibility to moisture damage tend to undergo stripping, and usually, after a certain number of cycles, the slope of the curve for rut depth versus number of passes suddenly increases. Figure 10-9 shows typical deformation curves for samples that do and do not exhibit significant moisture damage in the Hamburg test.

Post-compaction consolidation, creep slope, stripping slope, and stripping inflection point (SIP; Fig. 10-10) are widely used to evaluate the rut resistance and moisture-damage susceptibility of HMAs. Post-compaction consolidation is the deformation (in mm) at 1,000 wheel passes, assuming that the wheel densifies the mixture within the first 1,000 passes. Creep slope relates to rutting primarily due to plastic flow and is the number of wheel passes required to create 1 mm of rut depth. Stripping slope relates to rutting primarily due to moisture damage and is the number of wheel passes required to create 1 mm of rut depth after SIP (Yildirim et al., 2007), the point at which moisture damage starts and the number of wheel passes at the intersection of creep slope and stripping slope. A SIP over 10,000 load cycles and a

rutting depth of 12.5 mm indicate less susceptibility to moisture damage.

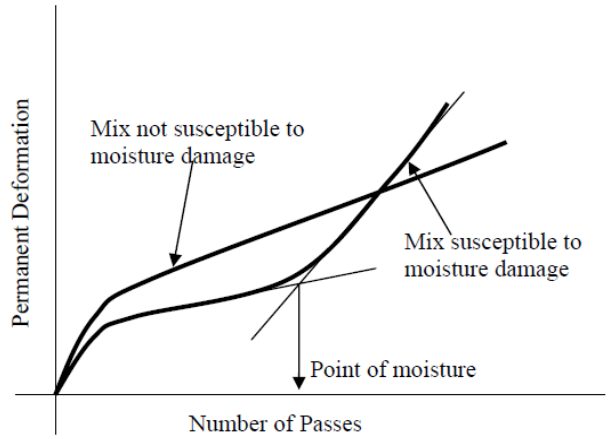

Figure 10-9. Two different outputs of the HWTD test (Bhasin et al. 2004)

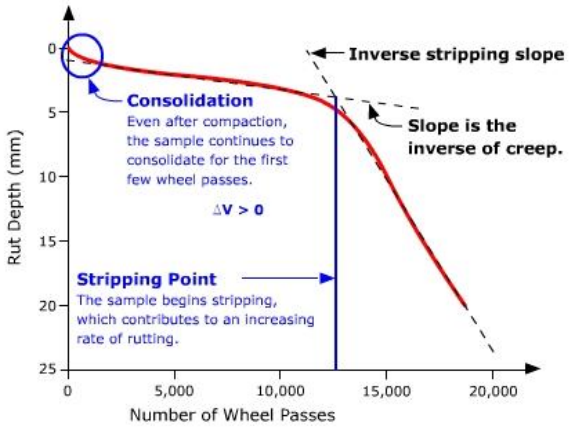

Figure 10-10. Stripping point determination

Figure 10-11 shows the top view of field core specimens after Hamburg testing. More asphalt binder moved onto the surface of cores containing rubberized OGFC, dry- or wet-processed, than those with control OGFC.

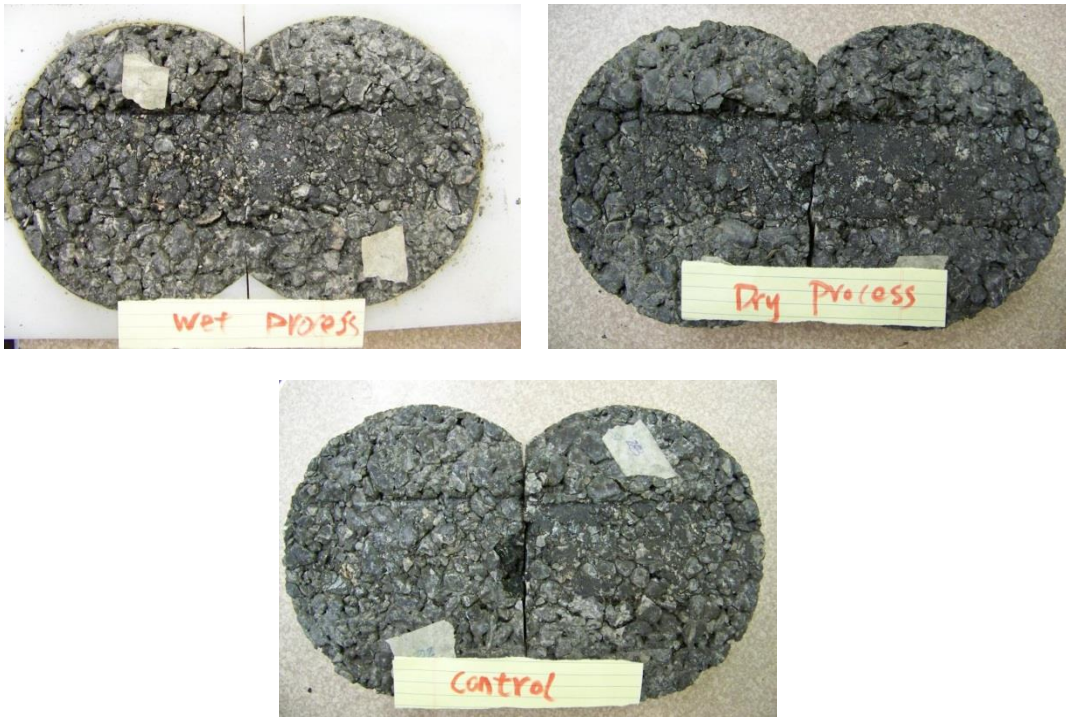

Figure 10-11. Top view of test specimens

Table 10-2 shows the deformation of the specimens after 1,000, 5,000, 10,000, and 20,000 wheel passes. Core samples of wet- and dry-processed materials had similar and significantly greater rut depth than control samples after 20,000 wheel passes, regardless of their origin (wheel path or center path).

Table 10-2. Rut depth per number of wheel passes

Passes	Rut Depth (mm)								
	Dry Process			Wet Process			Control		
	Wheel Path	Center Path	Average	Wheel Path	Center Path	Average	Wheel Path	Center Path	Average
1,000	2.35	2.15	2.25	3.00	1.93	2.47	1.91	1.68	1.80
5,000	4.41	4.27	4.34	5.72	4.08	4.90	3.29	3.38	3.34
10,000	5.29	5.84	5.57	6.88	5.64	6.26	4.03	4.39	4.21
20,000	6.96	7.86	7.41	8.01	7.02	7.52	4.91	5.70	5.31

Figure 10-12 shows curves comparing rut depth and number of wheel passes for the field core specimens. None exhibits a stripping inflection point, suggesting no significant moisture damage after 20,000 wheel passes. Therefore, test data could only record post-compaction consolidation and creep slope. Creep slope is the inverse of the rate of rutting in the linear region of the plot after compaction. Table 10-3 and Figure 10-13 present the values of post-compaction consolidation and creep slope.

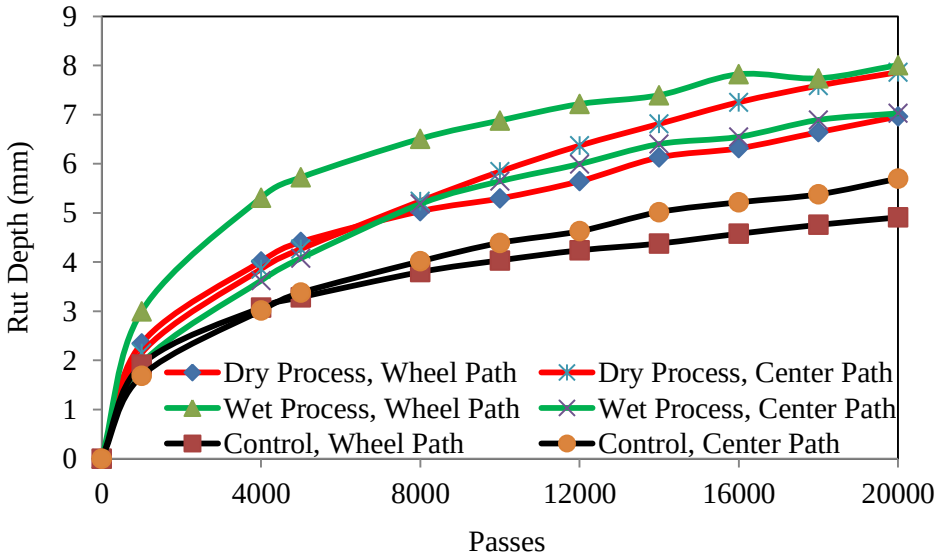

Figure 10-12. APA Hamburg test results

Table 10-3. Summary of test results

	Core Sample ID								
	Dry Process			Wet Process			Control		
	Wheel Path	Center Path	Average	Wheel Path	Center Path	Average	Wheel Path	Center Path	Average
Post-compaction (mm)	2.35	2.15	2.25	3.00	1.93	2.47	1.91	1.68	1.80
Creep Slope (passes/mm)	N/A	N/A	5625	N/A	N/A	5769	N/A	N/A	8513

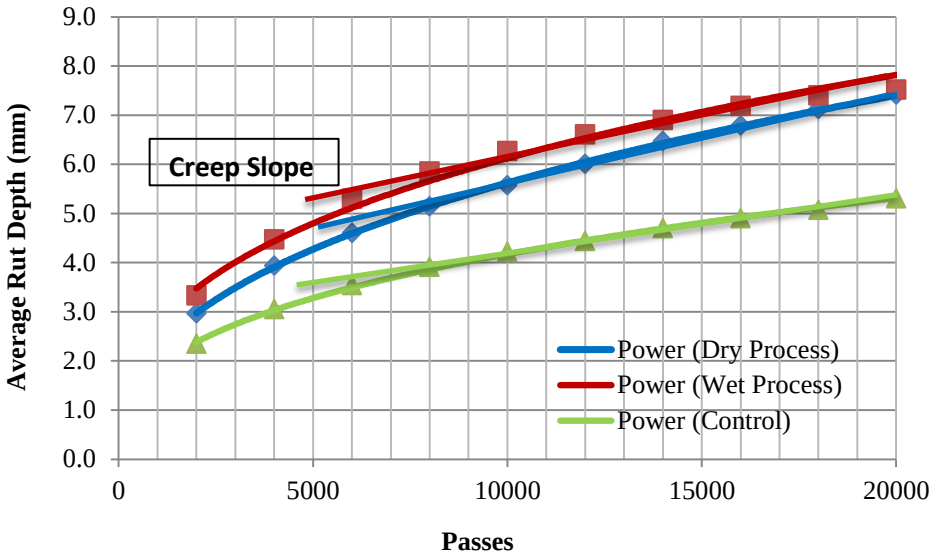

Figure 10-13. Creep slope for core samples

The core samples with dry- or wet-processed rubberized OGFC had significantly higher post-compaction values than control samples after 1,000 wheel passes, suggesting that they are more susceptible to densification within the first 1,000 wheel passes. They also have significantly lower creep slope than control samples, indicating greater plastic deformation under traffic loading.

To further analyze core sample performance, we calculated the rutting rates at 2,000-pass intervals; that is, from 0-2,000, 2,000-4,000, and 18,000-20,000 passes. We labeled 10 intervals of 2,000 passes from 0-2,000 to 18,000-20,000 as I-1 to I-10 (Table 10-4 and Fig. 10-14). We observed that rutting rates diminish as loading passes increase. All core samples had significantly higher rutting rates in the first two-cycle interval than the other intervals. Within the first 8,000 wheel passes, the rutting rates for core samples containing wet-processed binder OGFC were the highest, followed by those with rubberized OGFC; those with control OGFC had the least rutting. After 8,000 wheel passes, the core samples with rubberized OGFC had slightly higher rutting rates than wet-processed or control OGFC.

Table 10-4. Rates of rutting at the two-cycle interval

Two-Cycle Interval	Rates of Rutting (mm/2000 Passes)								
	Dry Process			Wet Process			Control		
	Wheel Path	Center Path	Average	Wheel Path	Center Path	Average	Wheel Path	Center Path	Average
I1(0-2,000)	3.06	2.87	2.97	4.07	2.58	3.33	2.26	2.43	2.35
I2(2,000-4,000)	0.95	0.99	0.97	1.24	1.04	1.14	0.75	0.64	0.70
I3(4,000-6,000)	0.53	0.79	0.66	0.85	0.81	0.83	0.61	0.37	0.49
I4(6,000-8,000)	0.49	0.59	0.54	0.35	0.75	0.55	0.39	0.35	0.37
I5(8,000-10,000)	0.26	0.60	0.43	0.37	0.46	0.42	0.38	0.24	0.31
I6(10,000-12,000)	0.35	0.53	0.44	0.33	0.35	0.34	0.24	0.21	0.22
I7(12,000-14,000)	0.48	0.44	0.46	0.18	0.41	0.29	0.39	0.14	0.26
I8(12,000-14,000)	0.19	0.44	0.31	0.43	0.15	0.29	0.20	0.20	0.20
I9(14,000-16,000)	0.33	0.34	0.33	0.09	0.34	0.22	0.16	0.18	0.17
I10(16,000-20,000)	0.32	0.27	0.30	0.10	0.13	0.12	0.32	0.15	0.24

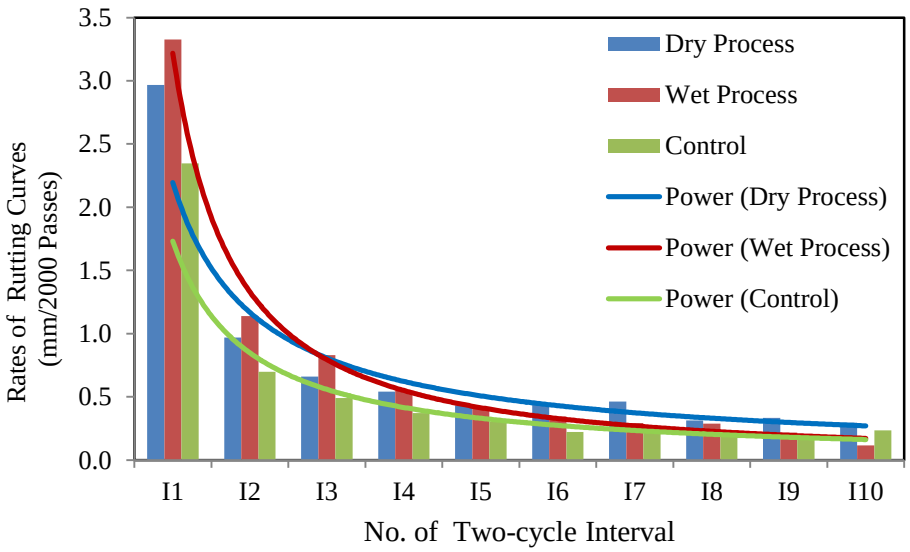

Figure 10-14. Rutting rates for rut profiles

10.3 Summary and Conclusions on Field Investigation

Test sections of rubberized and control OGFC were investigated by field visual inspection and laboratory testing of core samples. The following conclusions can be

drawn:

1. The pavements from SR 247 Macon all exhibited excellent performance after three or five years' service. Cracking, raveling, bleeding, pushing, and potholes were not found.
2. Hamburg tests indicated that no cores from any OGFC pavement exhibited significant moisture damage after 20,000 wheel passes. All the samples met the criterion of 12.5 mm after 20,000 passes.

CHAPTER 11 SUMMARY AND CONCLUSIONS

This project compared the long-term performance of hot asphalt mixes containing crumb rubber modifiers added in dry or wet processes to mixtures modified with SBS binder. A total of eight asphalt mixtures, four porous European mixtures (PEMs) and four stone matrix asphalts (SMAs), were designed with dry- and wet-processed CRM and SBS control binder in addition to hybrid binder. All of the modified binders had a PG 76-22.

Long-term performance properties were investigated after the samples weathered in the Georgia Asphalt Weathering Device for 1,000 or 3,000 hours. Tests measured dynamic modulus, fatigue life, rutting, and Catanbro loss for the mixtures and used the dynamic shear rheometer (DSR), gel permeable chromatography (GPC), and Fourier-transform infrared (FTIR) spectroscopy to study the extracted binders. Laboratory investigation and visual field inspection support the following conclusions:

1. G*/sin(σ) of unaged rubberized asphalt binder increased 14% and 20%, respectively, when 3% and 6% doses of TOR were added. The absolute difference in failure temperatures for the binders taken from the top and bottom of a tube was about 20% less than the controls' when 3% and 6% doses of TOR were added to PG 67-22 asphalt.

2. Following GDOT 114 and 123, PEM and SMA mixtures can be successfully designed to incorporate dry- and wet-processed CRM binders as well as hybrid and SBS-modified binders.

3. The volumetric and rutting, moisture susceptibility, drain-down, and Catanbro loss

properties of designed PEM and SMA met Georgia requirements, although the rutting depths of dry-processed rubberized PEM and SMA were higher than those of control SBS.

4. The dynamic modulus, |E*|, of dry-processed rubberized PEM or SMA did not differ significantly from that of other PEMs or SMAs, regardless of whether they were unaged or aged for 1,000 or 3,000 hours.

5. No differences were found in |E*| between unaged and 1,000-hour aged samples, whereas 3,000-hour aging had a significant effect on |E*| at lower frequency or higher temperature for both PEMs and SMAs.

6. The fatigue life of unaged dry-processed rubberized PEM or SMA was similar to that of wet-processed but generally lower than those of hybrid and SBS samples.

7. After 3,000-hour aging, the fatigue life of the dry-processed rubberized SMA was similar to that of the wet-processed modified mixture but shorter than that of hybrid and SBS SMA, regardless of strain and stress levels or test temperatures.

8. Rutting and Cantabro loss in both dry- and wet-processed PEM were greater than in the control SBS-modified and hybrid PEM, regardless of aging duration.

9. DSR, GPC, FTIR, and AFM results indicated an interaction between CRM and asphalt binder during the production and paving stages, regardless of the type of mixture.

10. Values of G*sin(δ) differed significantly among the four asphalt binders extracted

from PEM and SMA after weathering for 1,000 or 3,000 hours, based on DSR, GPC, and FTIR results, regardless of the type of mixture.

11. The dry-processed and control pavements from SR 247 Macon exhibited good condition after three years in service.

REFERENCES

AASHTO TP 79-12. Standard Method of Test for Determining the Dynamic Modulus and Flow Number for Hot Mix Asphalt (HMA) Using the Asphalt Mixture Performance Tester (AMPT).

Abdelrahman, M.A., Carpenter, S.H. (1999). The mechanism of the interaction of asphalt cement with crumb rubber modifier (CRM). *Transport Res Rec*, 1661:106–13.

Airey, G.D., Collop, A.C., Rahman, M.M. (2004). Mechanical properties of crumb rubber modified asphalt mixtures. 3rd Eurasphalt & Eurobitume Congress. Vienna.

Airey, G.D., Rahman, M.M., Collop, A.C. (2003). Absorption of bitumen into crumb rubber using the basket drainage method. *Int. J. Pavement Eng.*, 4(2):105–19.

Amirkhanian, S.N. (2001). Utilization of crumb rubber in asphaltic concrete mixtures – South Carolina's experience. Clemson University. Retrieved 21 December 2014 from http://www.clemson.edu/ces/arts/CRM.SC.Exper.prn.pdf.

Bandini, P. (2011). Rubberized asphalt concrete pavements in New Mexico: Market feasibility and performance assessment. http://www.nmenv.state.nm.us/swb/documents/RubberizedAsphaltConcretePavementsInNM_Final.pdf.

Bahia, H.U., Davies, R. (1994). Effect of crumb rubber modifiers (CRM) on performance-related properties of asphalt binders. *Journal of the Association of*

Asphalt Paving Technologists.

Bahia, H.U., Davies, R. (1995). Factors controlling the effect of crumb rubber on critical properties of asphalt binders. *Journal of the Association of Asphalt Paving Technologists*.

Bennert, T., Maher, A., Smith, J. (2004). Evaluation of crumb rubber in hot mix asphalt. U.S.D.O.T, Research and Special Programs Administration.

Billiter, T.C., Chun, J.S., Davison, R.R., Glover, C.J., Bullin, J.A. (1996). Investigation of the curing variables of asphalt-rubber binder. *American Chemical Society Symposium on Modified Asphalts*, Orlando, FL.

Brandon, J., Hines, S., Jared, D., Bui, B., Ahmed, Y. (2014). Comparison of procedures to predict moisture susceptibility characteristics in warm mix asphalt. *Transportation Research Board, 93rd Annual Meeting*, Washington, DC.

Bressette, T., Zhou, H., Stonex, A., Hicks, R. (2008). Asphalt rubber and its potential use in China. *Plan, Build, and Manage Transportation Infrastructure in China*，776-785.

Brown, D.R., Jared, D., Jones C., Watson, D. (1997). Georgia's experience with crumb rubber in hot-mix asphalt. *Journal of the Transportation Research Board*, 1583.

Buncher, M.S. (1994). The use of crumb-rubber modifier in hot mix asphalt. Proceedings of the 3rd Air Transport Conference, New York.

Buncher, M.S. (1995). Evaluating the effects of the wet and dry processes for including crumb rubber modifier in hot mix asphalt. Ph.D. Diss., Auburn University.

Chehovits, J.G. (1993). *Binder design procedures*. Federal Highway Administration, Washington, DC: Crumb Rubber Modifier Workshop Notes: Design Procedures and Construction Practices.

Davide, L.P. (2013). Recycled tyre rubber modified bitumens for road asphalt mixtures: A literature review. *Construction and Building Materials, 49,* 863–881.

Dong, R., Li, J., Wang, S. (2011). Laboratory evaluation of pre-devulcanized crumb rubber–modified asphalt as a binder in hot-mix asphalt. *J. Mater. Civ. Eng., 23*(8), 1138–1144.

Dong, Y., Tan, Y. Yang, L. (2012). Evaluation of performance on crumb-rubber-modified asphalt mixture. *Journal of Testing and Evaluation, 40,* 7.

Epps, J.A. (1994). Uses of recycled rubber tires in highways*: NCHRP synthesis of Highway Practice 198*. Washington, DC: Transportation Research Board.

Fager, G.A. Use of rubber in asphalt pavements – Kansas experience. http://www.asphaltrubber.org/ARTIC/Reports/RPA_A1380.pdf.

Fontes P.L., Glicerio T., Jorge C., Paulo A. (2010). Evaluating permanent deformation in asphalt rubber mixtures. *Construction and Building Materials, 24* (7): 1193–1200.

George, B.W. (1999). Asphalt rubber - the Arizona experience. Asphalt Rubber 1999: A Global Summary of Practices Rubber Pavements Association International Symposium Tempe, AZ.

Georgia moving forward with recycled rubber asphalt use. http://www.american-securities.com/news/georgia-moving-forward-with-recycled-rubber-asphalt-use/.

Gowda, G.V., Hall, K.D., Elliott, R.P. (1996). Arkansas experience with crumb rubber modified mixes using Marshall and Strategic Highway Research Program Level I Design Methods. *Transportation Research Record*, 25-33.

Green, E.L., Tolonen, W.J. (1977). The chemical and physical properties of asphalt-rubber mixtures. Arizona Department of Transport, Report ADOT-RS-14 (162).

Grzybowski, K., Rowe, G.M., Prince, S. (2012). Development of an accelerated weathering and reflective crack propagation test methodology. 7th RILEM International Conference on Cracking in Pavements, *4*, 125-135.

Gualliard, S., Leblanc, P. (2004). A rheometrical technique to study the swelling

kinetics of vulcanized rubber particles by paraffinic solvents using a torque. *J Appl Polym Sci.*, 94:142–53.

Hagos, E.T. (2008), *The Effect of Aging on Binder Properties of Porous Asphalt Concrete*. Delft University of Technology.

Heitzman, M.A. (1992). State of the practice - design and construction of asphalt paving materials with crumb rubber modifier, Washington, DC: FHWA-SA-92-022, Federal Highway Administration.

Hicks, R.G., Epps, J.A. (2000). Quality control for asphalt rubber binders and mixes. Report for Rubber Pavements Association.

Holikatti, S., Zhou, H., Vacura, P. (2013). Seven year itch: Evaluation of Caltrans full scale experiment on asphalt rubber modified pavements. http://www.ra-foundation.org/wp-content/uploads//02/003-PAP_019.pdf.

Hou, T. (2009). *Fatigue performance prediction of North Carolina mixtures using simplified viscoelastic continuum damage model*. North Carolina State University.

Hou, T., Underwood, B.S., Kim, Y.R. (2010). Fatigue performance prediction of North Carolina mixtures using simplified viscoelastic continuum damage model. *Journal of the Association of Asphalt Paving Technologists, 79,* 35–80.

Hsu, T., Chen, S., Hung, K. (2011). Performance evaluation of asphalt rubber in

porous asphalt-concrete mixtures. *J. Mater. Civ. Eng.*, *23*(3), 342–349.

Huang, B., Mohammad, L.N., Graves, P.S., Abadie, C. (2002). Louisiana experience with crumb-rubber modified hot-mix asphalt pavement. *Transportation Research Board*, 1-13.

Huffman, J.E. (1980). Sahuaro concept of asphalt-rubber binders. Proceedings of the 1st Asphalt Rubber User Producer Workshop, Scottsdale, AZ.

Hunt, E.A. (2002). Crumb rubber modified asphalt concrete in Oregon. Final Report SPR355. Oregon Department of Transportation and Federal Highway Administration.

Kaloush, K., Witczak, M., Sotil, A., Way, G. (2003). Laboratory evaluation of asphalt rubber mixtures using the dynamic modulus (E*) test. *Transportation Research Record*, 1-13.

Khalid, H., Artamendi, I. (2002). Exploratory study to evaluate the properties of rubberised asphalt modified using the wet and dry process. 3rd International Conference on Bituminous Mixtures and Pavements, Thessaloniki, Greece.

Kök, B., Yilmaz, M., Geçkil, A. (2013). Evaluation of low-temperature and elastic properties of crumb rubber- and sbs-modified bitumen and mixtures. *J. Mater. Civ. Eng.*, *25*(2), 257–265.

Kuennen, T. (2004). Asphalt rubber makes a quiet comeback. *Better Roads Magazine*,

(May): 32–42.

Lee, S.J., Akisetty, C.K., Amirkhanian, S. (2008). The effect of crumb rubber modifier on the performance properties of rubberized binders in HMA pavements. *Construction and Building Materials*, *22*(7): 1368–1376.

López, M., Francisco, J., et al. (2013). Microscopic analysis of the interaction between crumb rubber and bitumen in asphalt mixtures using the dry process. *Construction and Building Materials, 48*, 691-699

Lucas, M.J., Brehm, D. (1998). Evaluation of rubber-modified asphaltic concrete. Pennsylvania Department of Transportation.

Mashaan, N.S., Ali, A.H. Koting, S., Karim, M.R. (2013). Dynamic properties and fatigue life of stone mastic asphalt mixtures reinforced with waste tire rubber. *Advances in Materials Science & Engineering*.

Mashaan, N.S., Ali, A.H., Rehan K.M., Abdelaziz, M. (2014). A review on using crumb rubber in reinforcement of asphalt pavement. *Scientific World Journal*, Article ID 214612.

Miknis, F.P., Michon, L. (1997). Some applications of unclear magnetic resonance imaging to crumb rubber modified asphalt. *Fuel, 77*(5):393–7.

Moreno, F., Rubio, M.C., Martinez-Echevarria, M.J. (2011). Analysis of digestion

time and the crumb rubber percentage in dry-process crumb rubber modified hot bituminous mixes. *Construction and Building Materials, 25*(5), 2323–2334

National Cooperative Highway Research Program. (2003). 2002 Design Guide: Design of New and Rehabilitated Pavement Structures.

Olivares, F., Schultz, B., Fernández, M., Moro, B. (2009). Rubber-modified hot mix asphalt pavement by dry process. *Int. J. Pavement Eng. 10*(4):277-288.

Oliver, J. (1981). Modification of paving asphalts by digestion with scrap rubber. *Transportation Research Record*.

Oliver, J.W.H. (1982). Optimizing the improvements obtained by the digestion of comminuted scrap rubbers in paving asphalts. Proceedings of the Association of Asphalt Paving Technologists.

Ouyang, C., Wang, S., Zhang, Y., Zhang, Y. (2006). Improving the aging resistance of asphalt by addition of zinc dialkyldithiophosphate. *Fuel, 85*: 1060–1066

Page, G.C., Byron, E.R., Randy, C.W. (1992). Florida's approach using ground tire rubber in asphalt concrete mixtures. *Transportation Research Record 1339*, 16-22.

Pinheiro, J.H.M., Soares, J.B. (2003). The effect of crumb rubber gradation and binder-rubber interaction time on the asphalt-rubber mixture (dry process). Proc. of the Asphalt-Rubber Conference. Brasilia, Brazil.

Rebala, S.R., Estakhri, C.K. (1995). Laboratory evaluation of crumb rubber modified mixtures designed using TXDOT mixture design method. *Transportation Research Record*.

Renshaw, R.H. (n.d.). Bitumen-rubber: Its introduction and development in South Africa. http://www.asphaltrubber.org/ARTIC/International/RPA_A1168.pdf.

Richard, W., Rodezno J.C., Adam, T., Nam, T. (2014). Evaluation of a rubber-modified mixture in ALABAMA. NCAT Report 14-03.

Roberts, F.L., Kandhal, P.S., Brown, E.R., Dunning, R.L. (1989). Investigation and evaluation of ground tire rubber in hot mix asphalt. NCAT Report No. 89-3. Auburn, AL: National Center for Asphalt Technology.

Rosner, J.C., Chehovits, J.C. (1981). Chemical and physical properties of asphalt-rubber mixtures. Phase III summary report. Report HPR 1-19 (159), Arizona Department of Transportation, Phoenix, AZ.

Sabounjian, R. (1997). Performance of rubberized asphalt mixes in ALASKA. Transportation Research Board.

Sabouri, M.R., Kim, Y.R. 2014. Development of a fatigue failure criterion for asphalt mixtures under different modes of fatigue loading. Transportation Research Records 93th Annual Meeting.

Shen, J., Amirkhanian, S. (2005). The influence of crumb rubber modifier (CRM) microstructures on the high temperature properties of CRM binders. *International Journal of Pavement Engineering 6*(4), 265-271.

Shen, J., Xie, Z. (2012). Comprehensive evaluation of the long-term performance of rubberized pavement: Phase I: Laboratory study of rubberized asphalt mix performance. Georgia Department of Transportation. FHWA-GA-12-1119. 2012.

Shook, J.F. (1990). Experimental construction of rubber-modified asphalt mixtures for asphalt pavements in New York State. ARE Inc., Report Submitted to the New York State Department of Transportation.

Shuler, T.S., Pavlovich, R.D., Epps, J.A., Adams, C.K. (1985). Investigation of materials and structural properties of asphalt-rubber paving mixtures. Washington, DC: Federal Highway Administration.

Singleton, T.M., Airey, G.D., Collop, A.C., Widyatmoko, I. (2000). Residual bitumen characteristics following dry process rubber-bitumen interaction. Proceedings of the Asphalt Rubber 2000 Conference, Vilamoura, Portugal, pp. 463-482.

Swearingen, D.L., Newton, C.J., Anderson, K.W. (1992). Use of recycled materials in highway construction. Washington State Department of Transportation. Report No. WA-RD 252.1, Olympia, Washington.

Takallou, H.B. (1988). Development of improved mix and construction guidelines for

rubber modified asphalt pavements. *Transport Research Record, 1171*.

Takallou, H.B., Hicks, R.G, Esch, D.C. (1986). Effect of mix ingredients on the behavior of rubber-modified asphalt mixtures. *Transportation Research Record, 1096*, 68-80.

Takallou, H.B., Takallou, M.B. (2003), Effects of mixing time and temperature on the visco-elastic properties of asphalt rubber binder. Asphalt Rubber 2003, Proceedings. Brasilia, Brazil.

Tayebali, A.A., Vyas, B.B., Malpass, G.A. (1997). Effect of crumb rubber particle size and concentration on performance grading of rubber modified asphalt binders. In R.N. Jester (ed.), *Progress of Superpave (Superior Performing Asphalt Pavement): Evaluation and Implementation. ASTM STP 1322*. American Society for Testing and Materials.

Tortum, A. Celik, C. Aydin, A.C. (2005). Determination of the optimum conditions for tire rubber in asphalt concrete. *Build Environ, 40* (11):1492–504.

Turgeon, C.M. (1989). The use of asphalt-rubber products in Minnesota. Presented at the National Seminar on Asphalt-Rubber, Kansas City, MO.

Turner Fairbank Highway Research Center (TFHRC).（2005）. *User guidelines for waste and byproduct materials in pavement construction*. Washington, DC: Federal Highway Administration.

Typical RAC Binder Production.

http://maxlinktyrerecycling.com/our-solutions/bitumen-modifier-pellets/.

Vahidi, S., Mogawer, W., Booshehrian, A. (2014). Effects of GTR and treated GTR on asphalt binder and high-RAP mixtures. *J. Mater. Civ. Eng.*, *26*(4), 721–727.

Van, K., Jack, L. (1991). CalTrans experience with rubberized asphalt concrete. Presented at the Technology Transfer Session of an Introduction to Rubberized Asphalt Concrete, Topeka, Kansas.

Visser, A.T., Verhaeghe, M.B. (2000). Asphalt rubber: Lessons learned in South Africa. Proceedings of Asphalt Rubber 2000. Vilamoura, Portugal.

Volle, T.H. (2000). Performance of rubberized asphalt pavements in Illinois. Illinois Department of Transportation.

West, R.C., Page, G.C., Veilleux, J.G., Choubane, B. (1998). Effect of tire rubber grinding method on asphalt-rubber binder characteristics. Transportation Research Board.

Widyatmoko, I., Elliot, R. (2007). *A review of the use of crumb rubber modified asphalt worldwide*. UK: Waste & Resources Action Program (WRAP).

Witczak, M.W., Kaloush, K., Pellinen, T., El-Basyoun, M., Von Quintus, H. (2002). Simple performance test for Superpave mix design. NCHRP Rep. No. 465, National

Cooperative Highway Research Program, Transportation Research Board.

Xie, Z., Shen, J. (2013). Long-term performance of SMA mixtures added with crumb rubbers in dry process. *Airfield and Highway Pavement*. 1145-1155.